Geophysics Open - File Report 57
Geoscience Department and
Geophysical Research Center
New Mexico Tech
Socorro, NM 87801
December 1986

INVESTIGATION OF THE SEISMOGENIC ZONE

IN THE VICINITY OF SOCORRO, NEW MEXICO,

FROM AN ANALYSIS OF FOCAL DEPTH DISTRIBUTIONS

by

Kevin M. King

Submitted in partial fulfillment

of the requirement for

Geophysics 590

and the

Master's Degree Program

New Mexico Institute of

Mining and Technology

December 1986

ABSTRACT

A final data set consisting of 513 well located events, with average ERH = 0.40 (±0.155) km and average ERZ = 0.84 (±0.459) km, was used in the analysis of focal depths in the Socorro, New Mexico area. The depth distribution for the entire area reveals that over 89 percent of these earquakes lie between 6 and 12 km. No hypocenters shallower than 2 km were found and a sharp drop in focal depths near 12 km was also observed. This is interpreted as the rapid transition from a brittle to ductile crust, which occurs at estimated temperatures from 400-500°C for silicate rocks.

A grid of 16 different regions within the area was established in order to detect anomalous depth distributions when compared to the distribution of the entire area. One depth distribution profile running from the southwest to the northeast of Socorro displayed a bimodal distribution with peak activity between 6 to 8 km and 10 to 12 km. This suggests the possibility of a semi-ductile layer sandwiched between more brittle crust above and below. However, this interval (8-10 km) is not completely aseismic.

Another profile showed a region of relatively shallow seismicity with foci located predominantly between 4 to 8 km. This is also in the area of maximum surface uplift documented by Reilinger and others (1980), and the area in which Jarpe and others (1984) found compressional first motions throughout the entire focal sphere.

Cross section profiles of projected hypocenters provide several interesting examples of columns of seismicity. Further studies of these seismic pillars need to be pursued in order to substantiate their existence.

TABLE OF CONTENTS

ACKNOWLEDGMENTS

First and foremost, I must thank Dr. Allan R. Sanford for his knowledge, insights and advice. From these attributes, the study was given focus and direction. Also, I appreciate Dr. John S. Knapp, Jeff Minier, and Jon Ake for their helpful suggestions. I must also thank the NMT Computer Center for providing the facilities necessary to complete this study. Finally, I thank my wife and family for their patience and support.

INTRODUCTION

Purpose of Present Study

Just as global epicenter distributions can trace lithospheric plate boundaries, depth distributions of earthquake foci can indicate the seismic-aseismic (brittle-ductile) boundary within a region. The purpose of this study is to analyze epicentral and, more importantly, focal distributions of good-quality, well located microearthquakes in the Socorro, New Mexico area, in the attempt to better define the local seismogenic zone. In the process, local seismicity will be related to the major geologic features in the area.

Brittle-Ductile Transition

Much laboratory work has been performed to determine the brittle strength of crustal rocks. However, evidence for fractures, which include joints, faults, and bedding foliation (Brace, 1972), to depths from 5 to 10 km render these laboratory measurements useless in regard to actual in situ strengths of crustal rocks. Evidence for sub-surface fractures comes from a number of sources: earthquake studies, geologic studies of deeply exposed crust, seismic reflection and refraction profiles, direct observation in mines and drill holes and inferences from measured electrical or fluid conductivity (Brace and Kohlstedt, 1980). There is evidence for water-filled interconnected pore space to

about 5 km, and resistivity measurements indicate that these may exist perhaps as deep as 20 km (Nekut et al., 1977). A study of crustal permeability (Brace, 1980) argues for high fluid conductivities to 8 km, which in turn argues for interconnecting fractures, since intergrain porosity in crystalline rocks is probably only a percent or less (Brace and Kohlstedt, 1980).

Although the lower depth of interconnected pore space is not known, plastic flow (Brace, 1972) and the healing of cracks (Batzle and Simmons, 1977) appear to be the important limiting factors for the existence of fracture porosity. For silicate rocks, plastic flow begins around 400-500°C (Goetze and Brace, 1972; Tullis and Yund, 1977; Paterson, 1978). Brace and Kohlstedt (1980) suggest that brittle fractures and pore space may disappear below depths at which these temperatures occur. This agrees well with estimates of temperatures at depths of some of the deepest intracontinental events (250-450°C) found by Chen and Molnar (1983).

Byerlee (1968) showed that the brittle-ductile transition pressure in rocks is the pressure at which the stress required to form a fault is equal to the stress required to cause sliding on the fault. A sharp drop in seismicity with depth then, may indicate that the temperature and pressure are such that ductile deformation, rather than brittle fracture, is taking place, assuming similar stress conditions. The analysis of focal depths, then, can be very useful in assessing the brittle and ductile regimes within the crust.

Geologic Setting

Socorro and the associated seismic network are centrally located in the Rio Grande rift (Figure 1). The rift, consisting of a series of north trending grabens extending from southern Colorado to northern Mexico, formed during regional crustal extension which began approximately 30 million years ago (Chapin and Seager, 1975). For a detailed discussion of the RGR, refer to Rio Grande Rift: Tectonics and Magmatism (1979). Figures 2 and 3 show the physiographic and major geologic features of the area.

Socorro is located near the intersection of two crustal lineaments, the Morenci and the Capitan, along which magma has been intruded into the crust (Chapin et al., 1978). In particular, the Morenci lineament is a transverse shear zone and marks the boundary between oppositely tilted blocks to its north and south (Chapin et al., 1978).

Another important geological feature, extending from just south of Socorro to the San Mateo mountains, is a series of overlapping calderas. Exposed on Socorro Peak is the Socorro caldera which formed approximately 27 million years ago and became active again 12 to 7 million years ago.

Superposed on the lineaments and calderas are the major north-south trending faults of the Rio Grande rift. An important question in studies on the seismicity of the area has been whether the known fault zones are related to the observed seismicity. Although most of the studies have concluded that

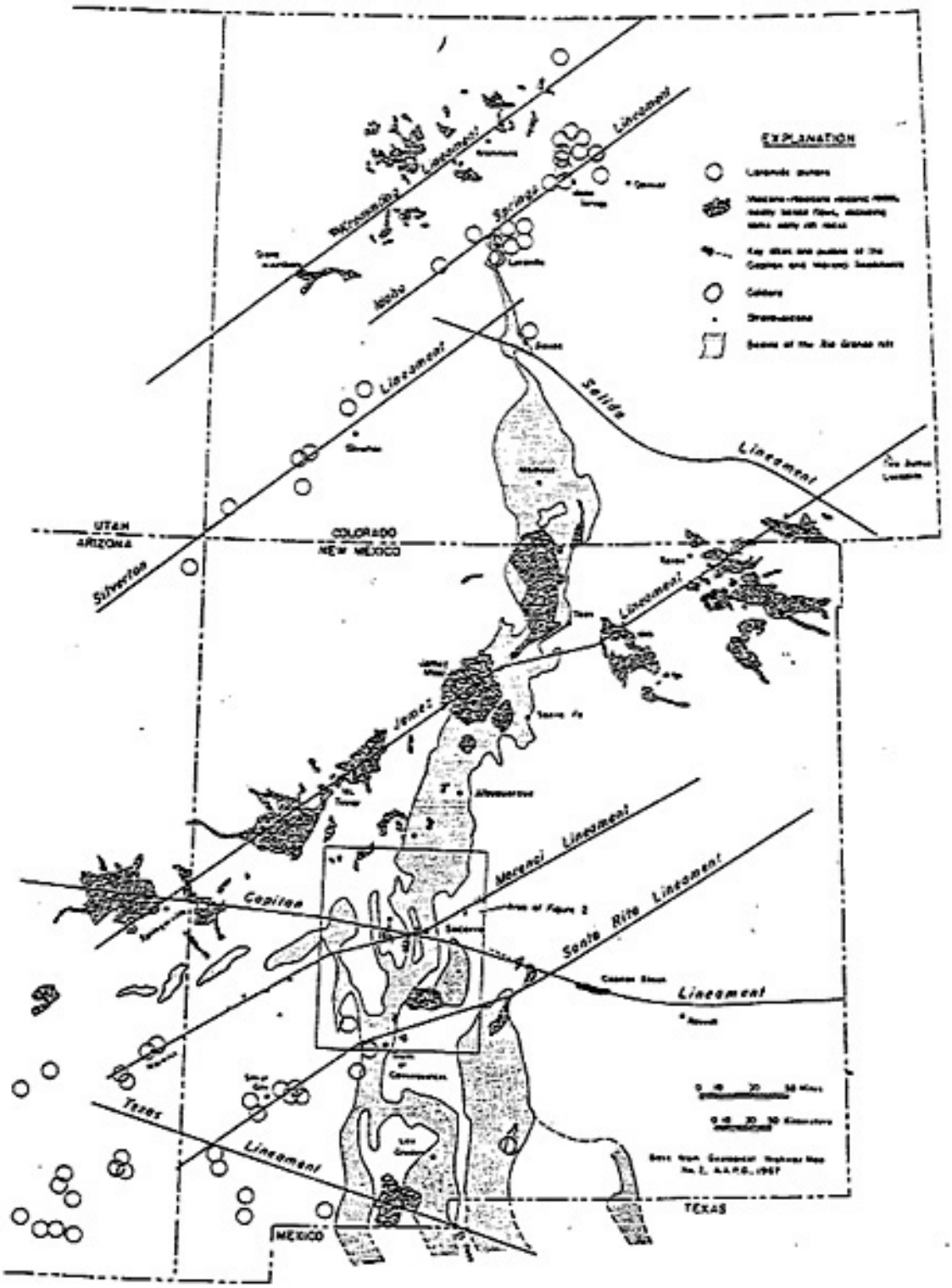

Figure 1. Extent of the Rio Grande rift with location of Socorro shown.

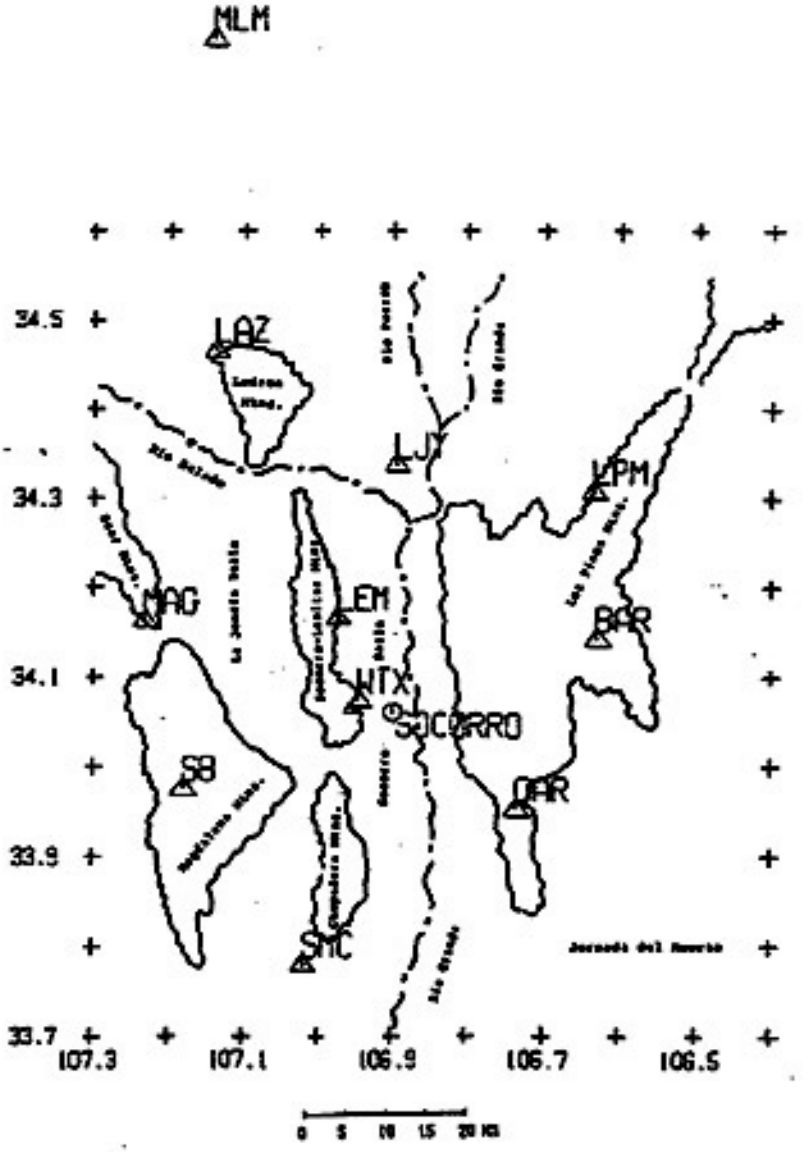

Figure 2. Physiographic character of the Socorro area. Seismic stations are given by triangles.

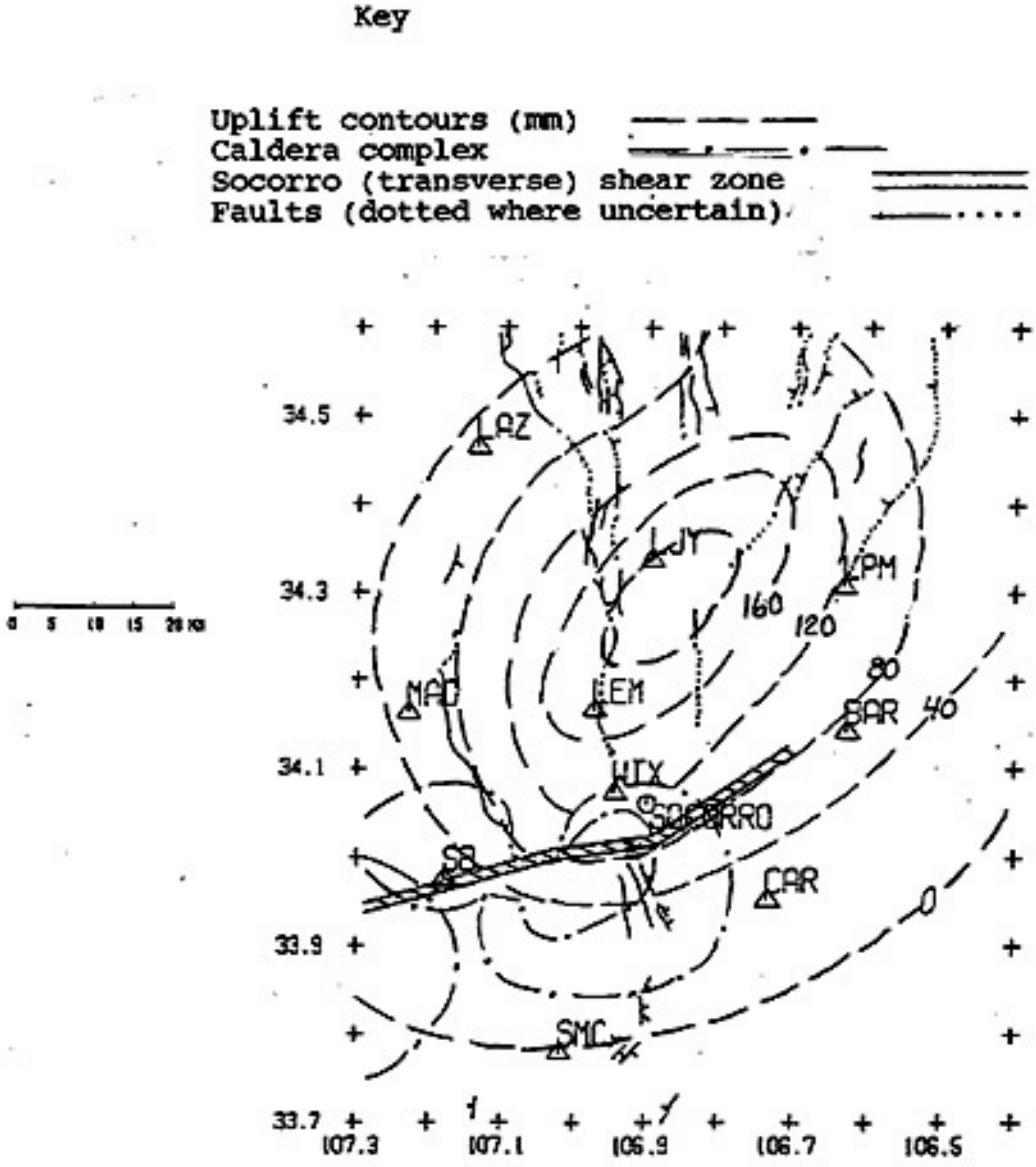

Figure 3. Major geologic features in the Socorro area. Uplift (after Reilinger and others, 1980); Pliocene or younger faults (after Machette and McGimsey, 1982; Machette, unpublished data); shear zone and caldera complex (after Chapin and others, 1978).

earthquakes cannot be directly correlated with the major faults in the area (Sanford et al., 1972; Mott, 1976; Sanford et al., 1979), the microearthquake foci do indicate active faults buried beneath the rift.

Underlying the geologic features discussed above is a mid-crustal magma body. Evidence for this body which has an areal extent of ~1700 km^2 at a depth near 19 km, comes from three major sources: 1) analysis of the strengths and times of S_zS reflections observed on microearthquake seismograms (Sanford et al., 1973; Sanford et al., 1977; Rinehart et al., 1979), 2) analysis of strong P reflections from a deep crustal reflection survey performed in the area (Brown et al., 1979; Brown et al., 1980; Brocher, 1981), and 3) observed uplift in the Socorro area determined from a releveling of benchmarks (Reilinger et al., 1980).

Other studies in the area suggest the existence of smaller, shallower magma bodies in the crust. High heat flows (Reiter and Smith, 1977; Sanford, 1977), regions of anomalous Poisson's ratio (Caravella, 1976; Fender, 1978; Frishman, 1979), screening of S waves from microearthquake foci (Shuleski, 1976; Johnston, 1978), anomalous crustal Q values (Carpenter and Sanford, 1985) and a first motion study which found compressions over the entire focal sphere (Jarpe et al., 1984), comprise most of the evidence for these shallow magma bodies.

Much of the seismic activity in the Socorro area, which is the highest of any area along the Rio Grande rift, occurs in swarms. Defined as a sequence of shocks in which there is no one

primary event, swarms typically occur in regions of recent, but not necessarily current, volcanic activity (Richter, 1958).

DATA

Locations

Locations of microearthquakes in the Socorro area are calculated using the algorithm HYP071 Revised (Lee and Lahr, 1975). An average P wave velocity of 5.85 km/sec and a Poisson's ratio of 0.25 are the two central parameters in a half-space crustal model used in the algorithm. Input is in the form of weighted P and S arrival times.

HYP071 solution quality ranges in grade from D to A, which corresponds to a range in quality from poor to excellent for epicenters and poor to good for hypocenters. Solution quality (Q) itself is based on (1) a statistical quality of the solution (QS) and (2) a station distribution quality factor (QD). QS is based on the calculated root-mean-square (RMS) of the time residuals, the standard epicentral errors (ERH), and standard focal depth errors (ERZ). QD is based on the number (NO) of station readings used, the largest azimuthal separation between stations (GAP) and the epicentral distance to the nearest station (DM) (see Appendix 1 for details on HYP071 parameters). ERH for B quality solutions are $\leq$ 2.5 km while ERZ can be > 5 km.

Preliminary Data Sets

A further criterion imposed on the data for this study, was that an 'equivalent' of six P arrivals per event be maintained. This became necessary once it was observed that for some weak events only S arrivals are recorded at some (distant) stations. Since good S arrivals are approximately half as clear as good P arrivals the appropriate P/S weighting ratio is 2/1 and, therefore, two S arrivals (from stations without P arrivals are 'equivalent' to one P arrival. For example, an event in which only three direct P arrivals are recorded will require an additional three 'equivalent' P arrivals (six S arrivals) in order to meet this criteria. A total of nine station recordings would, then, be required in this case. This criterion has the effect of requiring a larger number of stations to be used when a good quality solution consists of a small number of P readings and many S readings.

Two data sets were used in the present study. Data set A contained 220 events that occurred between May, 1975 and January, 1978 and data set B contains 497 events that occurred between September, 1982 through December, 1985. Events in data set A were recorded by high gain, short period seismic recording instruments (MEQ-800S) stationed at temporary field locations in the Socorro area. Event signals in set B were picked up by the permanent array of stations, set up jointly by the USGS and New Mexico Tech (NMT) in 1982. Plots of epicenters and depth distributions are given for data sets A and B in Figures 4-7.

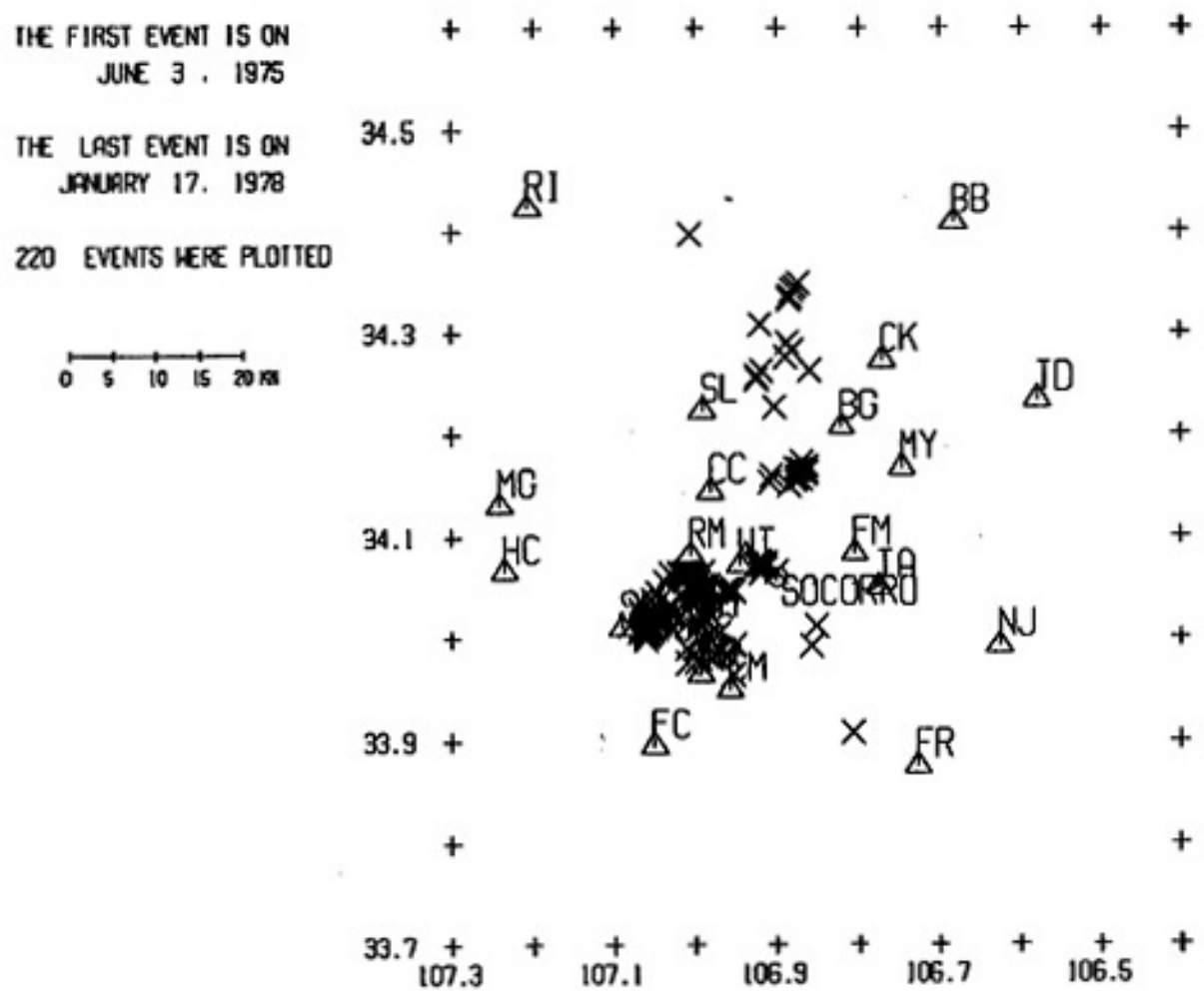

Figure 4. Epicenters of 220 B-quality events occurring in the period from May 20, 1975 through January 20, 1978 (Data set A).

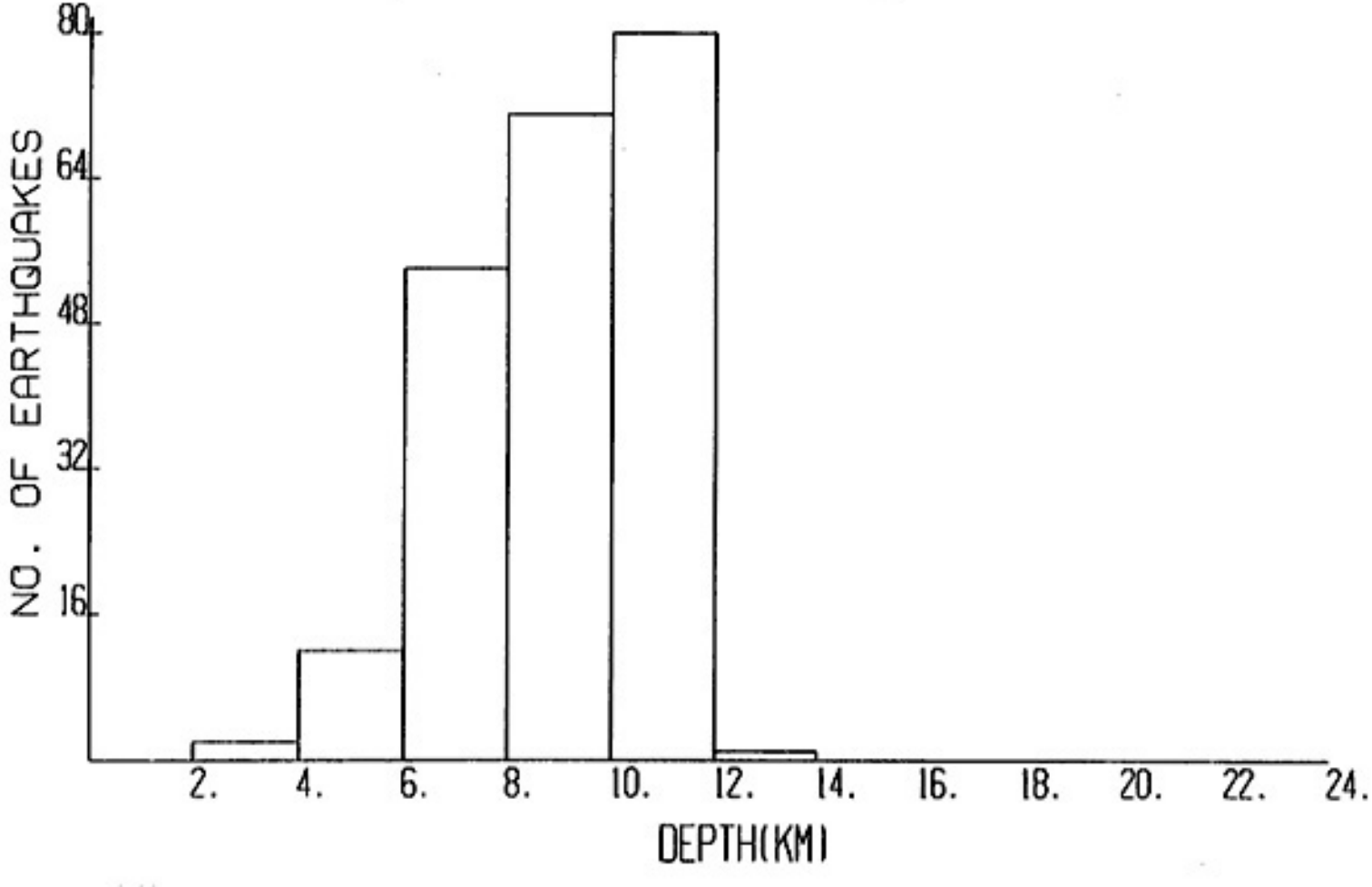

Figure 5. Depth distribution of events shown in Figure 4.

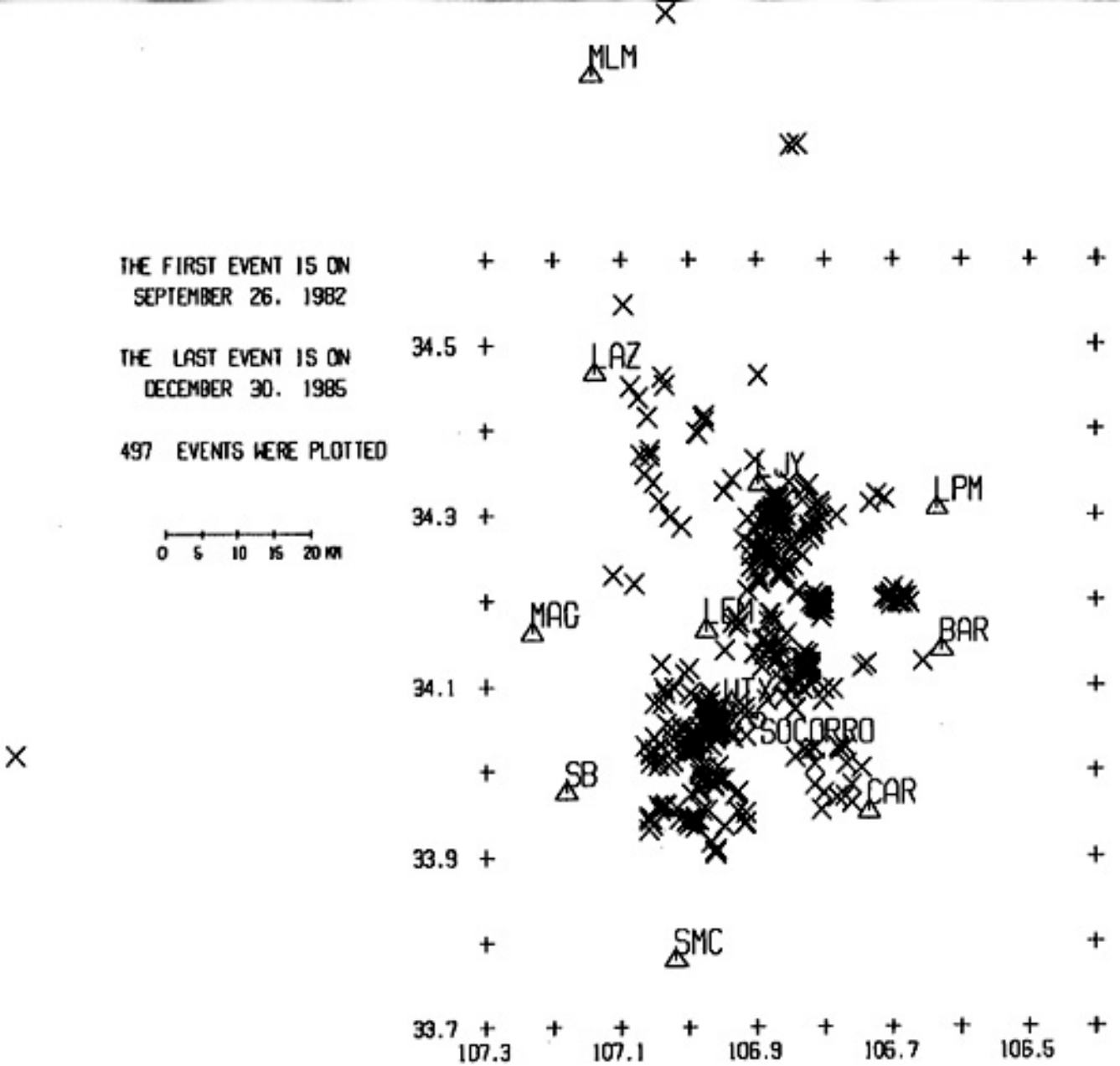

Figure 6. Epicenters of 497 B-quality events occurring in the period from September 22, 1982 through December 31, 1985 (Data set B).

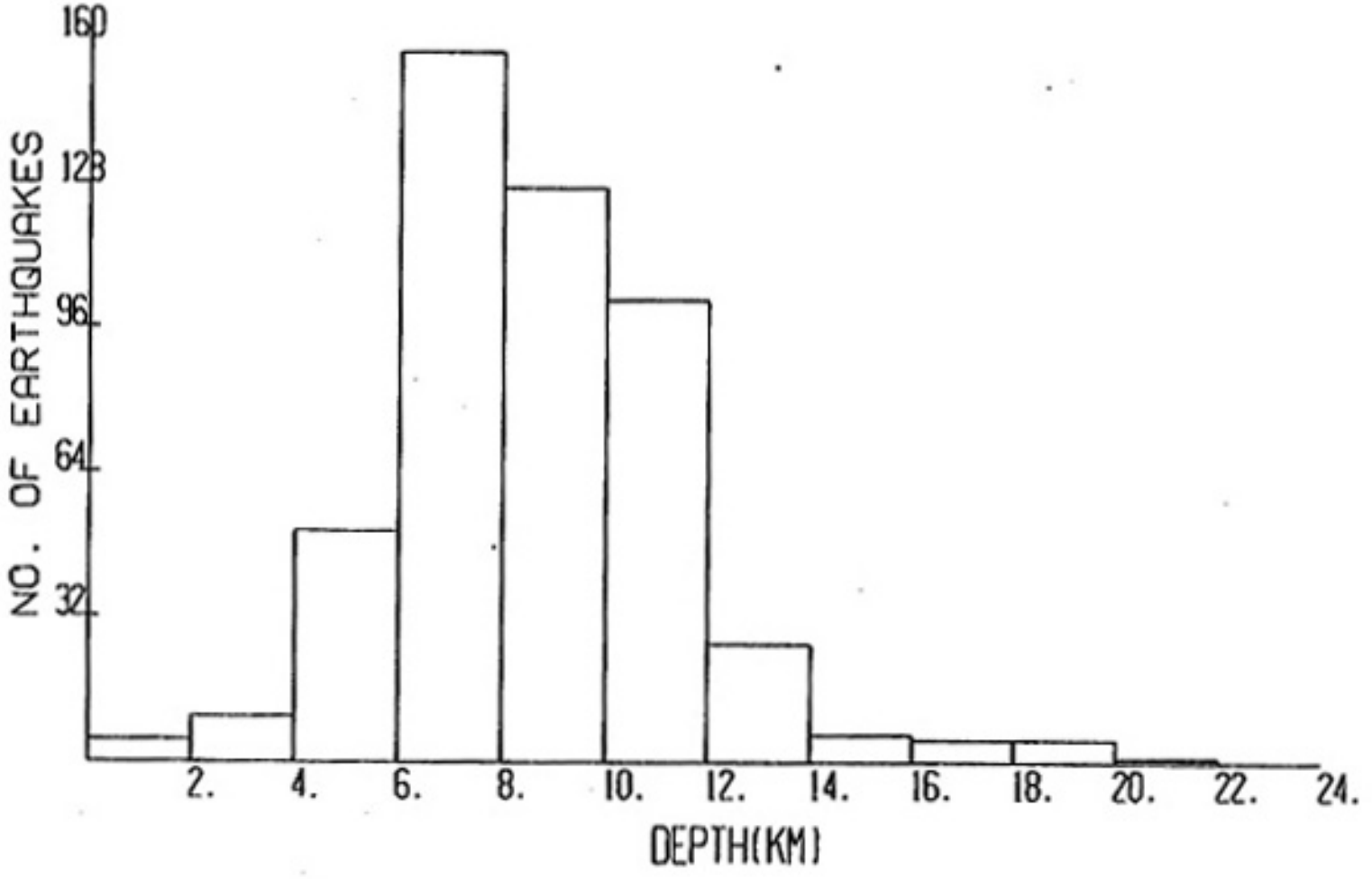

Figure 7. Depth distribution of events shown in Figure 6.

Epicenters and depth distribution for the combined data are given in Figures 8 and 9, respectively.

Magnitudes have been calculated for data set B, but not for data set A. These magnitudes are based on a duration magnitude scale derived by Los Alamos National Laboratory (LANL). The LANL formula, given by

$$M = 2.79 \cdot \mathrm{Log}(t) - 3.63,$$

where t is the signal duration in seconds measured from the onset of the P-arrival to the loss of signal into the background noise, was originally derived for use in northern New Mexico (Newton et al., 1976), but was subsequently found applicable in central New Mexico (Ake et al.,1983) as well. This equation was derived from data with magnitudes ranging from one to four and, hence, the accuracy of this scale for small magnitudes (M <0.0) is uncertain. The advantage of a magnitude scale based on signal duration rather than signal amplitudes, is that magnitudes can be calculated even though instrument saturation (amplitude clipping) has occurred.

Approximately 80 percent of the B-quality microearthquakes in data set B have a duration magnitude in the range from -0.5 to 1.0 (Figure 10). A plot of frequency versus magnitude is given for the entire data set in Figure 11a. The relation $\log(\Sigma N) = a - bM$, was applied to the segment of the graph between magnitudes 0.1 and 1.8. Results of the linear regression yielded values of 2.55 and -0.706 (±0.009 s.d.) for a

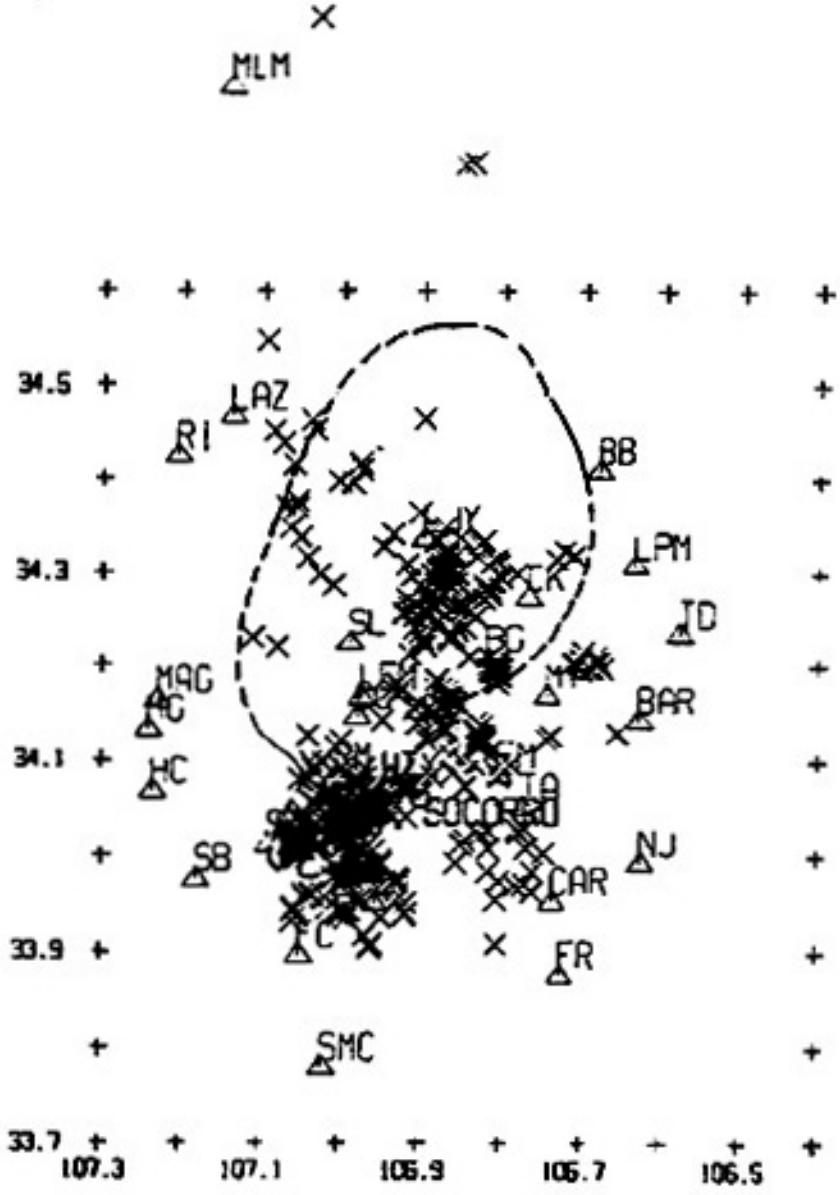

Figure 8. Epicenters for the 717 events shown in Figures 4 and 6 (Data sets A and B). Also shown is the outline of the Socorro magma body (after Rinehart and others, 1979) and locations of stations for the two data sets.

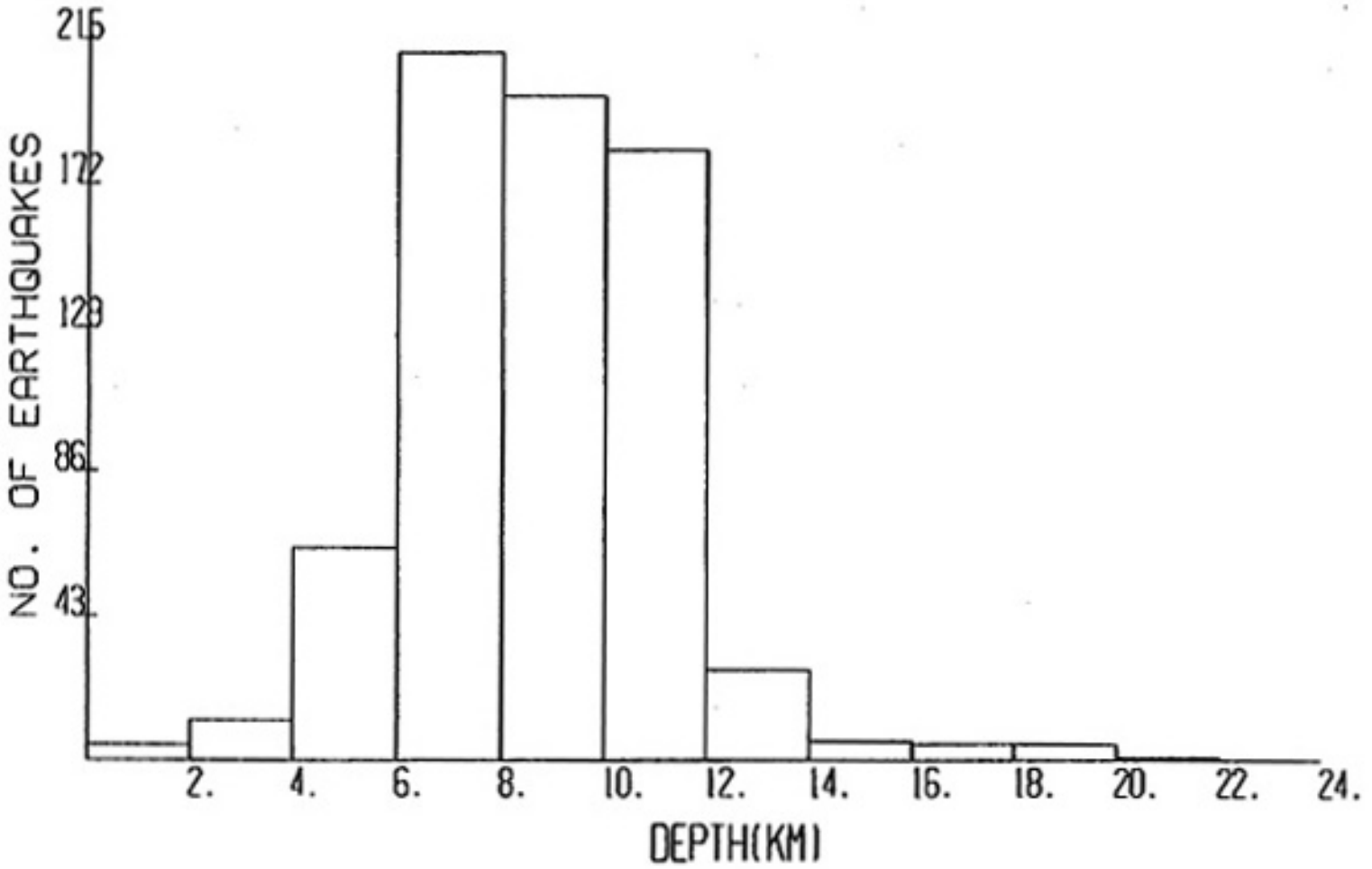

Figure 9. Depth distribution for events shown in Figure 8.

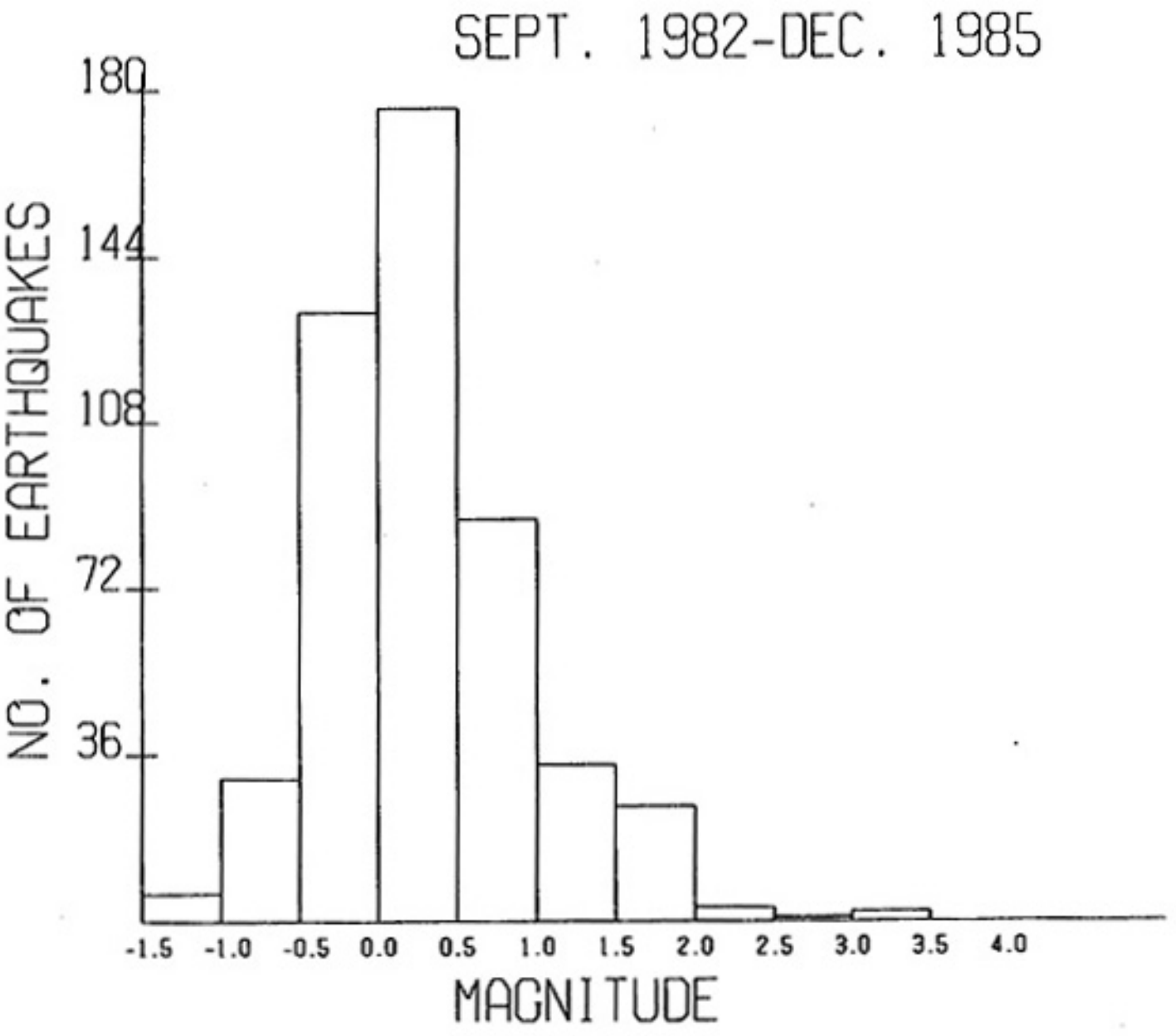

Figure 10. Magnitude distribution of B quality events occurring from September 22, 1982 through December 31, 1985.

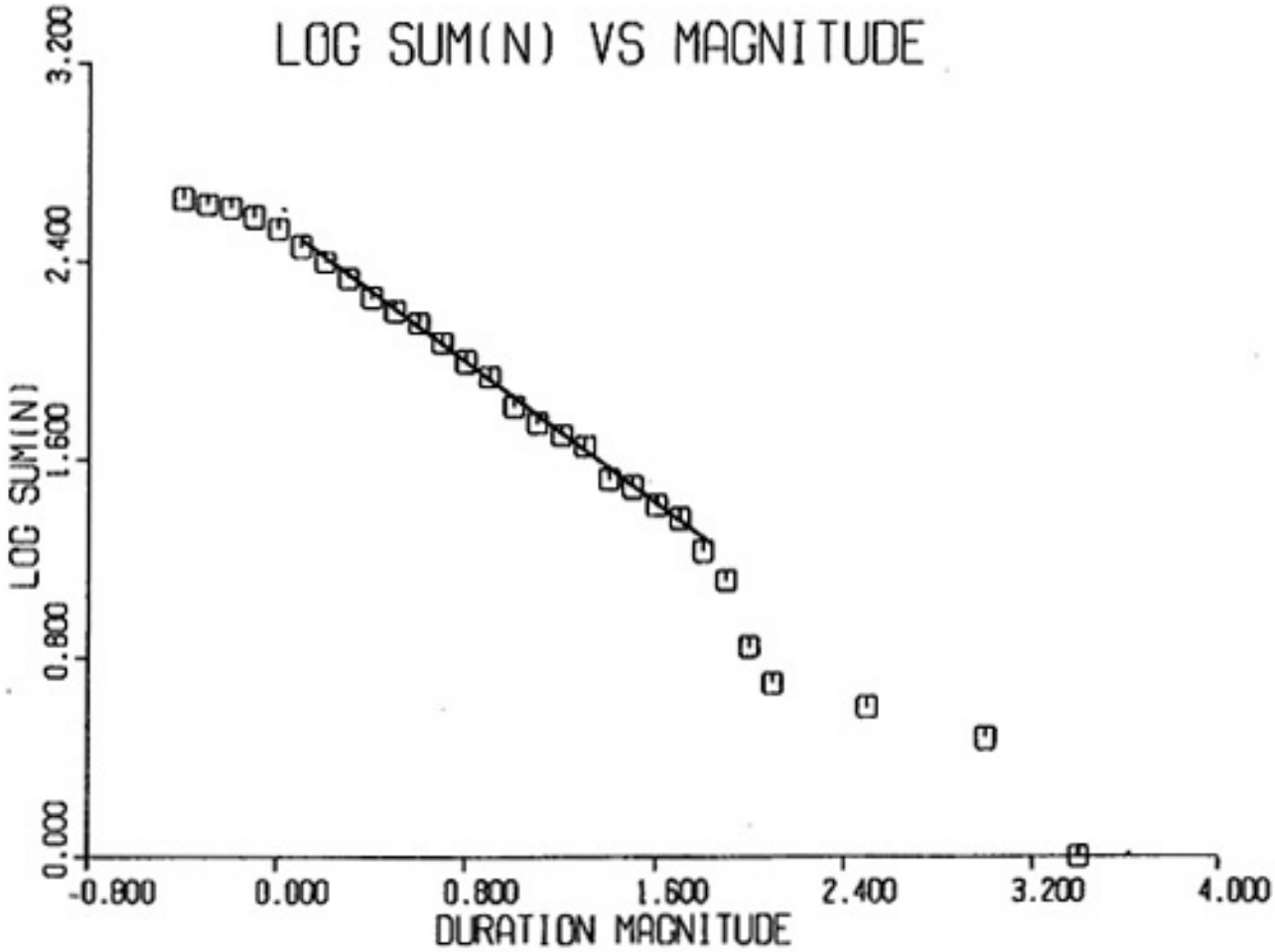

Figure 11(a). Frequency (Log(ΣN)) versus magnitude (M_τ). In the interval from M equal to 0.1 to 1.8, Log(ΣN) = a - bM, where a = 2.55 and b = 0.706 (±0.009).

and b, respectively. b-values calculated from frequency versus magnitude plots for events with depths less than 9.0 km (Figure 11b) and greater than or equal to 9.0 km (Figure 11c) were found to be 0.578 (±0.014) and 0.824 (±0.016), respectively. The calculated b-value found for the entire data set (-0.706) is less than most b-values found previously in the area. For example, Ake (1984) found two b-values for two different swarms to be -0.802 and -0.603; Jarpe (1984) found a b-value of -0.81 for a local earthquake swarm; Jaksha (1983) found a b-value of -0.87 for the events occurring within the geographical area of the Socorro magma body. However, it is known that b-values are heavily data-set dependent and, therefore, a reliable b-value requires that a large data set be obtained over a long time period.

First Modification of Data Set

In the effort to better define the upper and lower bounds of the seismogenic zone, events shallower than 4 km and deeper than 12 km were relocated. The location procedure involved a timing of P and S arrivals from the appropriate records, unbiased by the formerly picked arrivals. Reflections from the mid-crustal magma body were also used as a depth constraint when clearly observed on the seismograms. (See Appendix II for examples of S_zS phases, and their use in calculating depths.)

The combined data sets initially contained only 17 events

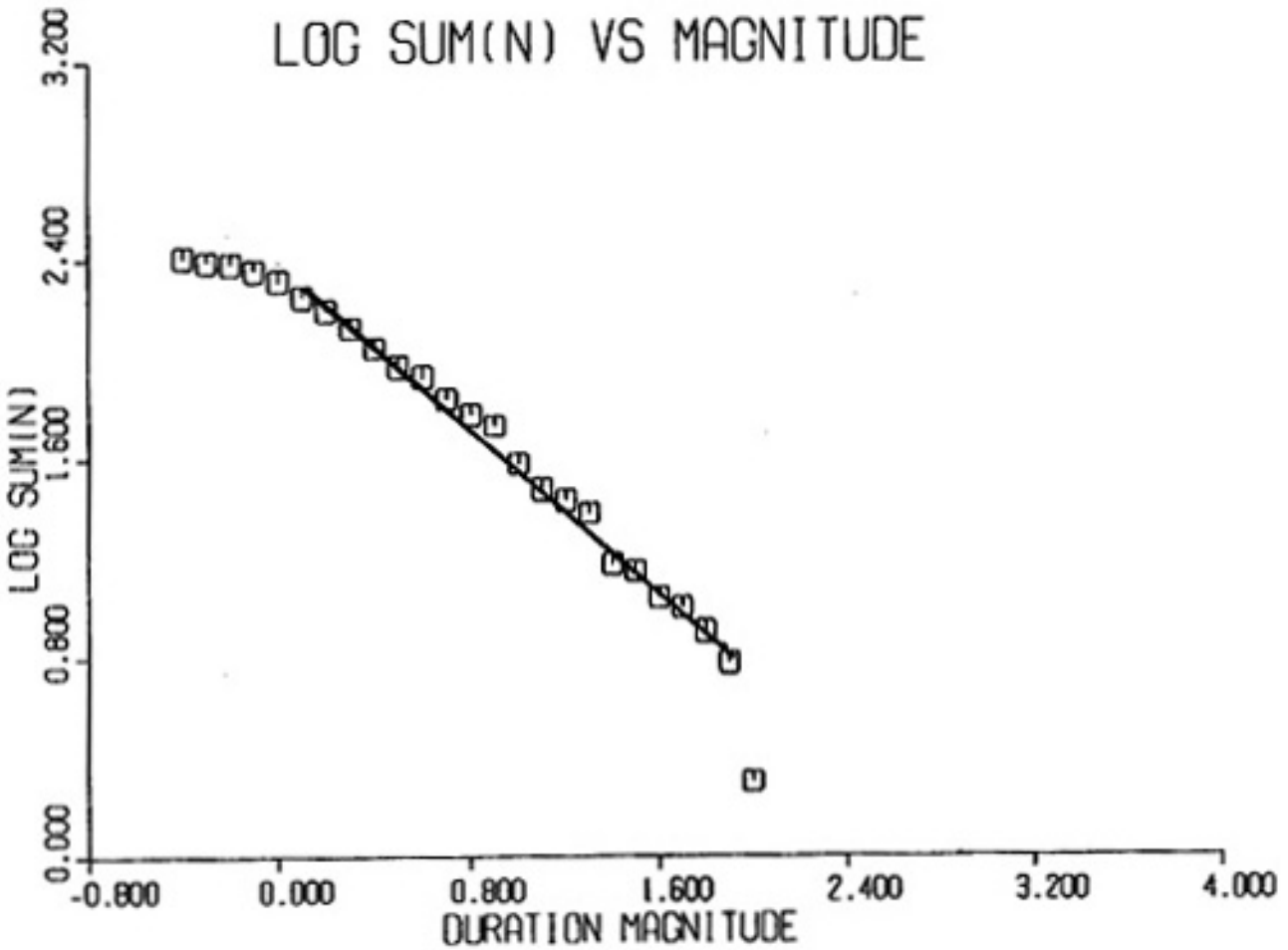

Figure 11(b). Frequency (Log(ΣN)) versus magnitude (M_τ). For depths less than 9.0 km: Log(ΣN)= a - bM, where a = 2.07 and b = 0.578 (±0.014).

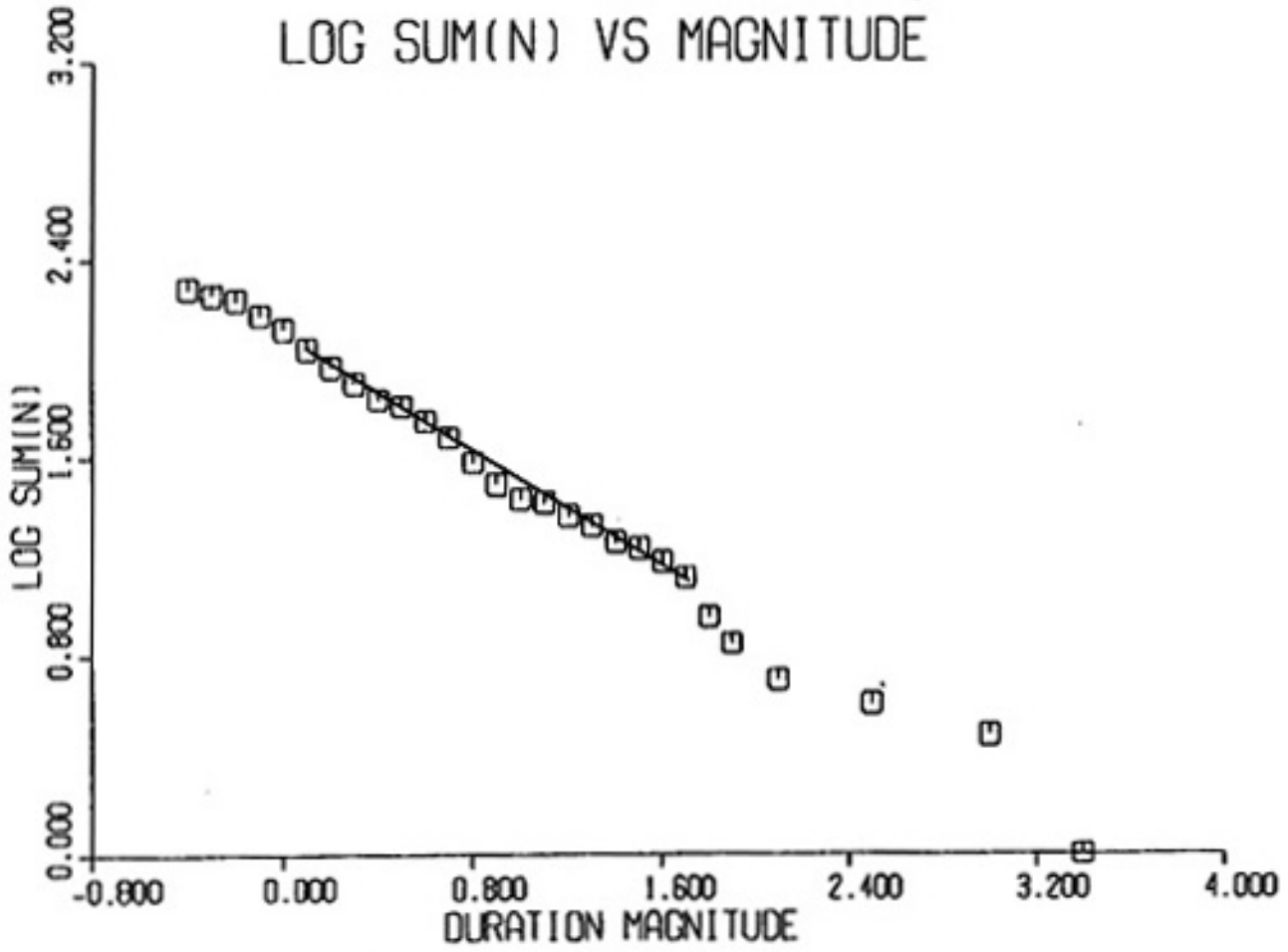

Figure 11(c). Frequency (Log(ΣN)) versus magnitude (M_τ). For depths greater than 9.0 km: Log(ΣN)= a - bM, where a = 2.39 and b = 0.824 (±0.016).

with depths shallower than 4 km and 46 events deeper than 12 km. After relocating, only 8 of the 17 shallow earthquakes retained B quality status; 6 of those remained at depths less than 4 km, but none shallower than 2 km. For the deep earthquakes, 17 of the 46 relocated events retained B quality solutions, but with only 2 focal depths greater than 12 km. Of these two, one was located well beyond the confines of the local array, so that its depth is believed to be poorly constrained despite its B rating. The other event was found to have a depth of 12.39 km.

The data set was further modified by removal of explosions (2), events outside the confines of the central network, and events with solution qualities (Q) equal to B due to a QS/QD = C/A, because, for this case, ERZ > 5.0 km. Epicentral and depth distributions for this modified data set, consisting of 676 events, are shown in Figures 12 and 13, respectively. Of particular tectonic significance is the fact that there is a very sharp dropoff in hypocenters at 12 km.

Seismicity and Geologic Features

Depth distributions were found for (1) the regions north and south of the Socorro shear zone (the Morenci lineament), (2) the central Rio Grande valley region and (3) the region within the confines of the caldera complex to the south of Socorro. These distributions were made in the attempt to determine any significant or anomalous relations between those features and focal depths.

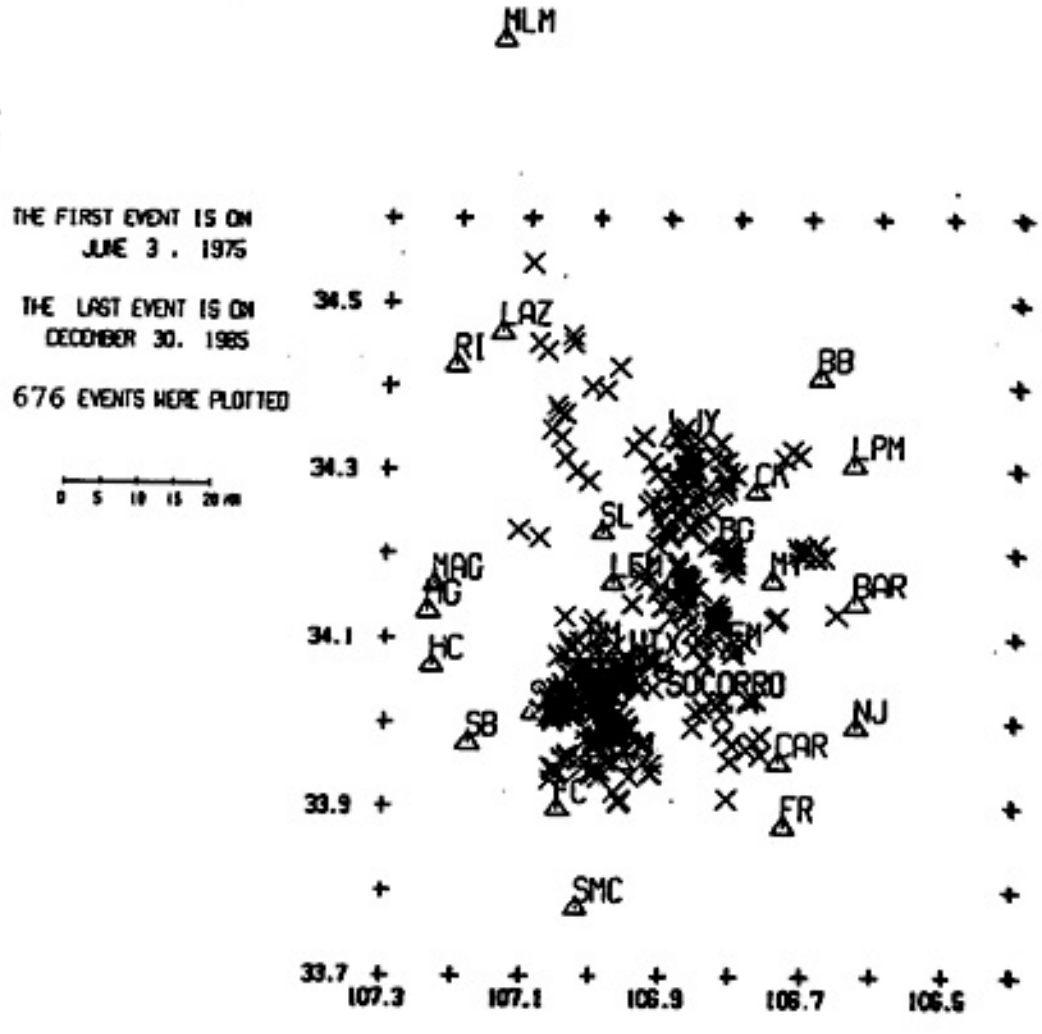

Figure 12. Epicenter distribution of 676 (QS=) A and B-quality events.

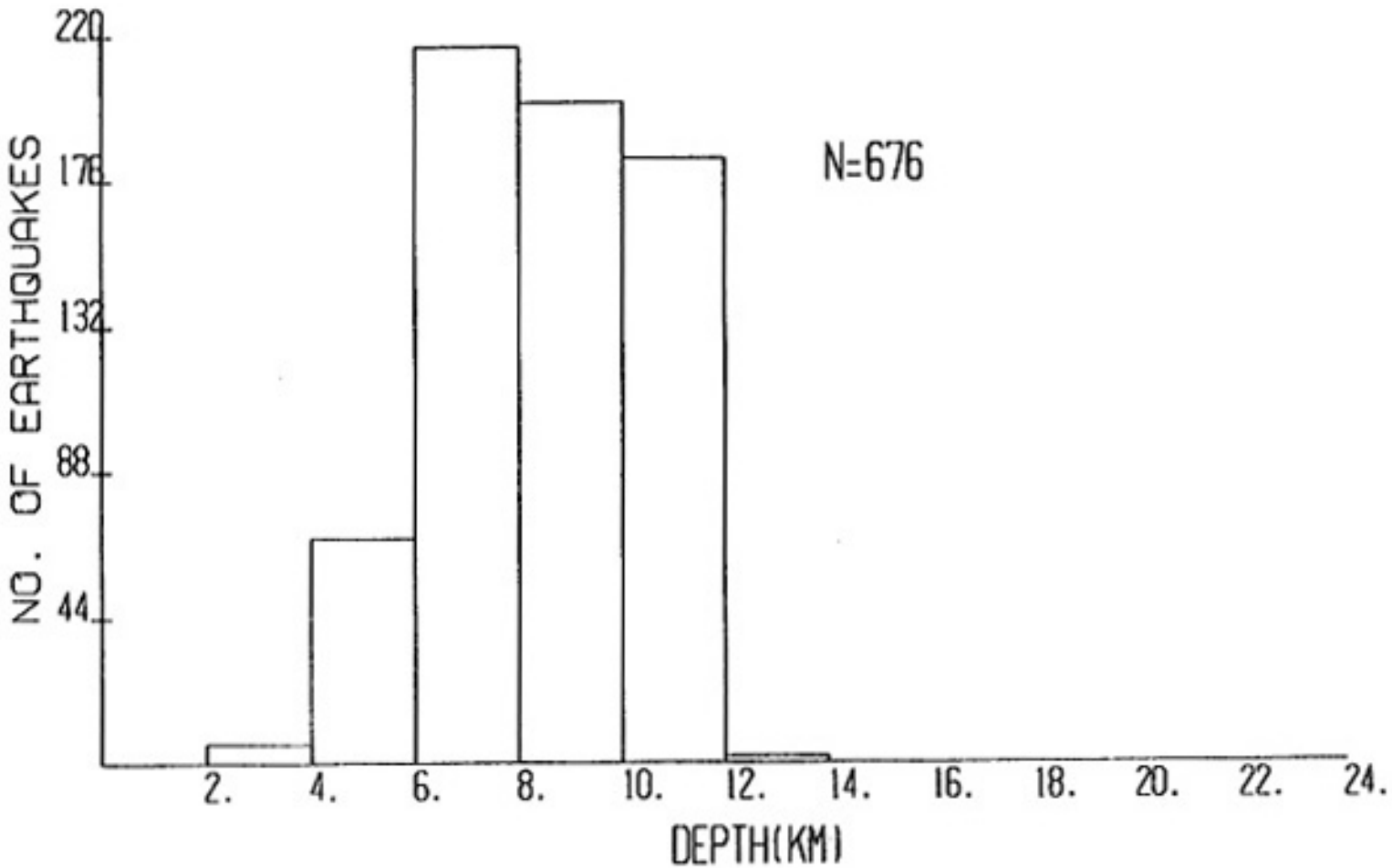

Figure 13. Depth distribution of 676 events shown in Figure 12 (QS- A and B-quality events).

The depths of foci north of the Morenci shear zone (Figure 14) does not vary significantly from the distribution found for the entire area. Clearly, most of the hypocenters were located between 6 and 12 km, with a very sharp drop off at 12 km. For the region south of the Socorro shear zone (Figure 15), the distribution is, again, similar to that for the entire Socorro area, but with fewer focal depths between 10 and 12 km.

Depth distributions were found for a circular region with a radius equal to 10.0 km (Figure 16), centered in the Socorro caldera complex (33.978°, 106.979°). The distribution shows that the largest number of events occurs between 8 and 10 km and, again, drops off sharply at 12.0 km.

Lastly, the depth distribution for the region bounded by the uncertain faults located in the central portion of the network just east of station LEM, (from latitudes 34.1° to 34.35° and longitudes 106.85° to 106.95°) shows an asymmetric distribution with earthquake depths located predominantly between 4 and 8 km (Figure 17). Compared to the distribution for the entire region, the decrease in hypocenters below depths of 8 km appears anomalous. In order to determine whether the hypocentral locations might suggest activity along fault planes, two cross sections across the rift were made (Figure 18), one in the south (Lat.=34.15°) and one in the north (Lat.=34.3°). Hypocenters within ±5 km of the vertical cross section plane were projected onto the plane along a line normal to it. The resulting sections show a cluster of activity at depths from 4 to 8 km and again, particularly in the northern cross section, between 10 and 12 km.

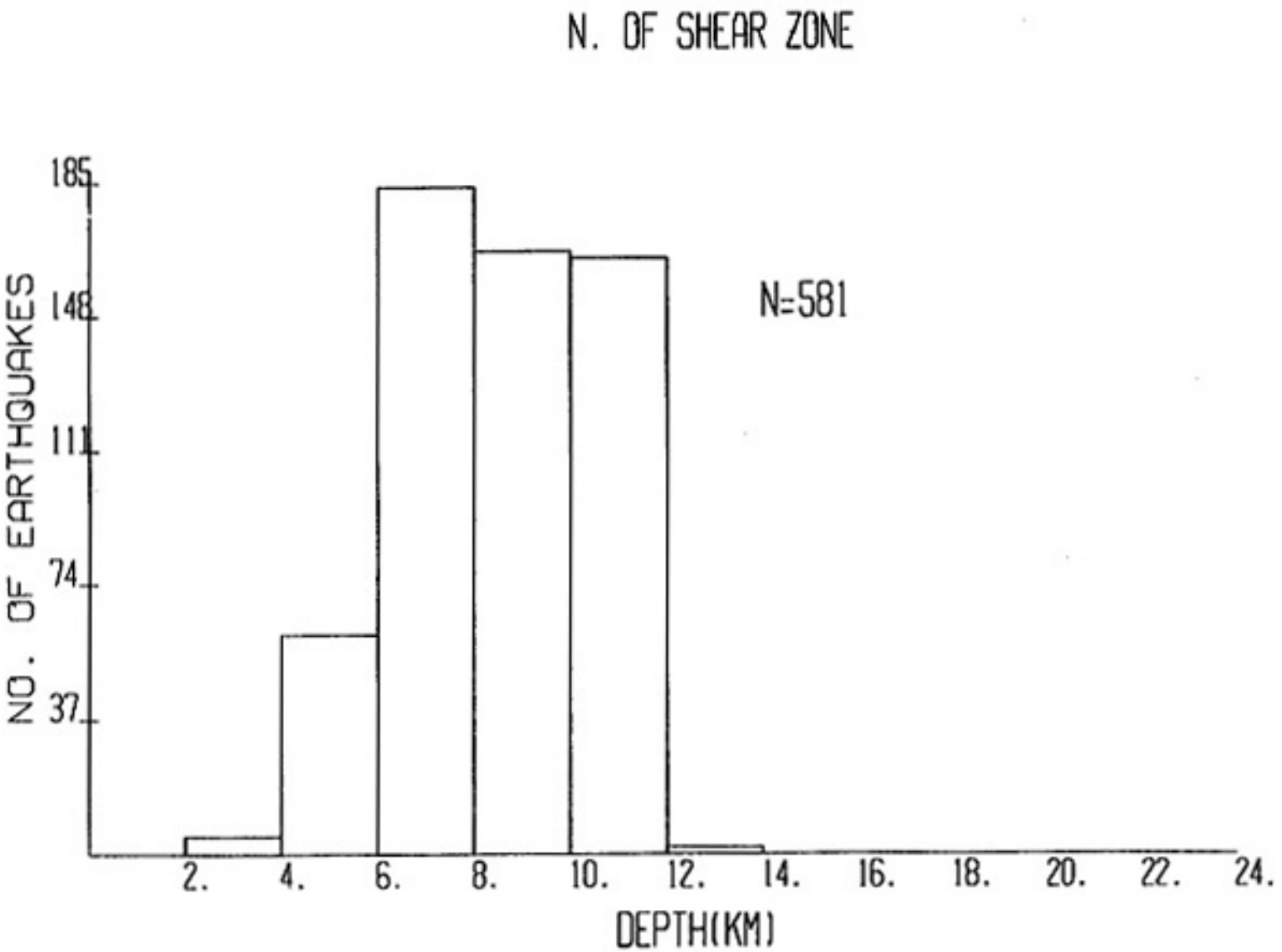

Figure 14. Depth distribution of events north of the Socorro transverse shear zone (QS- A and B-quality events).

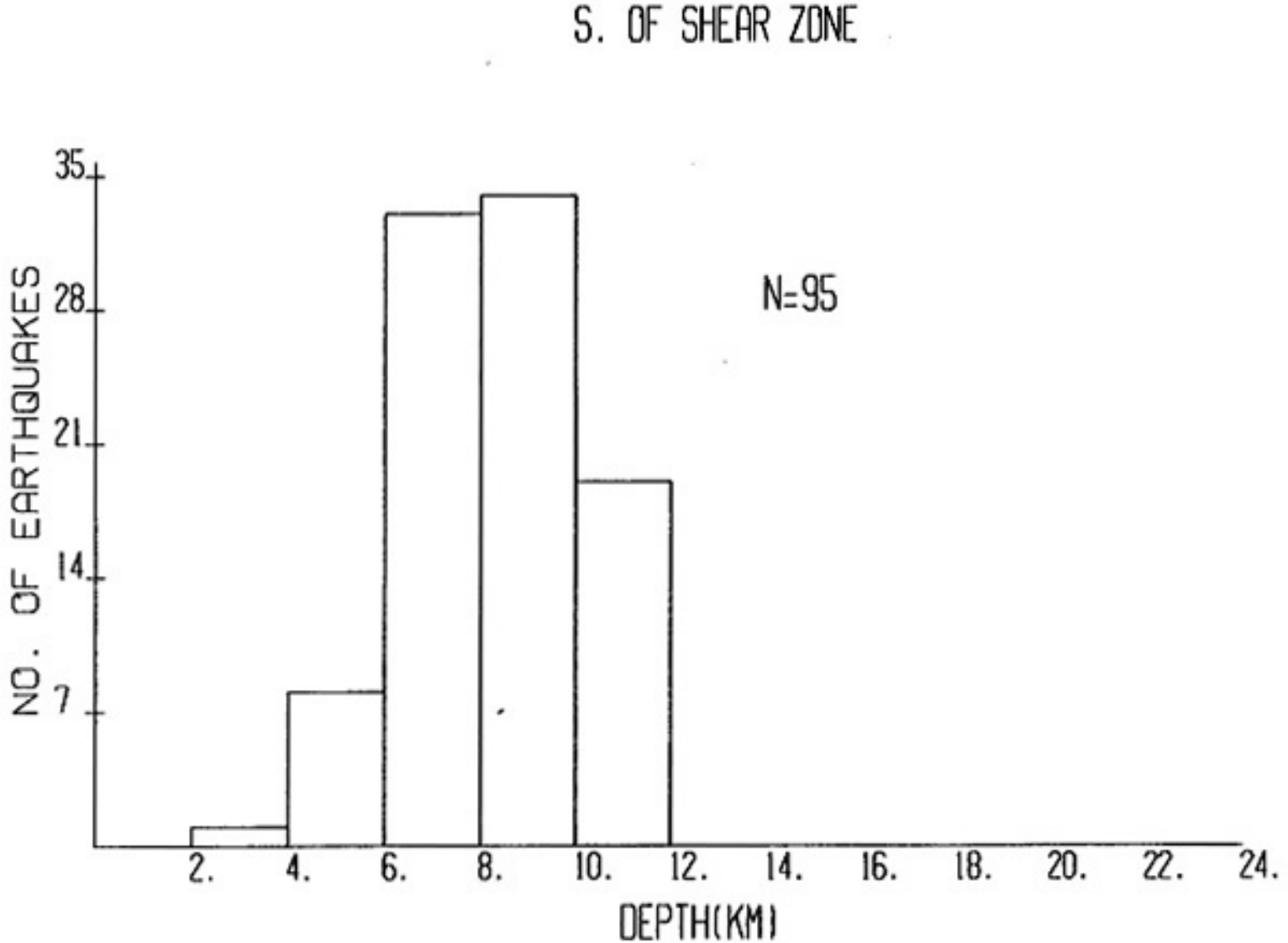

Figure 15. Depth distribution of events south of the Socorro transverse shear zone (QS= A and B-quality events).

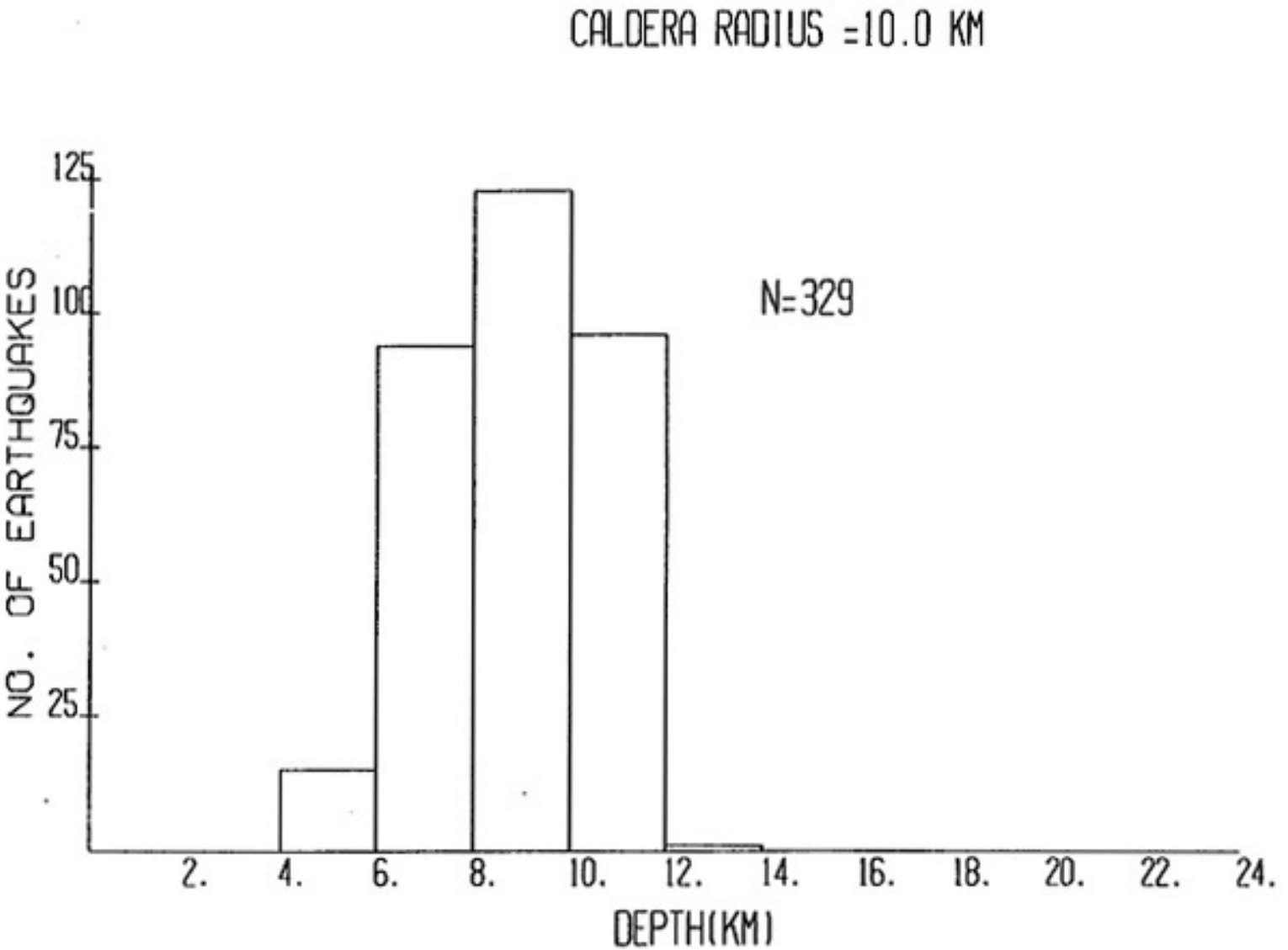

Figure 16. Depth distribution for a circular region with 10 km radius centered in the caldera complex (Lat-N = 33.978° and Long-W = 106.979°), south of Socorro (QS= A and B-quality events).

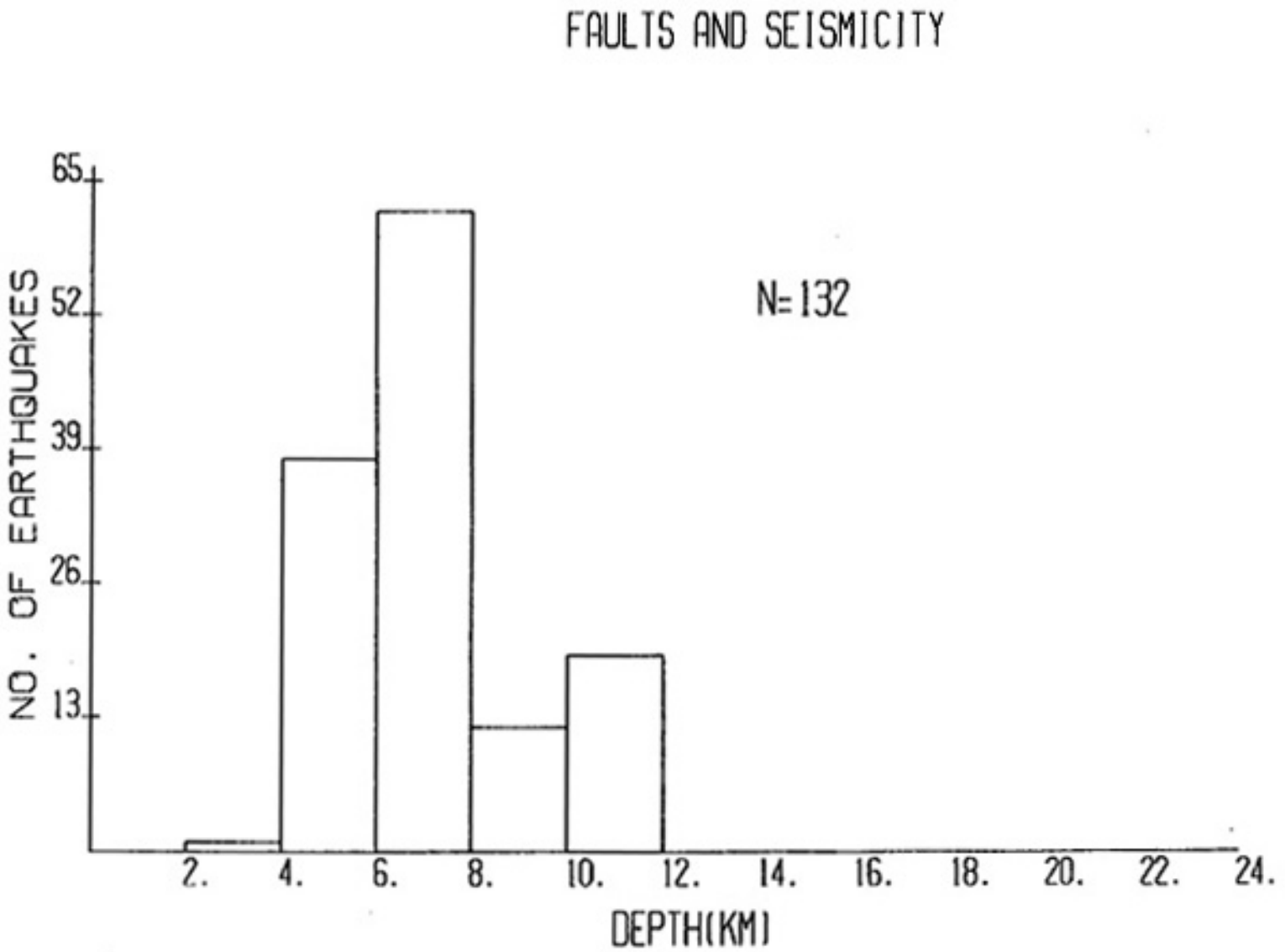

Figure 17. Depth distribution of QS- A and B quality events between bounding rift faults, from latitudes 34.1° to 34.35° and from longitudes 106.85° to 106.95° (see Figure 3).

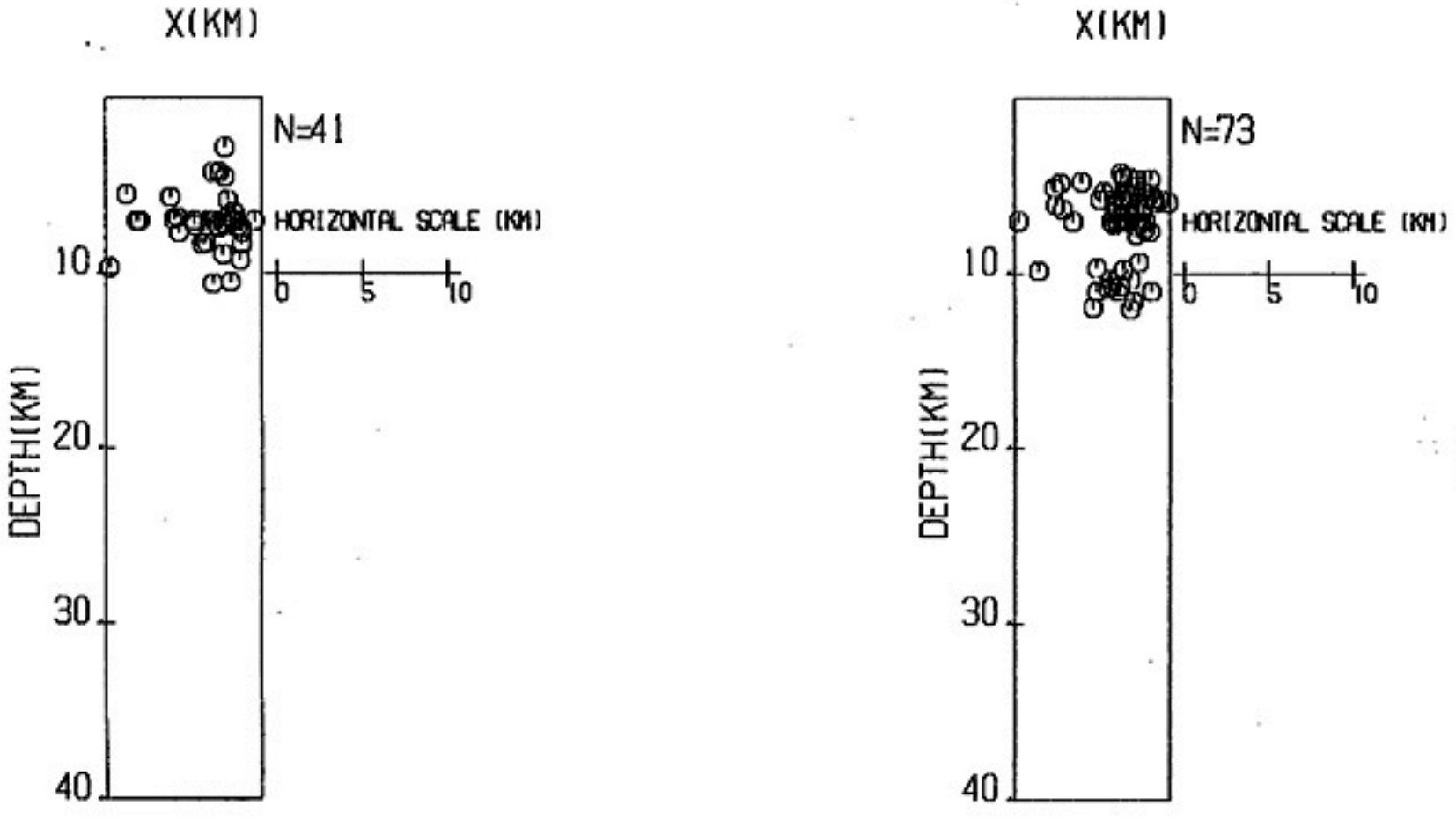

Figure 18. Cross section profiles (width=10 km) across the Rio Grande rift at (1) latitude 34.15° (left) and (2) latitude 34.3° (right) between the bounding faults of the inner graben (no vertical exaggeration).

The seismic activity does not seem to be associated with any extensive planar surfaces.

Depth Distributions and Cross Sections

In order to compare focal depth distributions within the network, a grid was established which divided the major zones of seismicity into sixteen regions (Figure 19). In zones of high seismicity smaller regions were used, and in zones of widely distributed activity larger regions were utilized. The depth distributions for these specific regions are shown in Figures 20 (a-d).

One interesting feature of these distributions can best be viewed by a profile which runs very close to the centers of swarms in regions 14, 10, 7, and 16 moving from the southwest to the northeast. The depth distributions for the regions 10, 7, and 16, are bimodal with peaks between 6 and 8 km and 10 and 12 km (Figure 21). A physical reason for this decrease in activity between 8 and 10 km is the possibility of a ductile layer sandwiched between more brittle crust above and below.

A cross section running from south to north through regions 6, 4, and 2 respectively, has the depth distributions given in Figure 22. In region 6, foci are concentrated in the depth interval 6-8 km, whereas in region 2, they occur predominantly from 4 to 8 km. Between these two regions, the distribution of focal depths is bimodal with peaks at 6-8 km and 10-12 km.

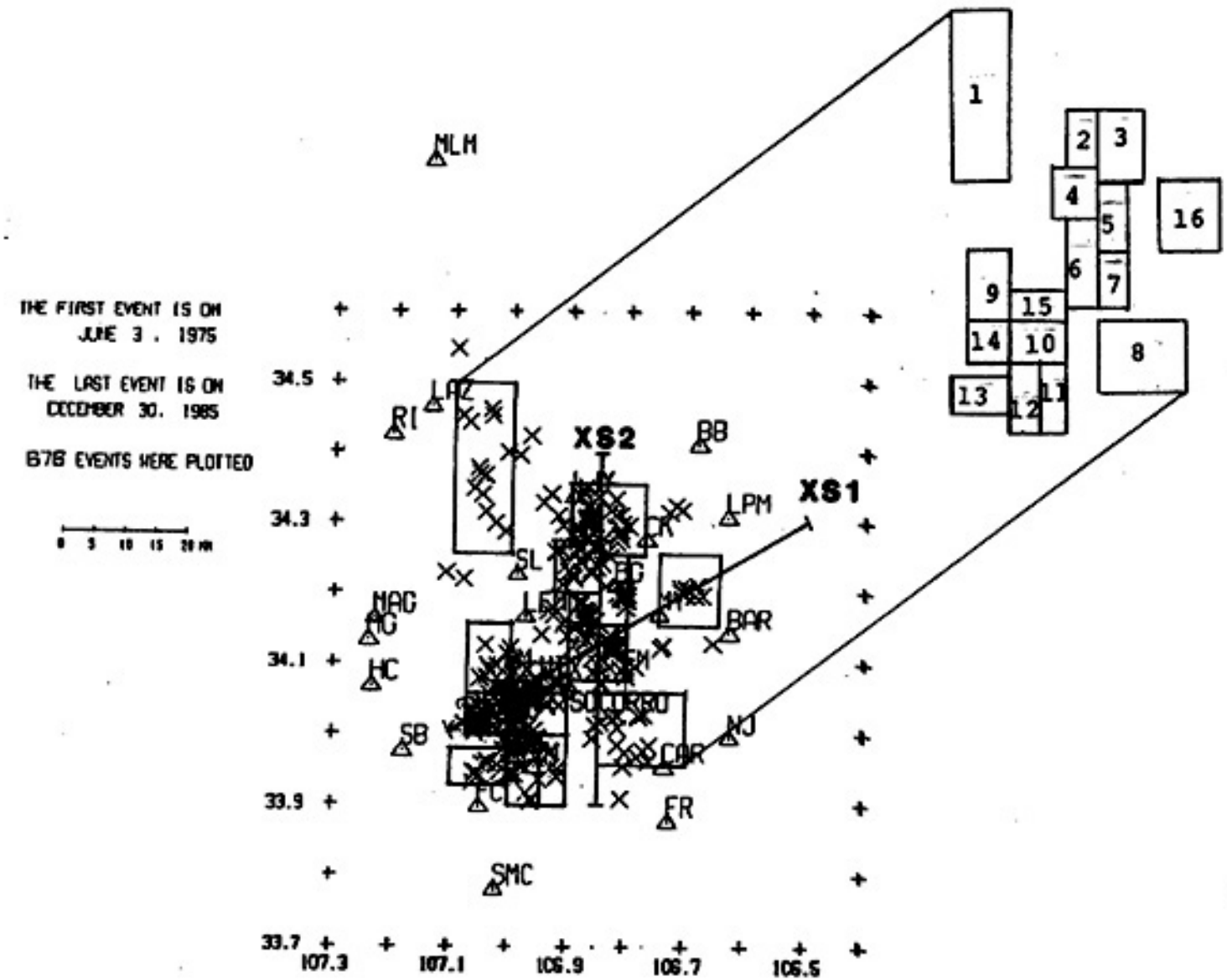

Figure 19. Location of regions used to compare focal depth distributions. Position of cross section lines XS1 and XS2 are also shown.

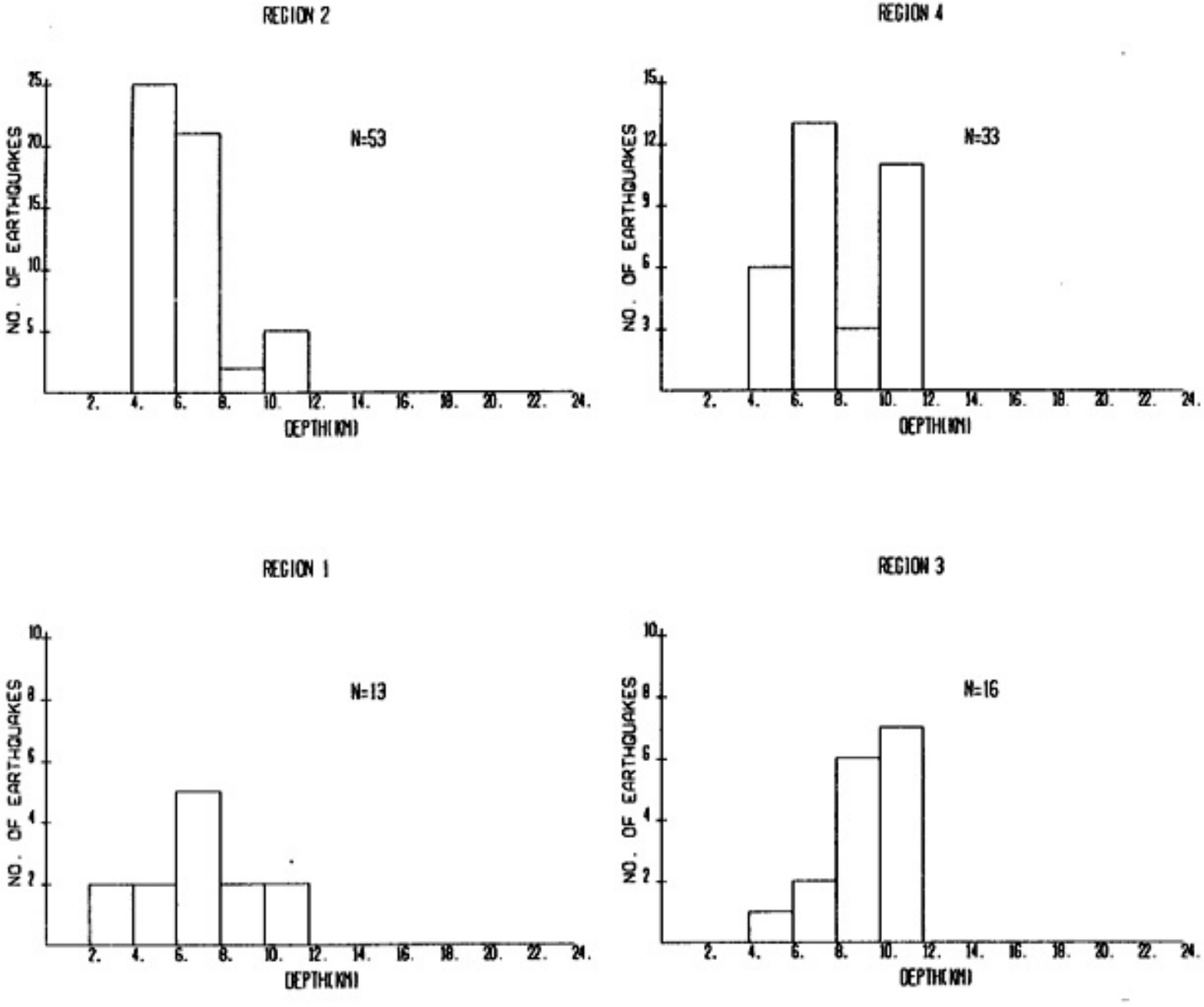

Figure 20(a). Distribution of focal depths within regions 1-4 shown in Figure 19.

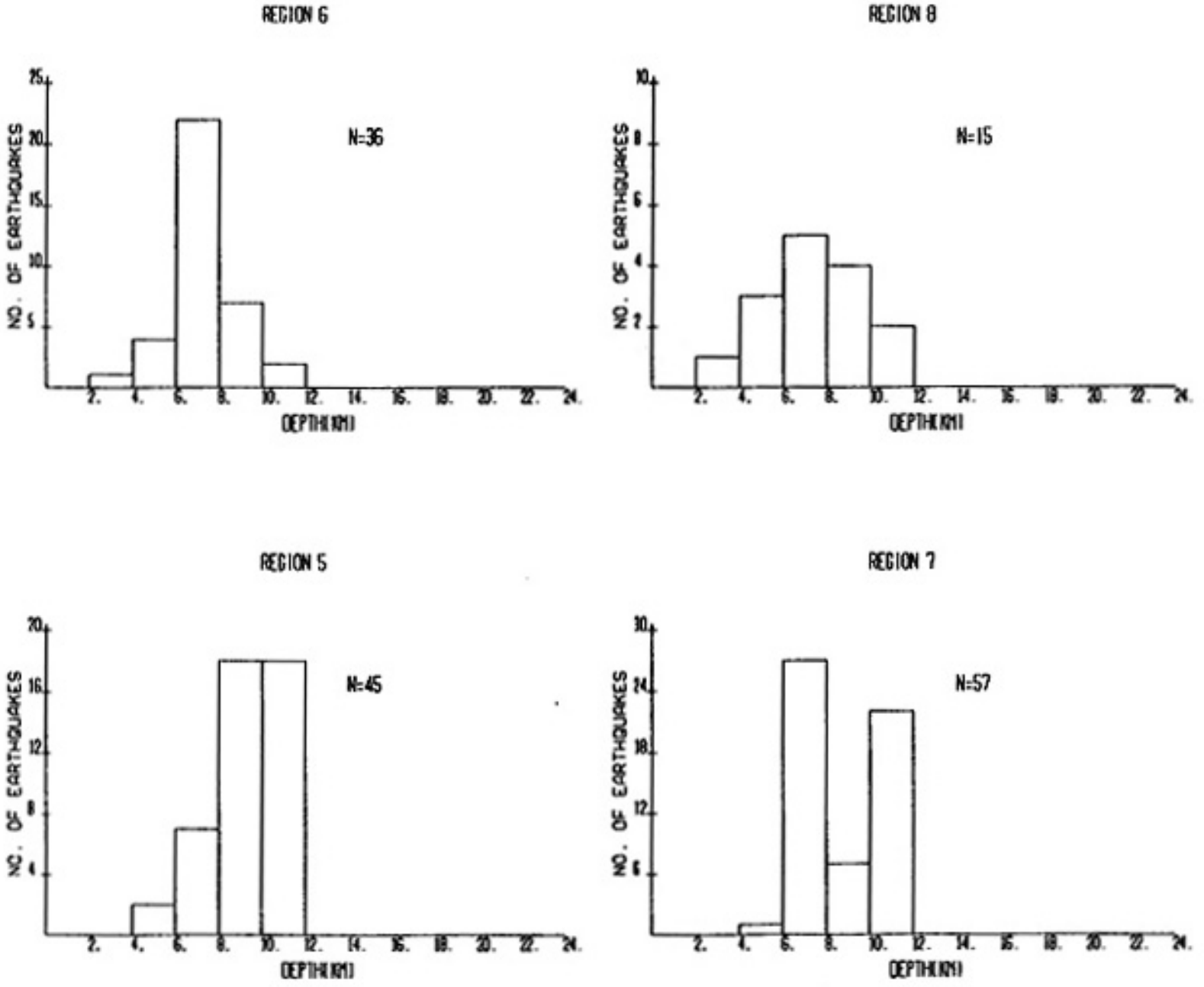

Figure 20(b). Distribution of focal depths within regions 5-8 shown in Figure 19.

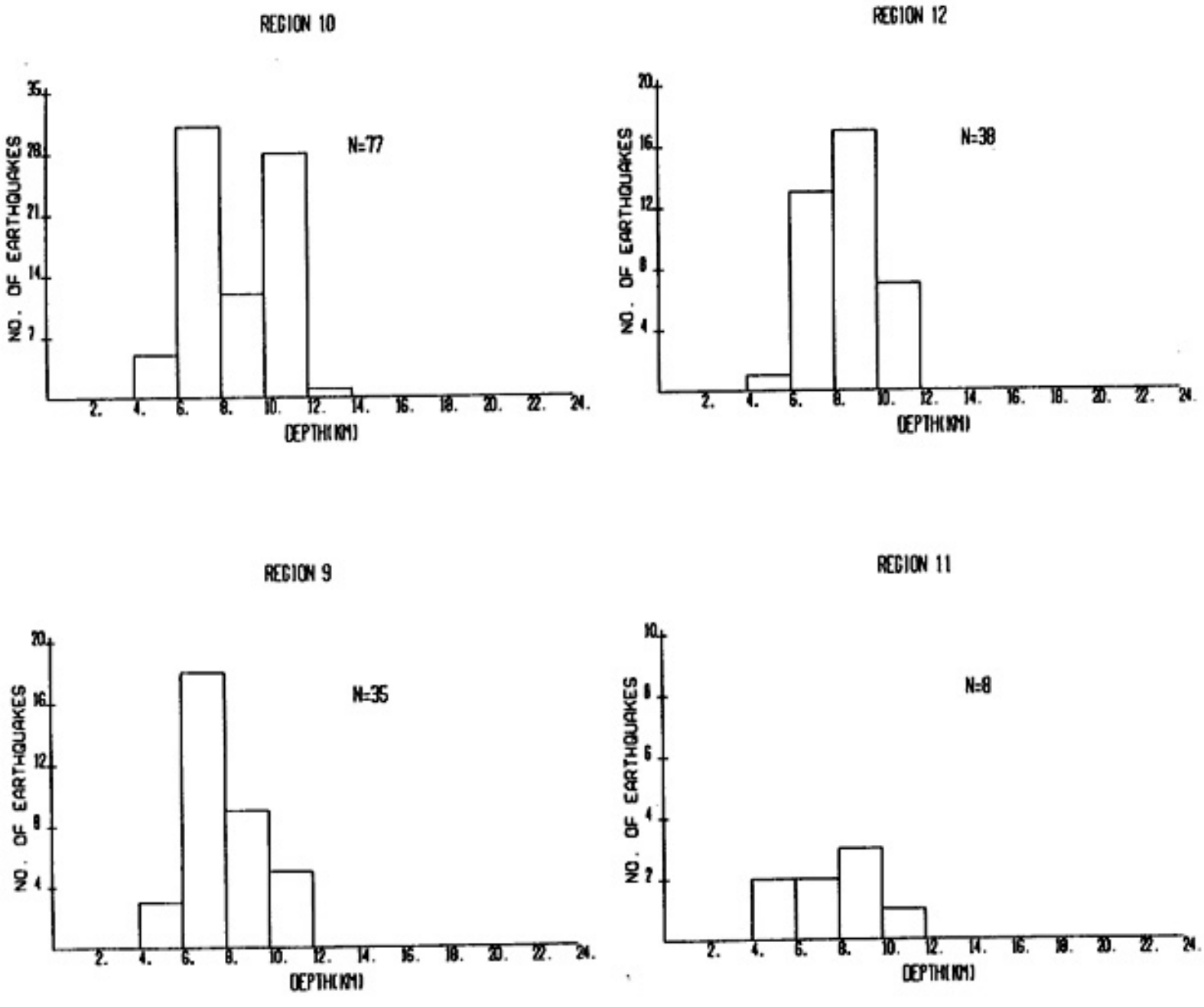

Figure 20(c). Distribution of focal depths within regions 9-12 shown in Figure 19.

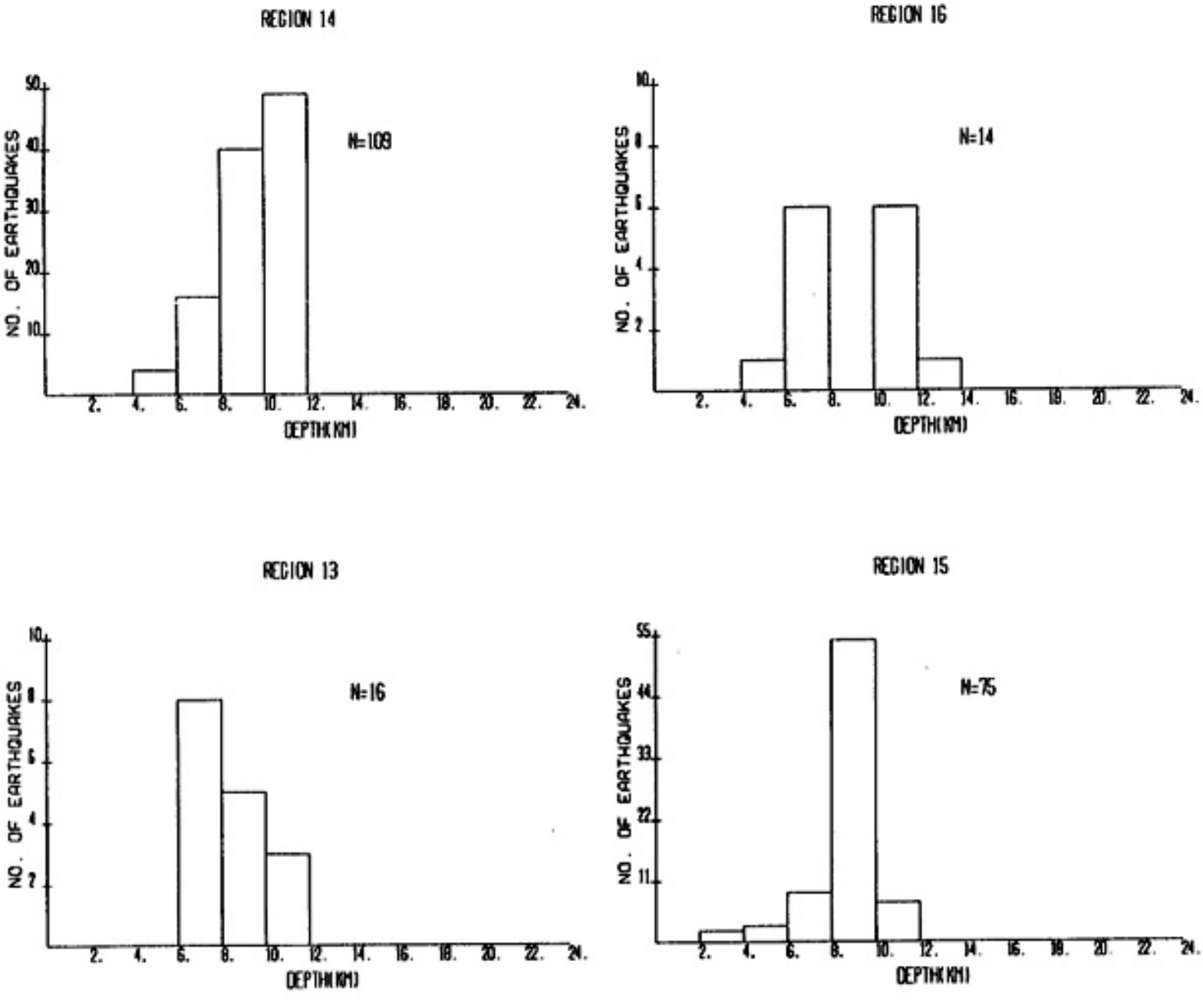

Figure 20(d). Distribution of focal depths within regions 13-16 shown in Figure 19.

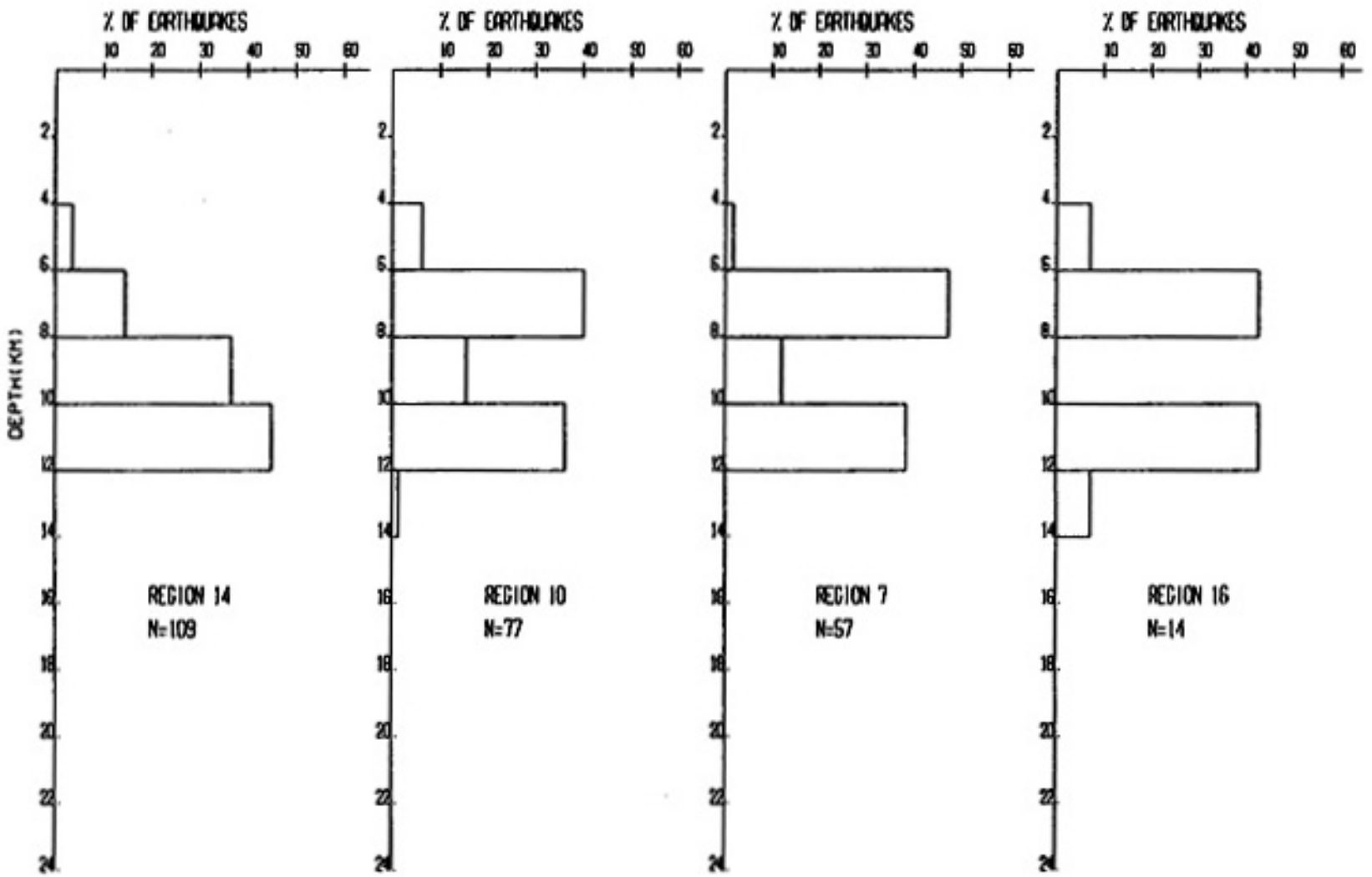

Figure 21. Depth distributions (based on percentage of events within each region) along a line running across regions 14, 10, 7 and 16, from the southwest to the northeast (see Figure 19). Note the drop in the number of events between 8 and 10 km in regions 10, 7 and 16.

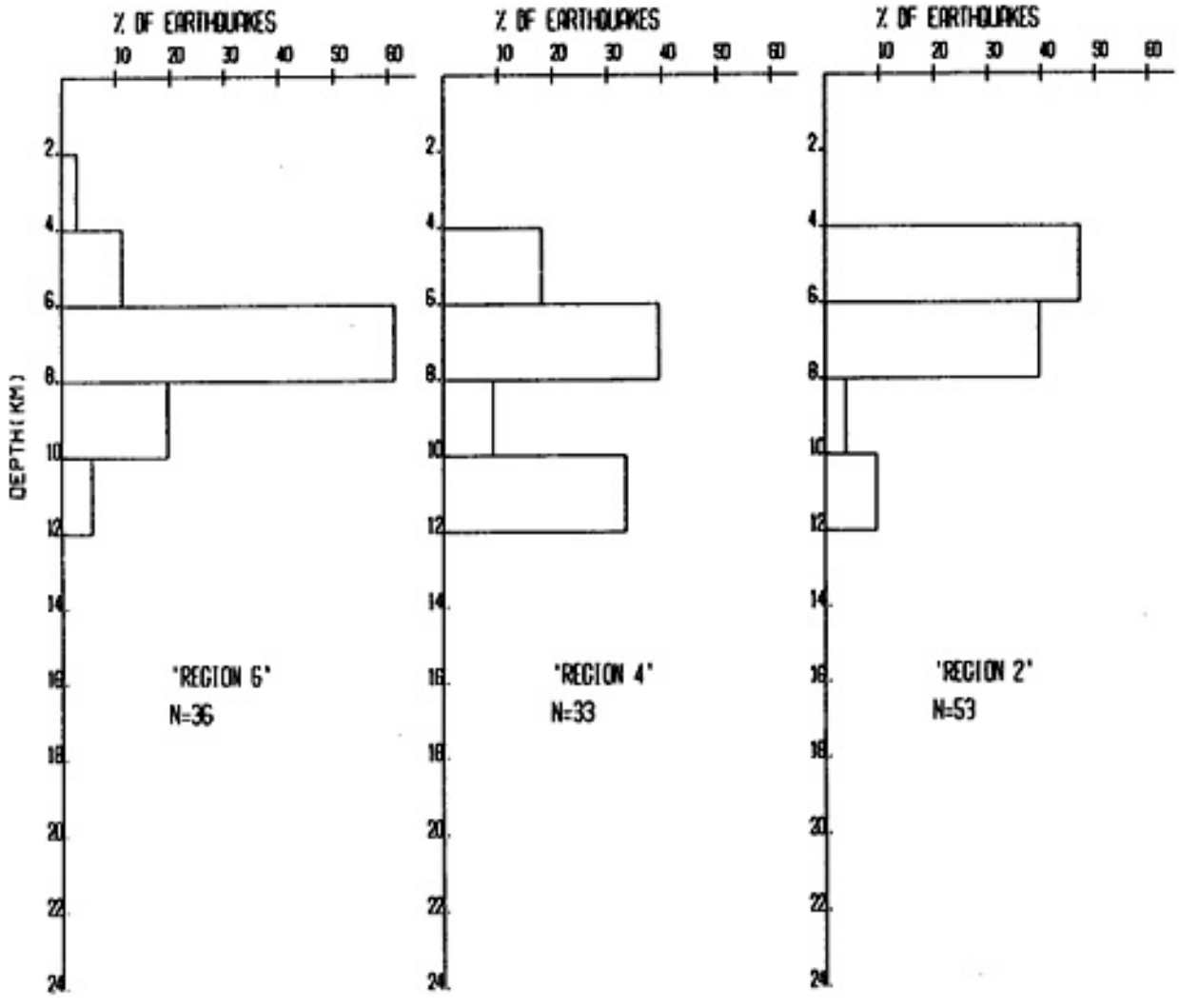

Figure 22. Depth distributions along a line running across regions 6, 4, and 2, from south to north.

A third line from south to north crosses region 8, 7, 5, and 3, respectively (Figure 23). Again the bimodal distribution in region 7 is very different from the distributions to the north and south.

Two cross-sections, one from the southwest to the northeast, XS1, and one from the south to the north, XS2, (see Figure 19 for locations), are shown in Figures 24 and 25 with no vertical exaggeration. Hypocentral depths were projected onto the cross section plane from perpendicular distances within +2.5 km.

Errors in Focal Depths

The cross sections shown in Figures 24 and 25 reveal several interesting features. First, several regions display pillar-like clusters of foci. Secondly, there is an inordinate number of hypocenters with depths of exactly 7.0 km. Some events comprising the seismic pillar observed in Figure 25 (XS2) were analyzed in order to determine whether vertical extension of foci was caused by uncertainty of focal depths. The pillar consists almost entirely of events occurring in a September, 1985 swarm. Fifteen of a total of 45 events, both shallow and deep, were relocated by an experienced reader of seismograms. Of the three shallowest events, only one event maintained a B quality solution. Its depth increased from 6.27 to 7.0 km. The remaining 12 events retained B quality status.

For 6 of the 15 events, S_zS phases were observed at station

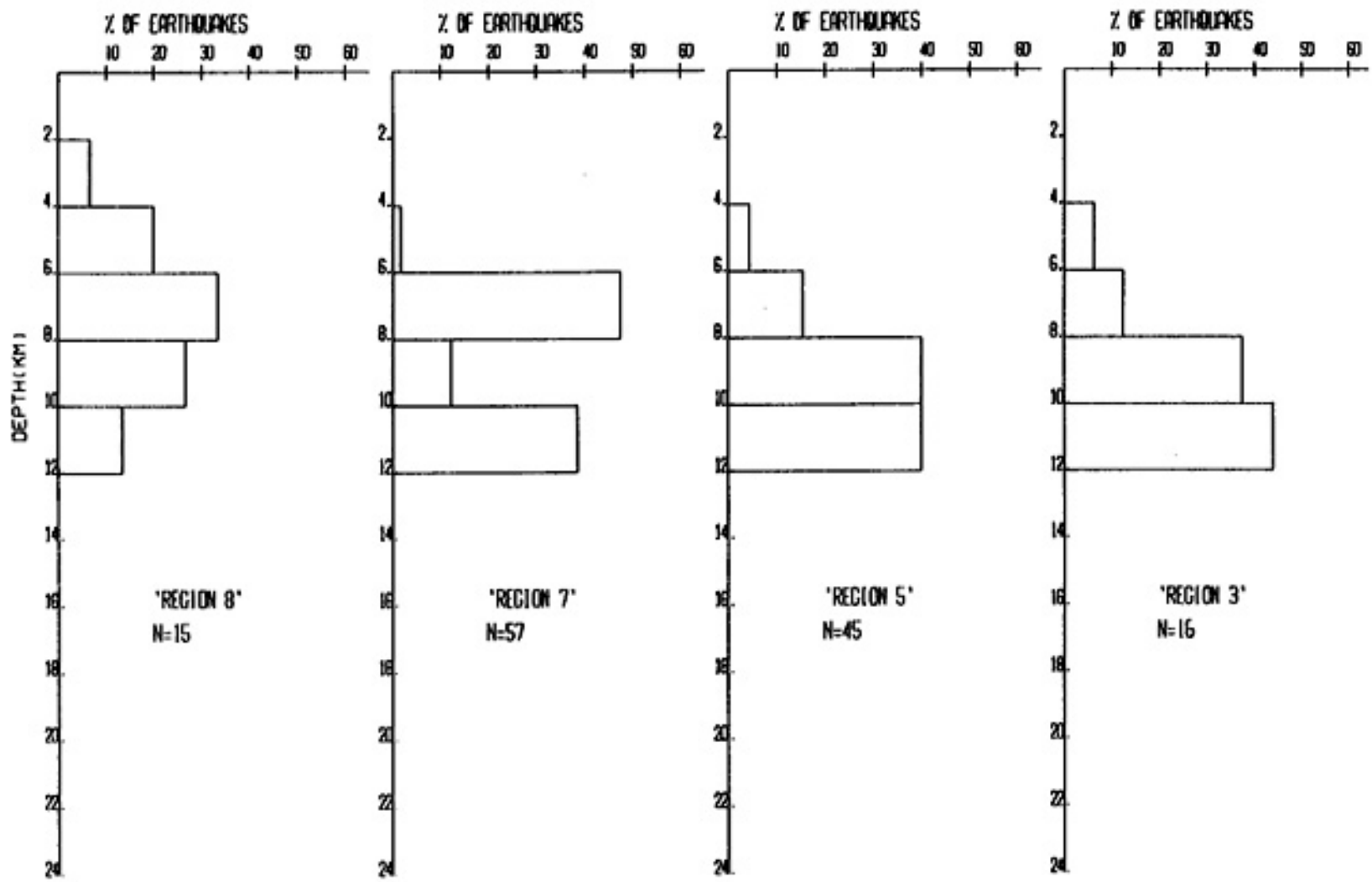

Figure 23. Depth distributions along a line running across regions 8, 7, 5 and 3, from south to north.

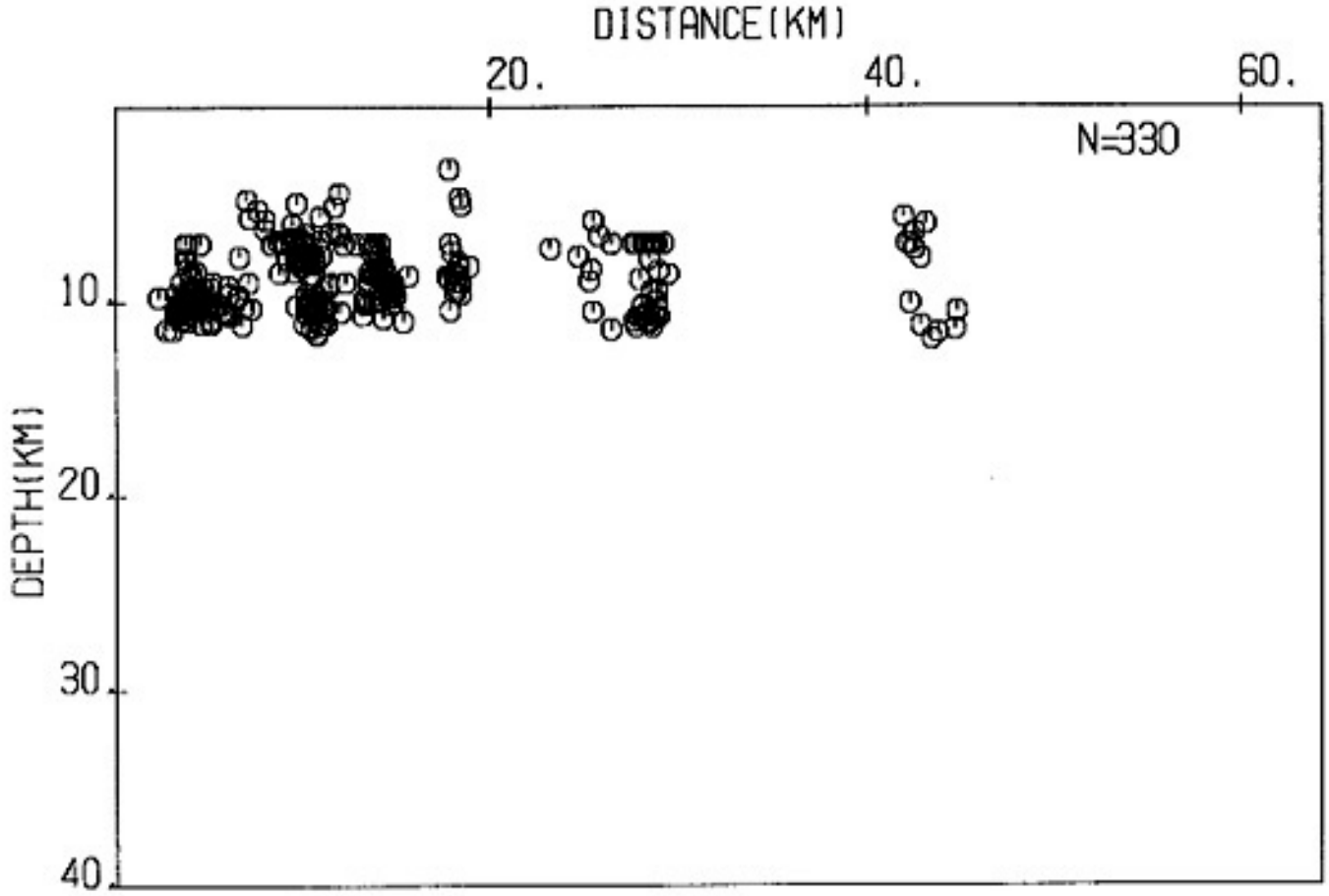

Figure 24. Cross section profile (XS1) from the southwest, near station SB, to the northeast, south of station LPM, (see Figure 19). Hypocenters within +2.5 km were projected onto the cross section plane.

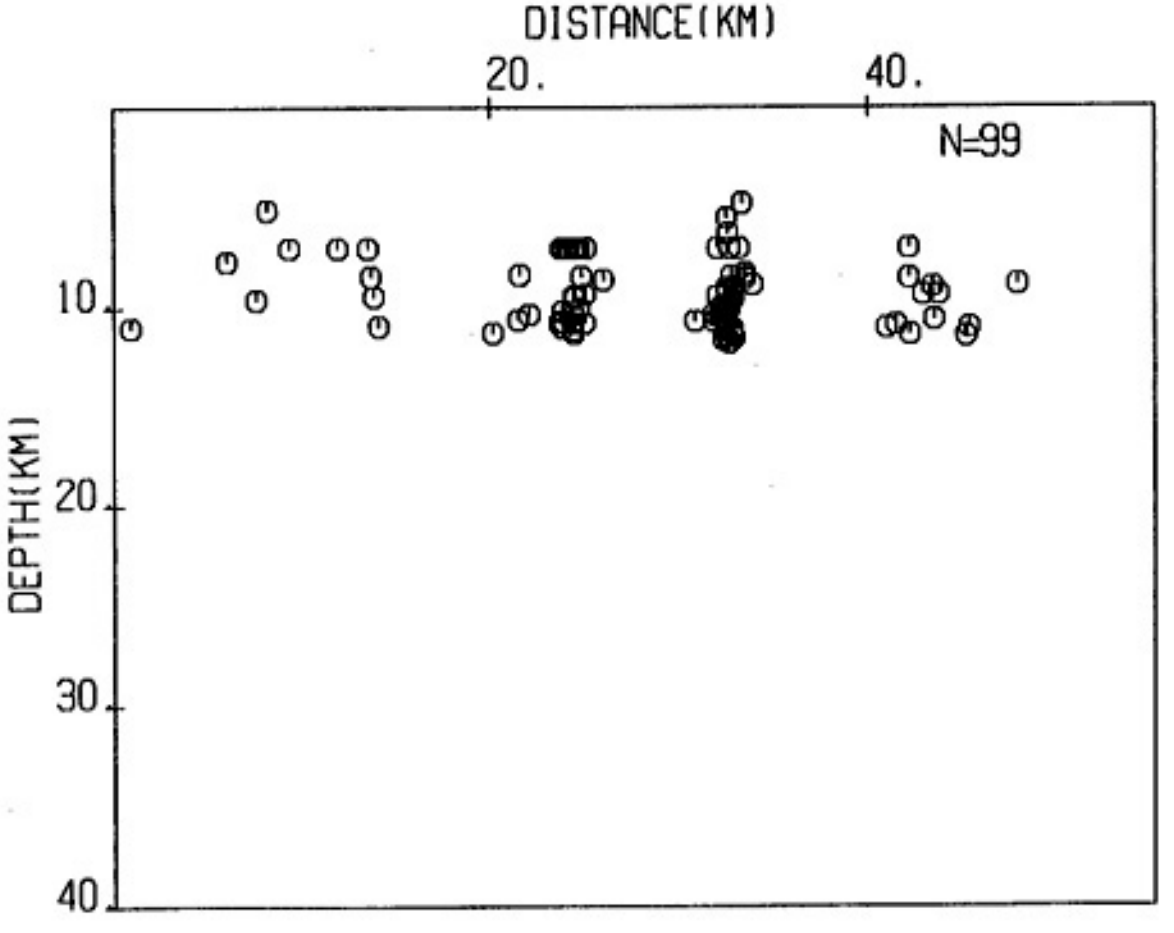

Figure 25. Cross section profile (XS2) from south to north (see Figure 19). Hypocenters within +2.5 km were projected onto the cross section plane.

MAG, and depths were calculated using these reflections. The depths calculated ranged from 7.31 to 9.48 km, with 5 of the 6 ranging from 9.05 to 9.48 km. HYPO71 depths for these 6 earthquakes ranged from 10.50 to 11.96 km. Possible explanations for the discrepancy in the calculated depths are: (1) the velocity of the lower half of the uppercrust, through which the reflected phase must travel, may be lower than the upper half of the upper crust; and/or (2) the depth to the magma body used in the calculation (19.2 km) is too shallow.

In the cross-section profiles (Figures 24 and 25) many events (100) are located exactly at the depth of 7.0 km. This is caused by the HYPO71 parameter, ZTR, which is referred to as the default or test depth. If a solution cannot be constrained to a depth better than the test depth, the value assigned to ZTR is given as the focal depth. For the Socorro area, the test depth entered into HYPO71 is 7.0 km. The epicenter plot (Figure 26) of the 100 events with focal depths equal to 7.0 km displays a scattering of locations throughout the network, indicating that the assignment of this depth is not restricted to one particular area. Also, the ERZ associated with these 100 events (2.17 km ±1.00) is approximately twice that of the ERZ of the remaining events in the data set (1.03 ±0.719 km).

The HYPO71 standard or test depth (ZTR) was varied in order to determine its effect on calculated focal depths. Solutions for the 15 test events were found for each value of the test depth (see Table 1). Nine of the 15 solutions retained qualities QS/QD of A/B for all values of the test depth (3, 5, 7,

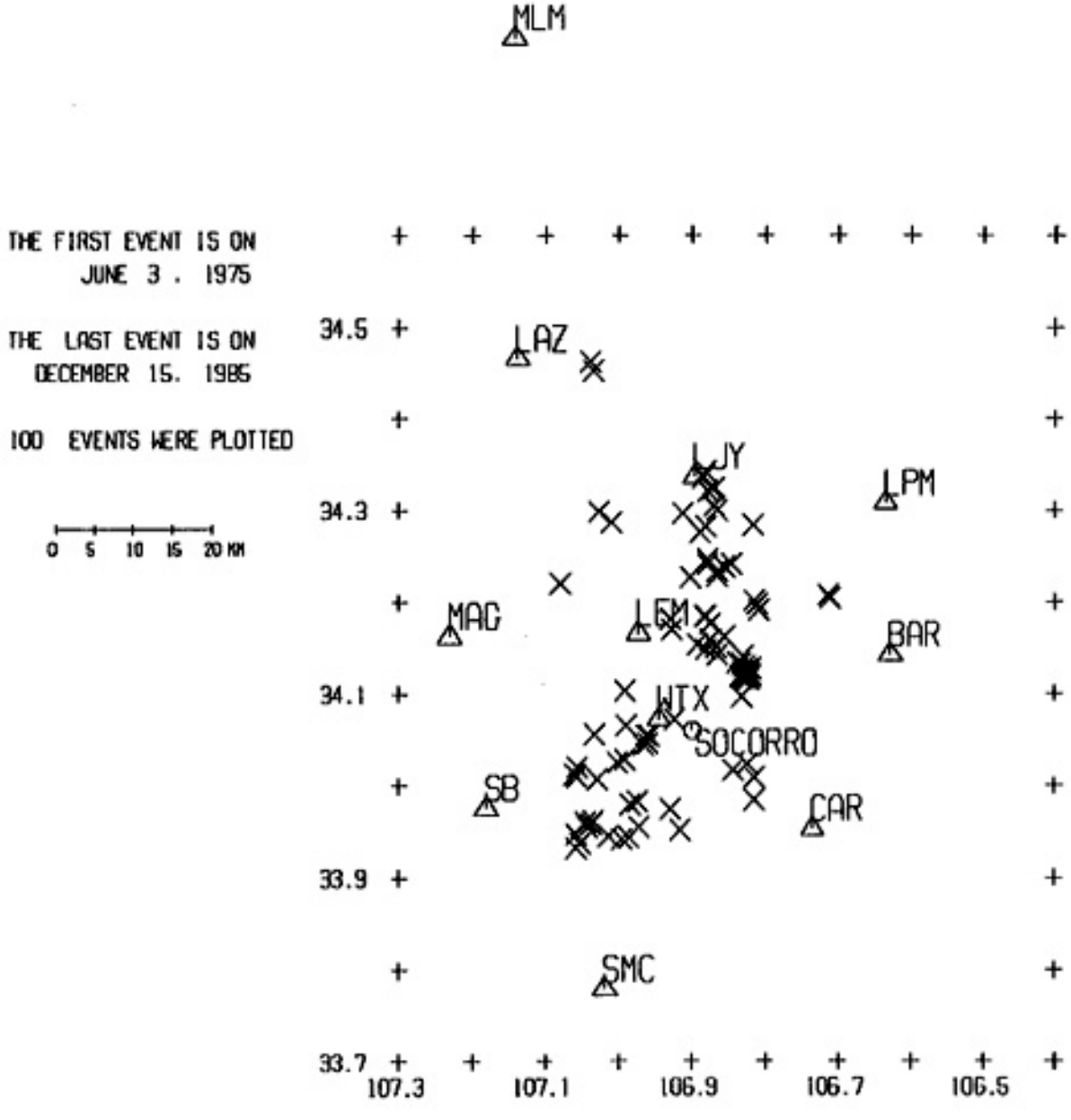

Figure 26. Epicenter distribution for events with focal depths equal to 7.00 km (QS= A and B-quality events).

Table 1. Focal depths as a function of varying HYPO71 test depths.

	ETR: (Test Depth)		3	5	7	9	11	13	
	Date Yr/Mo/Day	OT UT	Depth (OS/QD)	Depth (OS/QD)	Depth (OS/QD)	Depth (OS\QD)	Depth (OS/QD)	Depth (OS/QD)	Range
1	850917	10:36	6.58 (A/C)	5.00 (B/C)	7.00 (A/C)	6.65 (A/C)	6.18 (A/C)	6.07 (A/C)	2.00 km, mixed quality; 0.93 (A/C)
2	"	10:41	7.34 (B/C)	7.45 (B/C)	7.00 (B/C)	6.96 (B/C)	7.28 (B/C)	7.60 (B/C)	0.64 km (B/C)
3	"	11:42	7.55 (B/C)	5.00 (B/C)	7.00 (B/C)	9.00 (B/B)	7.39 (B/C)	8.15 (B/B)	4.00 km, mixed quality
4	"	19:50	8.22 (B/B)	9.53 (B/B)	12.70 (B/B)	12.31 (B/B)	11.00 (B/B)	13.00 (B/B)	4.78 km (B/B)*
5	850918	17:01	10.95 (A/B)	11.65 (A/B)	11.96 (A/B)	11.67 (A/B)	11.00 (A/B)	13.00 (A/B)	2.05 km (A/B)
6	"	18:02	10.66 (A/B)	10.63 (A/B)	10.81 (A/B)	11.29 (A/B)	11.00 (A/B)	11.07 (A/B)	0.66 km (A/B)
7	"	20:23	11.10 (A/B)	11.12 (A/B)	11.92 (A/B)	11.38 (A/B)	11.00 (A/B)	11.59 (A/B)	0.92 km (A/B)
8	850919	02:27	11.67 (A/B)	11.67 (A/B)	10.50 (A/B)	11.43 (A/B)	11.00 (A/B)	11.80 (A/B)	1.30 km (A/B)
9	"	02:57	11.60 (A/B)	11.65 (A/B)	11.66 (A/B)	12.18 (A/B)	11.00 (A/B)	11.74 (A/B)	1.18 km (A/B)
10	"	03:03	10.14 (A/B)	10.10 (A/B)	10.95 (A/B)	10.25 (A/B)	10.24 (A/B)	10.69 (A/B)	0.85 km (A/B)
11	"	09:38	10.88 (A/B)	11.07 (A/B)	11.71 (A/B)	12.15 (A/B)	11.00 (A/B)	12.01 (A/B)	1.27 km (A/B)
12	"	10:05	10.46 (A/B)	10.60 (A/B)	10.82 (A/B)	10.66 (A/B)	11.00 (A/B)	11.01 (A/B)	0.55 km (A/B)
13	850920	14:26	6.76 (A/C)	5.00 (A/C)	7.00 (A/C)	6.66 (A/C)	7.20 (A/C)	6.59 (A/C)	2.20 km (A/C)
14	"	14:37	9.58 (B/B)	10.55 (A/B)	11.06 (A/B)	9.00 (B/B)	11.00 (A/B)	10.58 (A/B)	2.06 km, mixed quality; 0.51 (A/C)
15	"	16:20	9.05 (A/B)	9.26 (A/B)	9.45 (A/B)	9.00 (A/B)	9.34 (A/B)	9.79 (A/B)	0.79 km (A/B)

$\text{Range}_{\text{ave}}$ (A/B) = 1.063 (± 0.455) km

9, 11, and 13 km). The largest depth range among these nine events was 2.05 km, and the mean depth range for these nine events was found to be 1.063 (±0.455) km. Three events were found to have solutions of mixed (QS/QD) quality and three events had the qualities A/C, B/B and B/C. The range in depths as a function of the varying test depths was 2.20 km for the A/C event, and 4.78 km for the B/B event. From these tests it was determined that events with statistical quality QS=B would have to be dropped from the data set in order to obtain an accurate view of the focal distributions.

Final Data Set

After eliminating all events with QS/QD qualities B/A and B/B, the final data set consisted of 513 well located events. The average ERH and ERZ for these events are 0.40 (± 0.155) km and 0.84 (± 1.871) km, respectively. Figures 27 and 28 display the epicenter and depth distributions, respectively, for this final data set.

Although the depth increment was decreased from 2 to 1 km, focal depth distribution plots for the 16 regions within the network (see Figure 29) for the QS = A quality events (Figures 30a-d) do not change drastically from the distributions found from the larger QS = A and B data set. In Figure 30, the seismic gap in regions 10 and 7, between depths 8 and 10 km, is observed. In both regions (10 and 7), approximately 80 percent of the microearthquakes occurred between 6 to 8 km and 10 to 12 km with

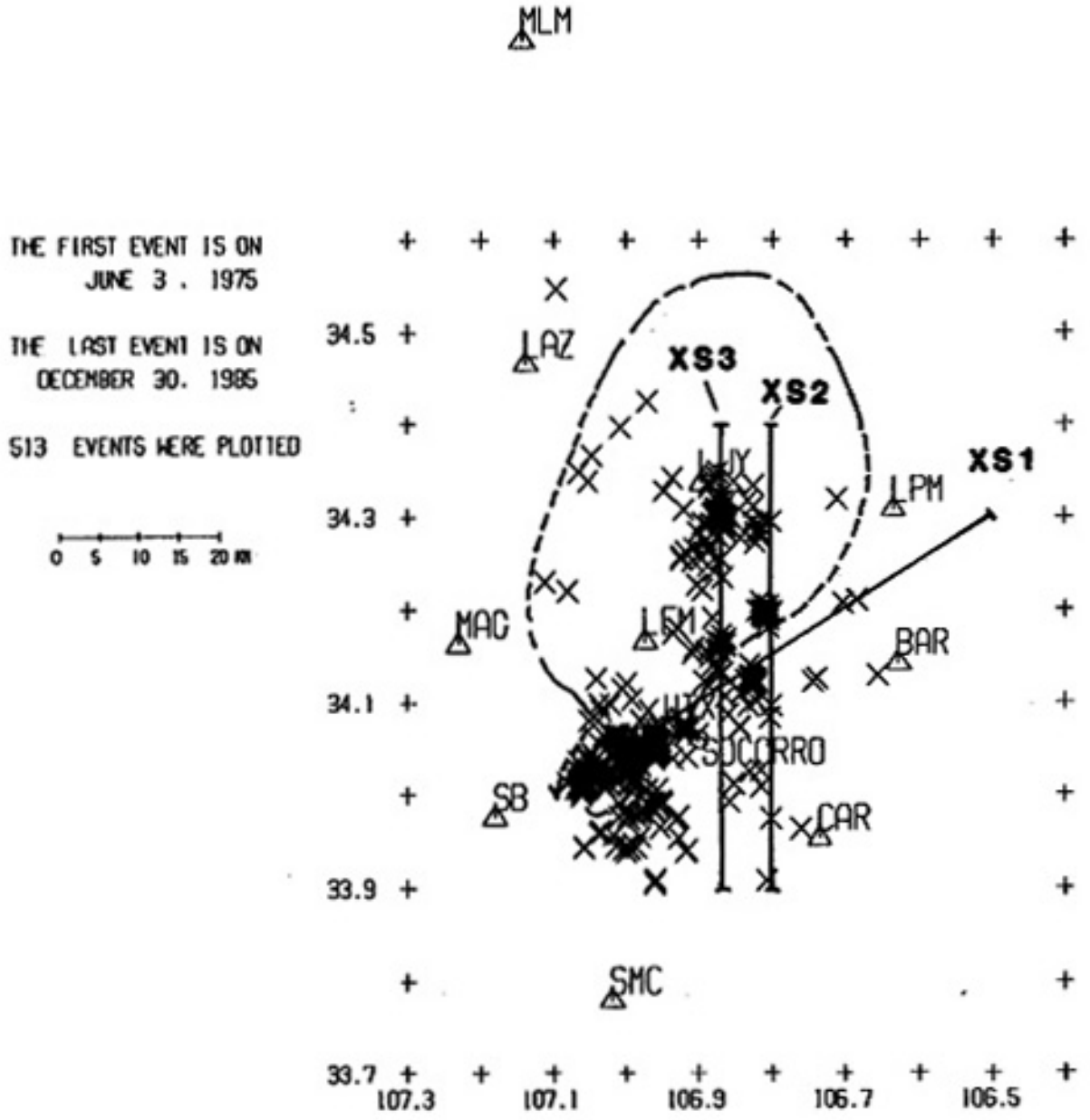

Figure 27. Epicenter distribution for 513 (QS-A) events in the final data set. Socorro magma body outlined (after Rinehart and others, 1979) and location of cross section lines XS1, XS2, and XS3 included.

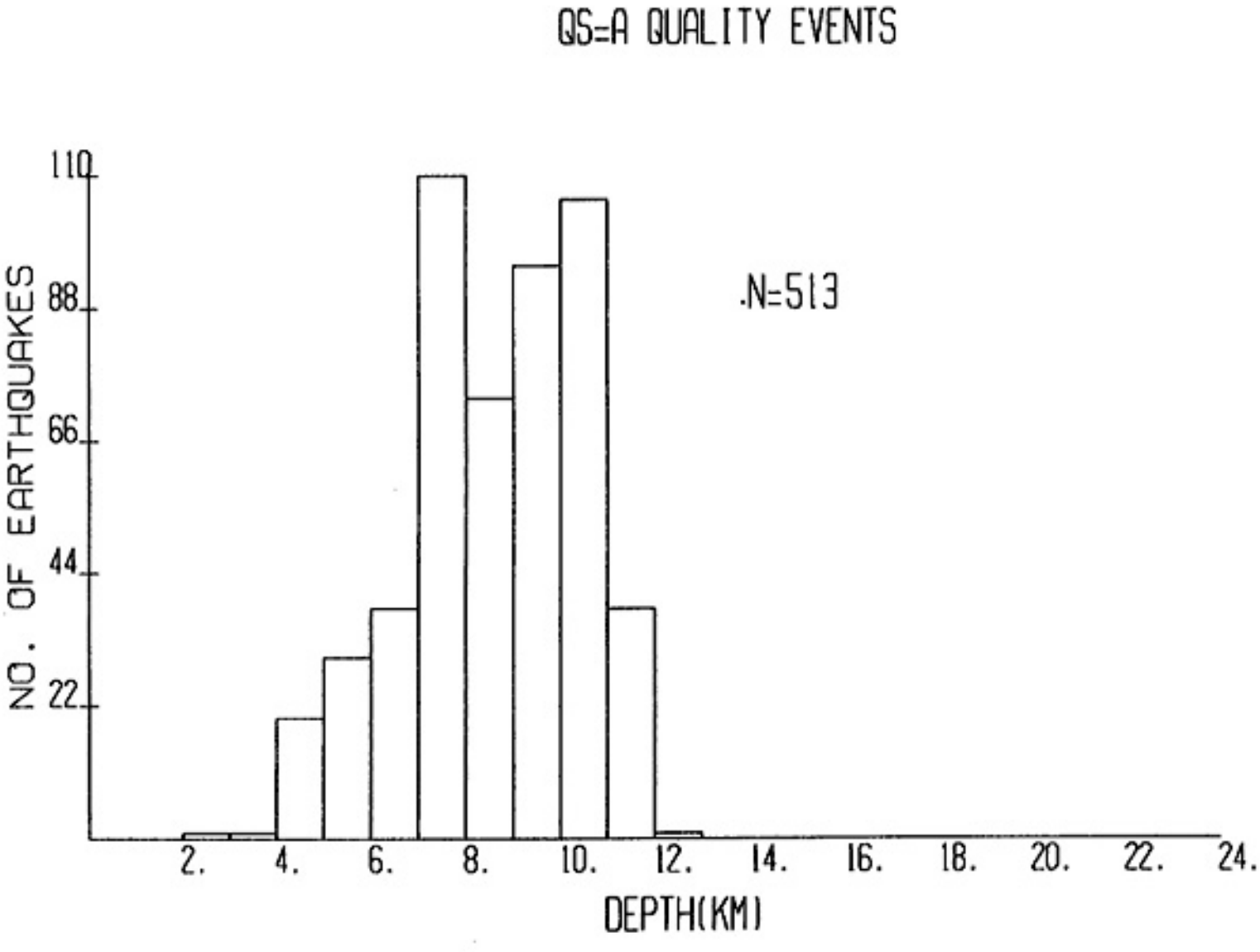

Figure 28. Depth distribution for the 513 events shown in Figure 27.

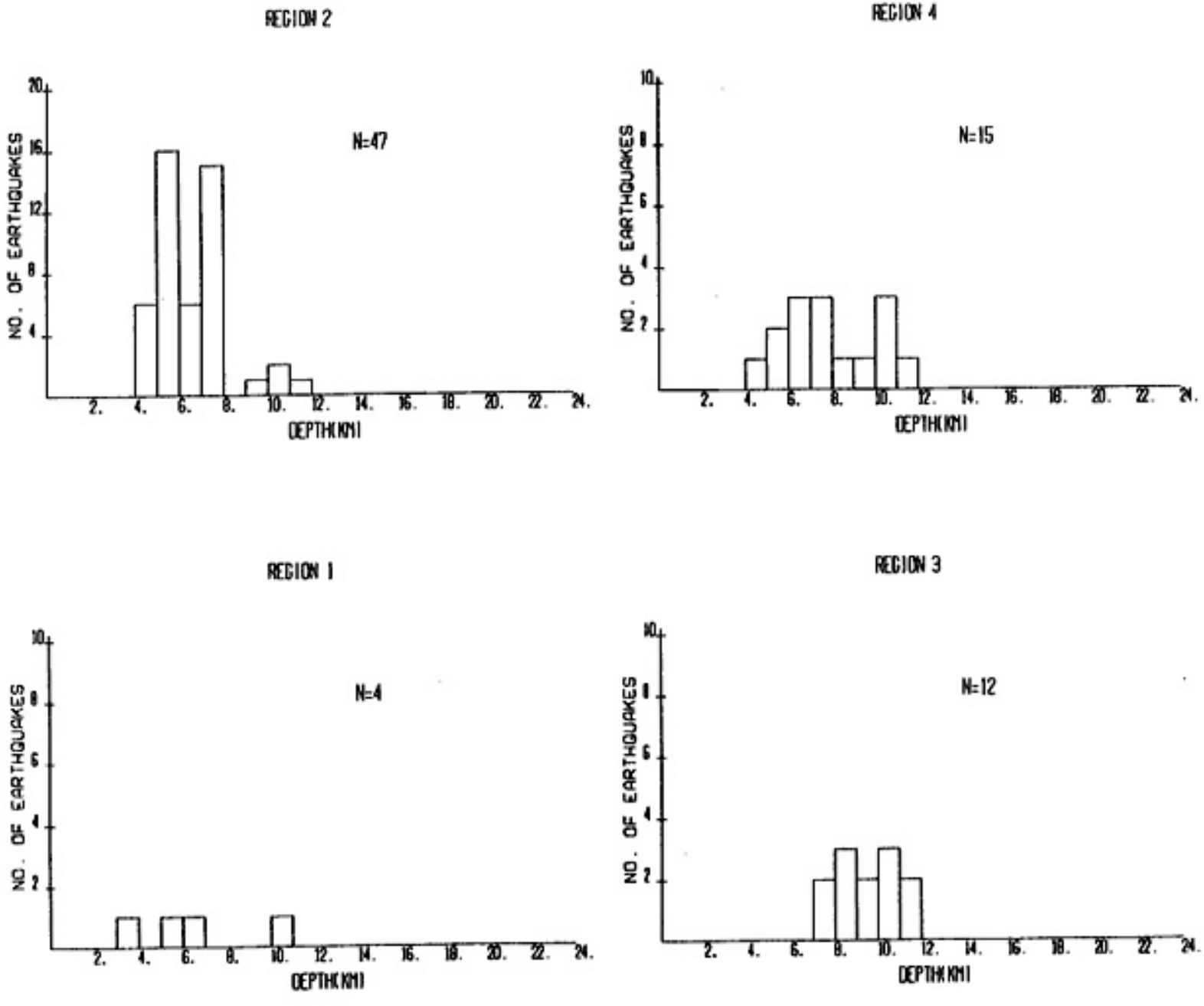

Figure 29(a). Distribution of focal depths within regions 1-4 for QS = A quality events only.

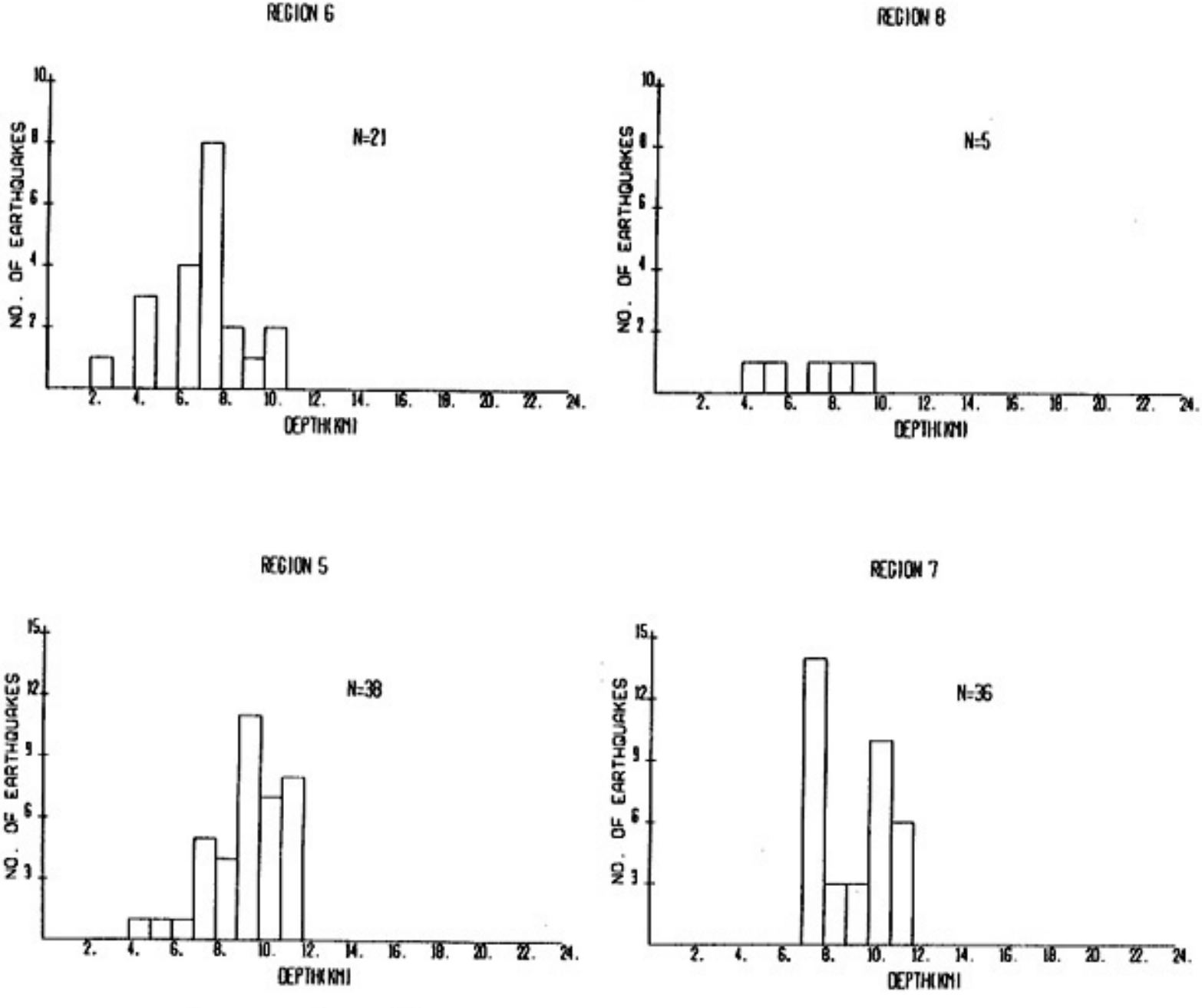

Figure 29(b). Distribution of focal depths within regions 5-8 for QS = A quality events only.

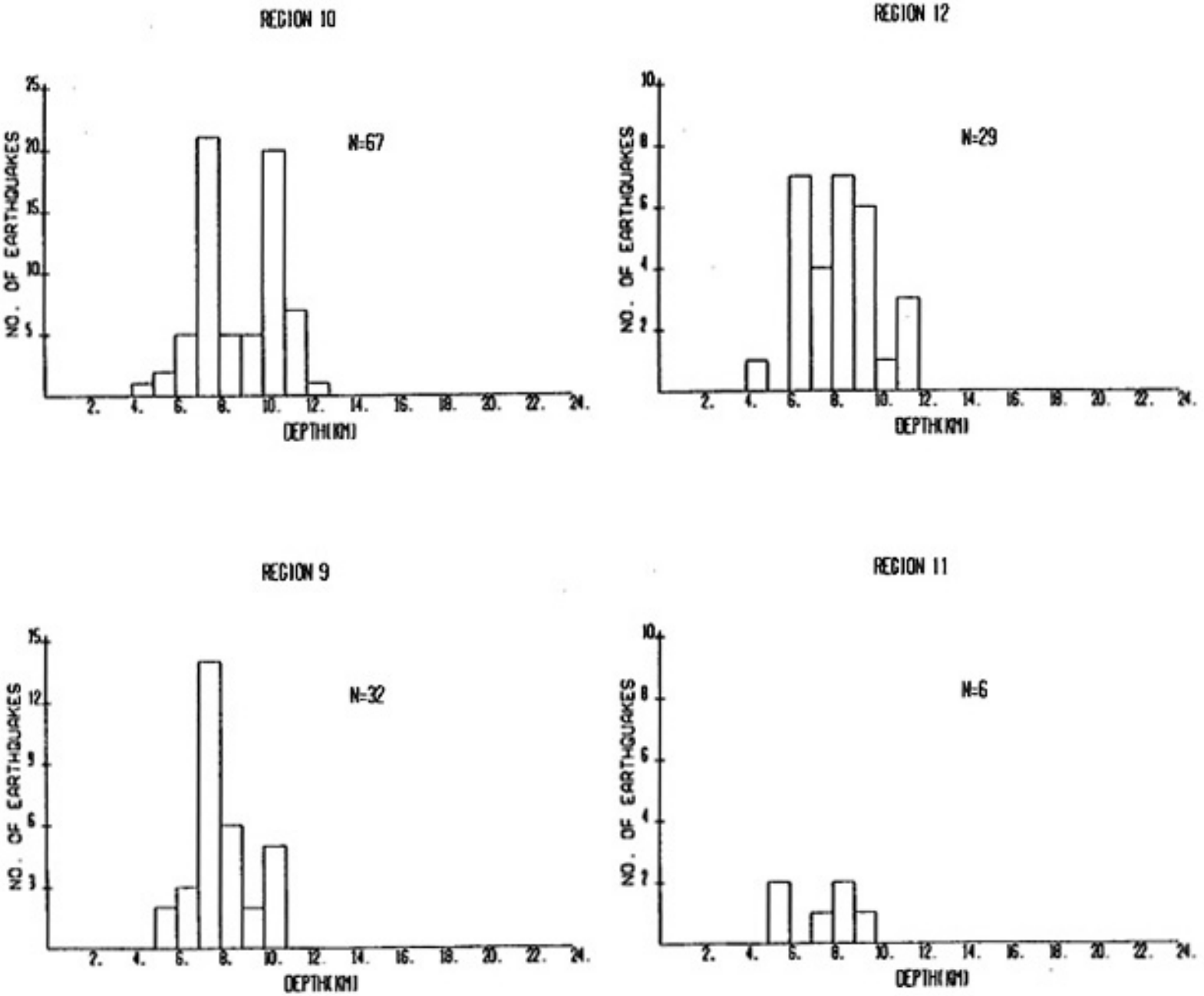

Figure 29(c). Distribution of focal depths within regions 9-12 for QS = A quality events only.

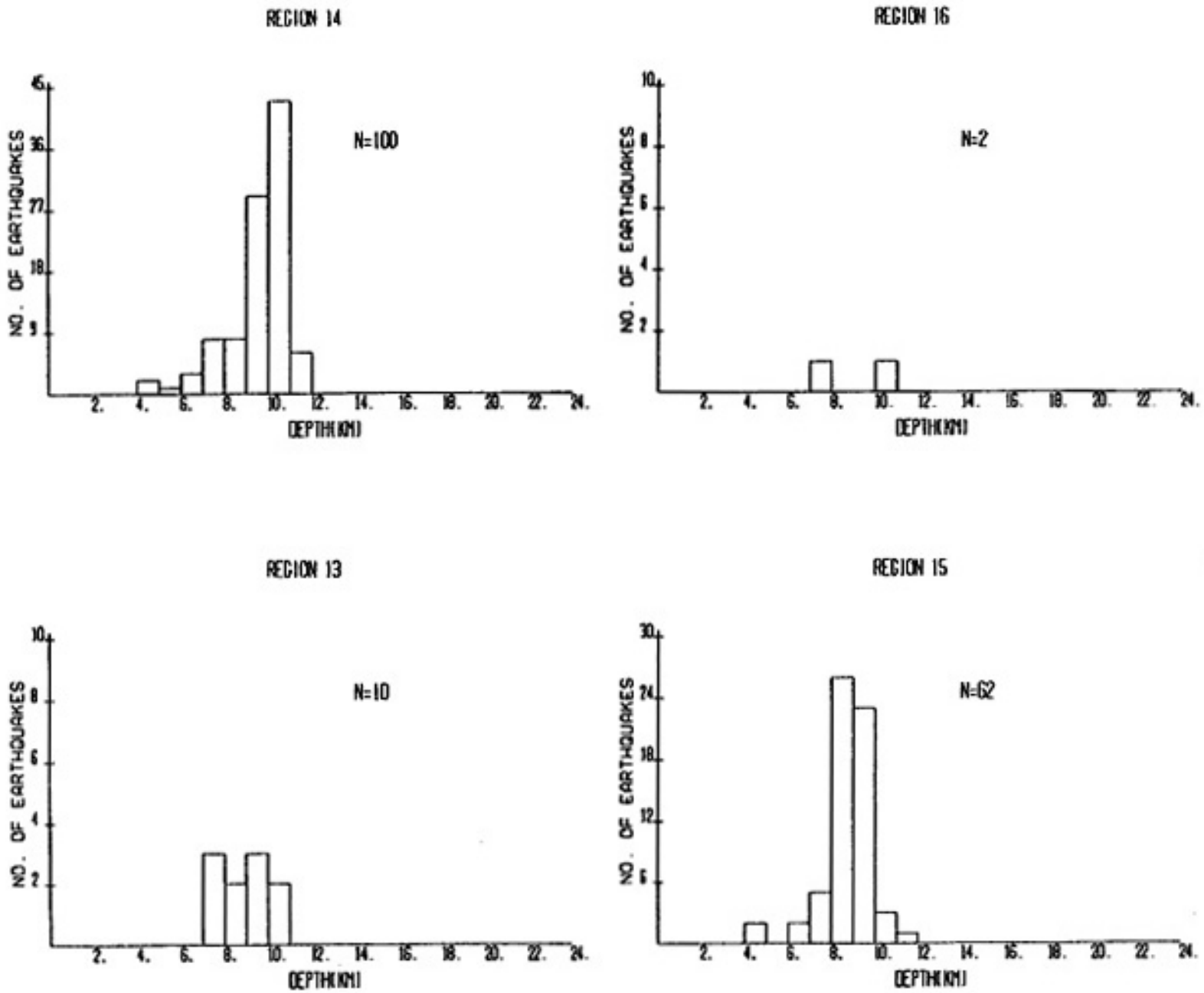

Figure 29(d). Distribution of focal depths within regions 13-16 for QS = A quality events only.

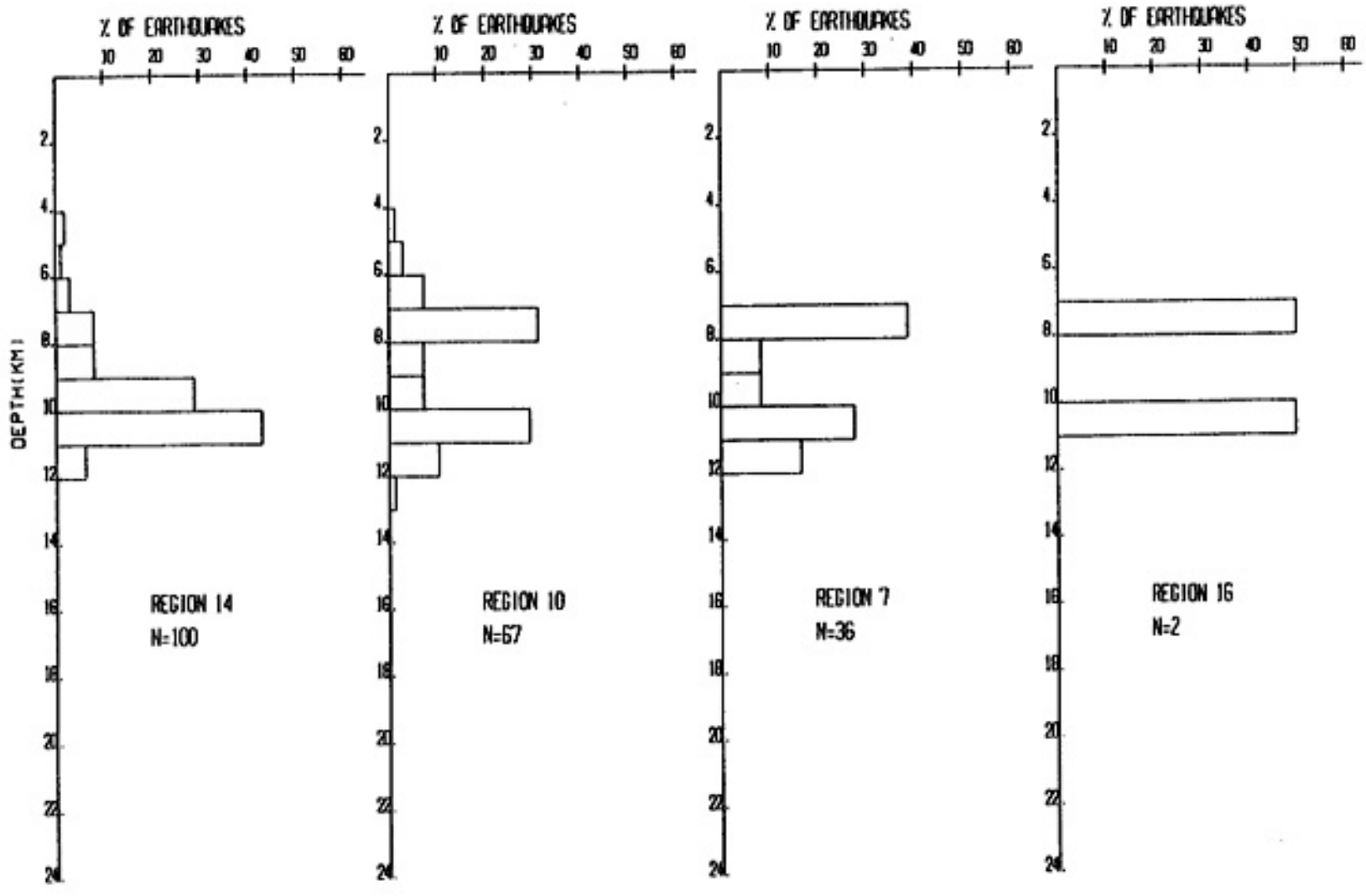

Figure 30. Depth distributions (based on percentage of events within each region) along a line running across regions 14, 10, 7 and 16, (see Figure 19) from the southwest to the northeast (for QS= A quality events only).

approximately 40 percent in each interval. The depth distribution for the entire area, now incremented at 1 km intervals, shows a significant decline in activity below 11 km, which the distribution at 2 km increments (Figure 13) could not show.

The distributions in regions 8, 7, 5, and 3 (Figure 31) are again similar to the former distributions with the exception of region 8, which was reduced to only 5 (QS = A) events. Distributions for regions 6, 4, and 2 (Figure 32), moving from south to north, show the predominance of events between 6 and 8 km in region 6, a bimodal distribution with peak numbers of events occurring from 6 to 8 km and 10 to 12 km in region 4 and a bimodal distribution with peak activity occurring from 5 to 6 km and 7 to 8 km in region 2.

Three cross-sectional views (XS1, XS2 and XS3 in Figure 27) of hypocenter depths, projected from perpendicular distances of less than or equal to ±2.5 km from the cross section plane, are viewed in Figures 33-35, with and without vertical exaggeration. From cross sections XS1 and XS2, it is apparent that much of the well-located clustered activity occurs to the south and southwest of station WTX, while hypocenters near the center of the rift, in cross section XS3, are much more dispersed.

Figures 36 and 37 show the depth distribution for events with magnitudes less than 1.0 and greater than or equal to 1.0, respectively. (Only events from data set B with QS=A are included in these plots.) It should first be noted that the

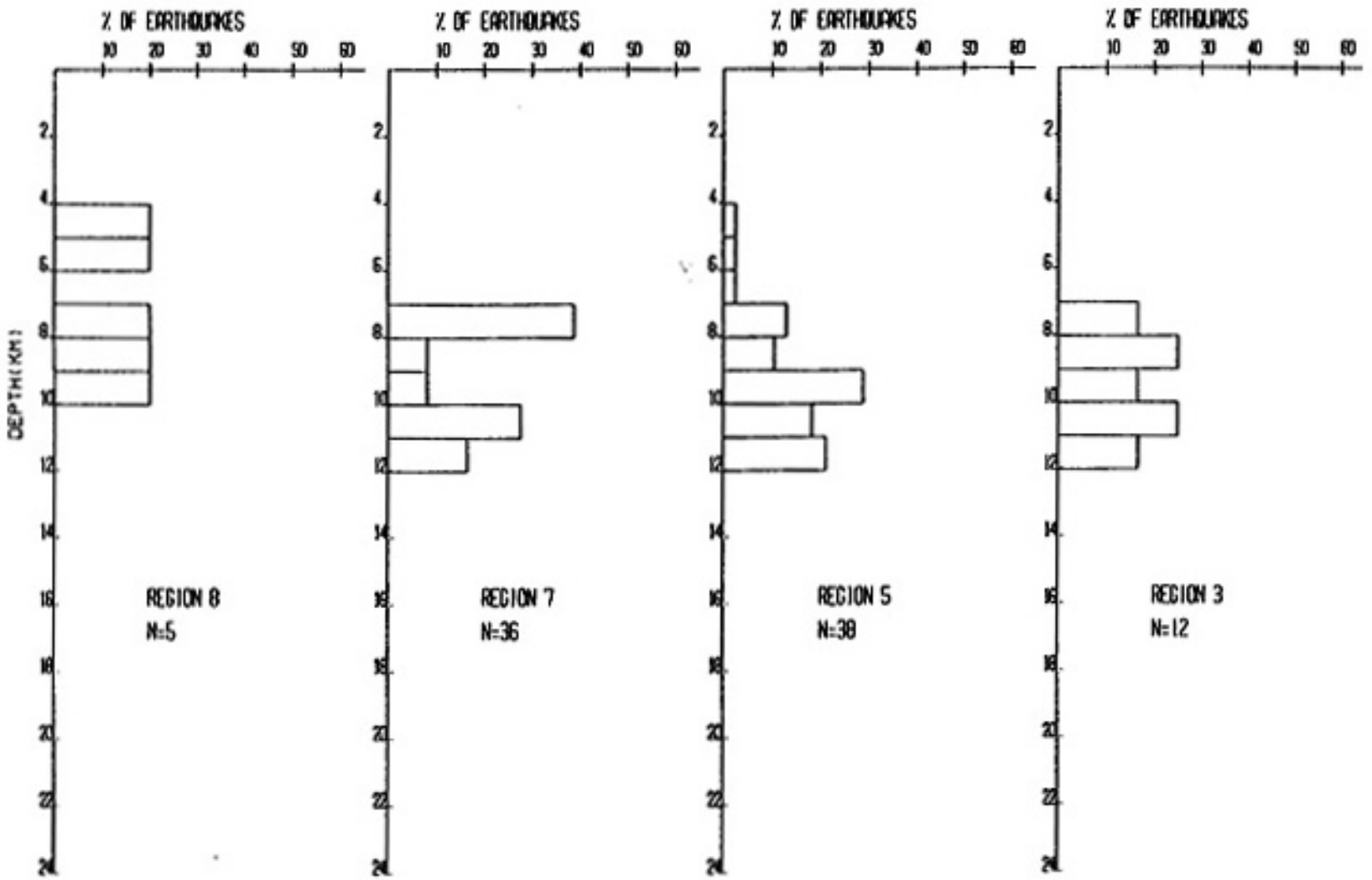

Figure 31. Depth distributions along a line running across regions 8, 7, 5 and 3, from south to north (for QS = A quality events only).

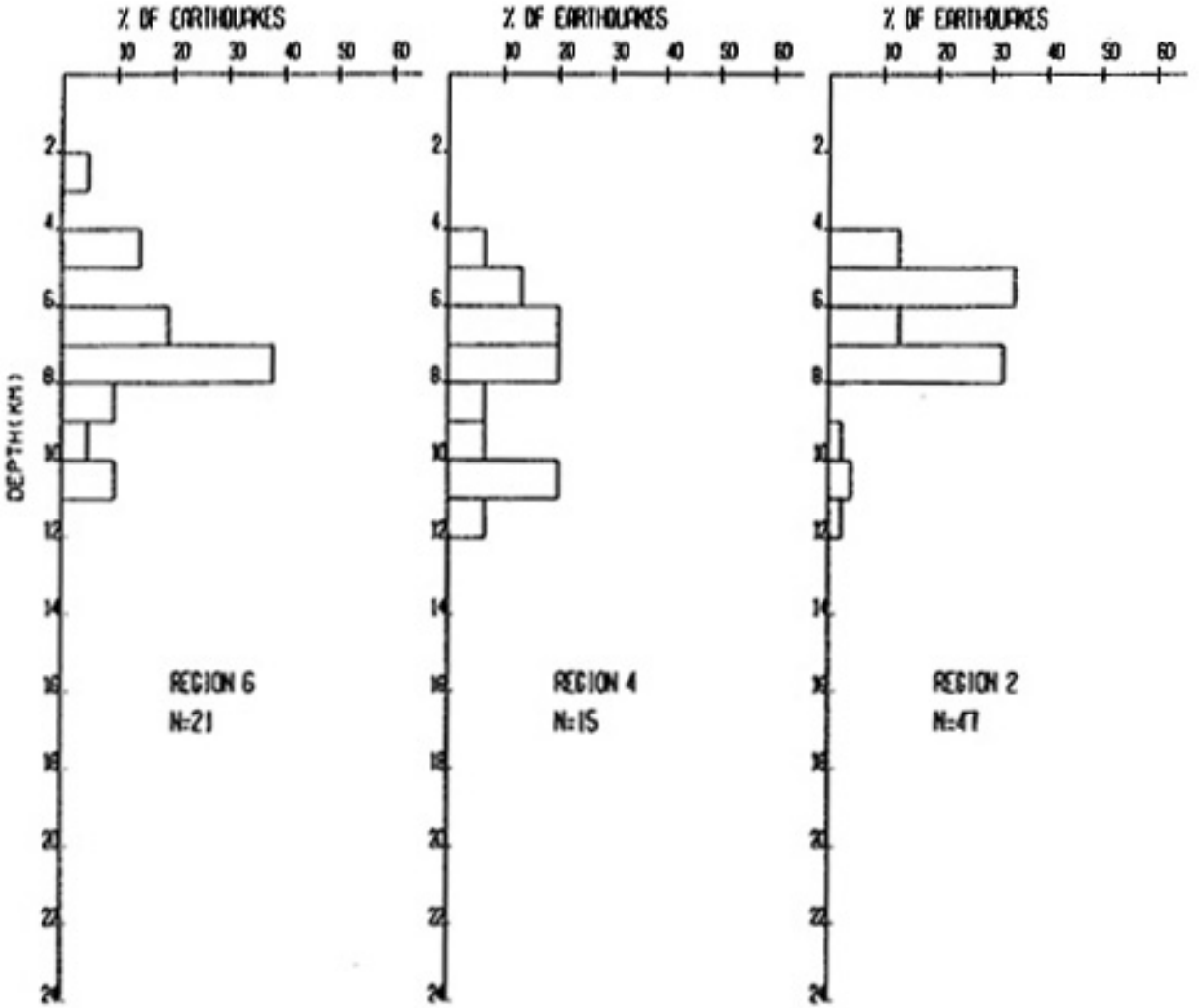

Figure 32. Depth distributions along a line running across regions 6, 4, and 2, from south to north (for QS = A quality events only).

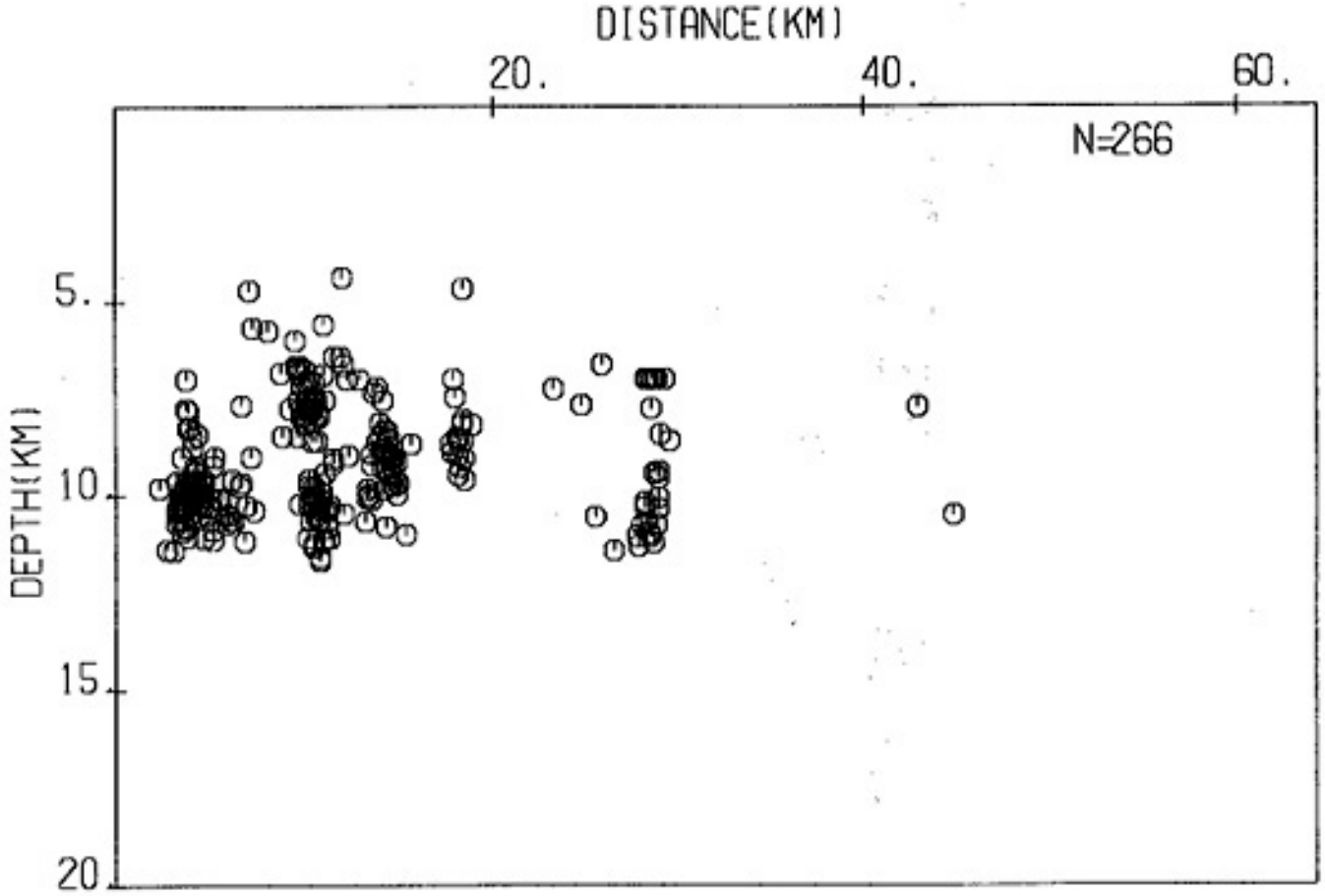

Figure 33(a). Cross section profile (XS1 in Figure 27) of QS = A quality events with two times vertical exaggeration. Events within ±2.5 km of the profile were projected onto the cross-section.

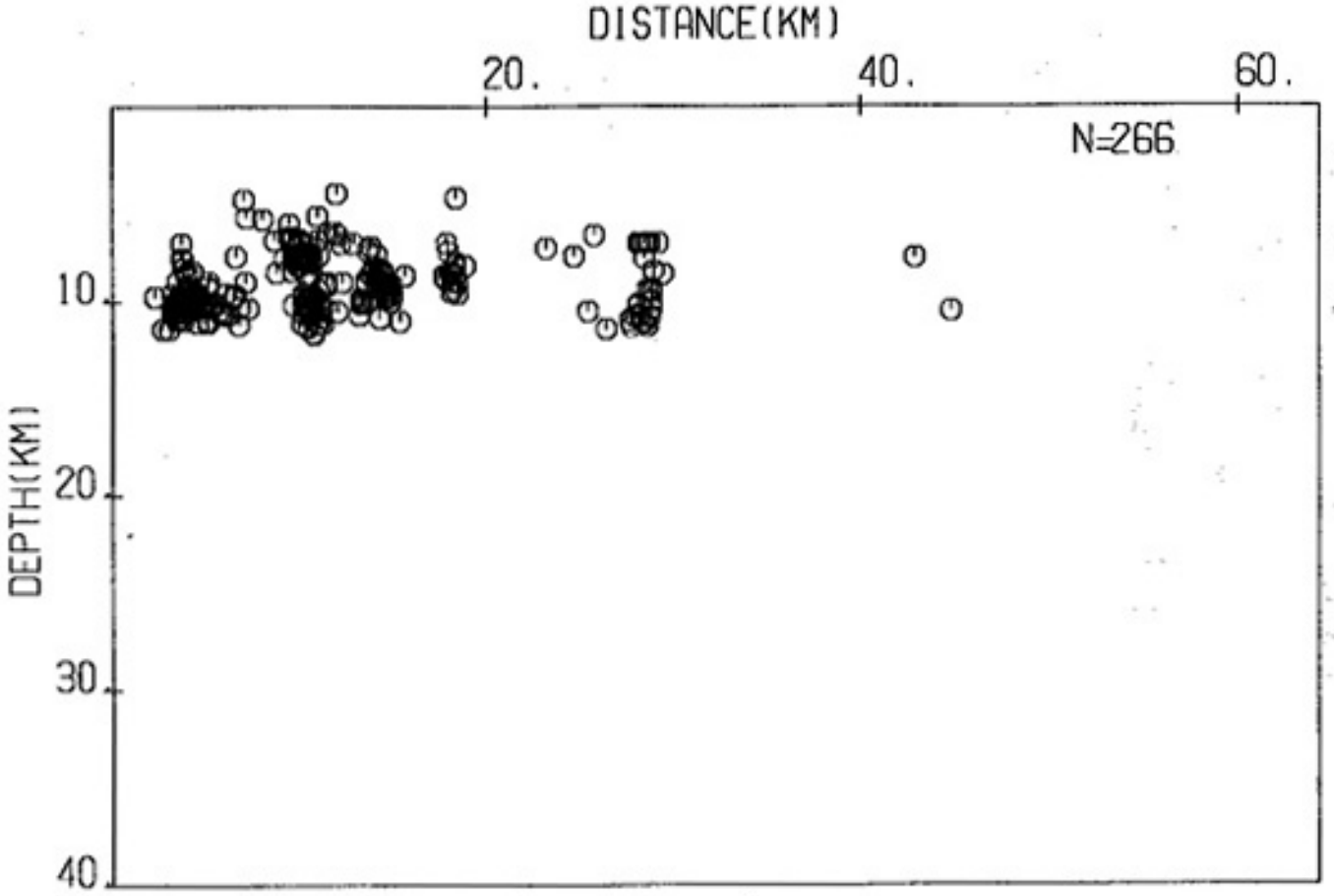

Figure 33(b). Cross section profile (XS1 in Figure 27) of QS = A quality events with no vertical exaggeration. Events within ±2.5 km of the profile were projected onto the cross-section.

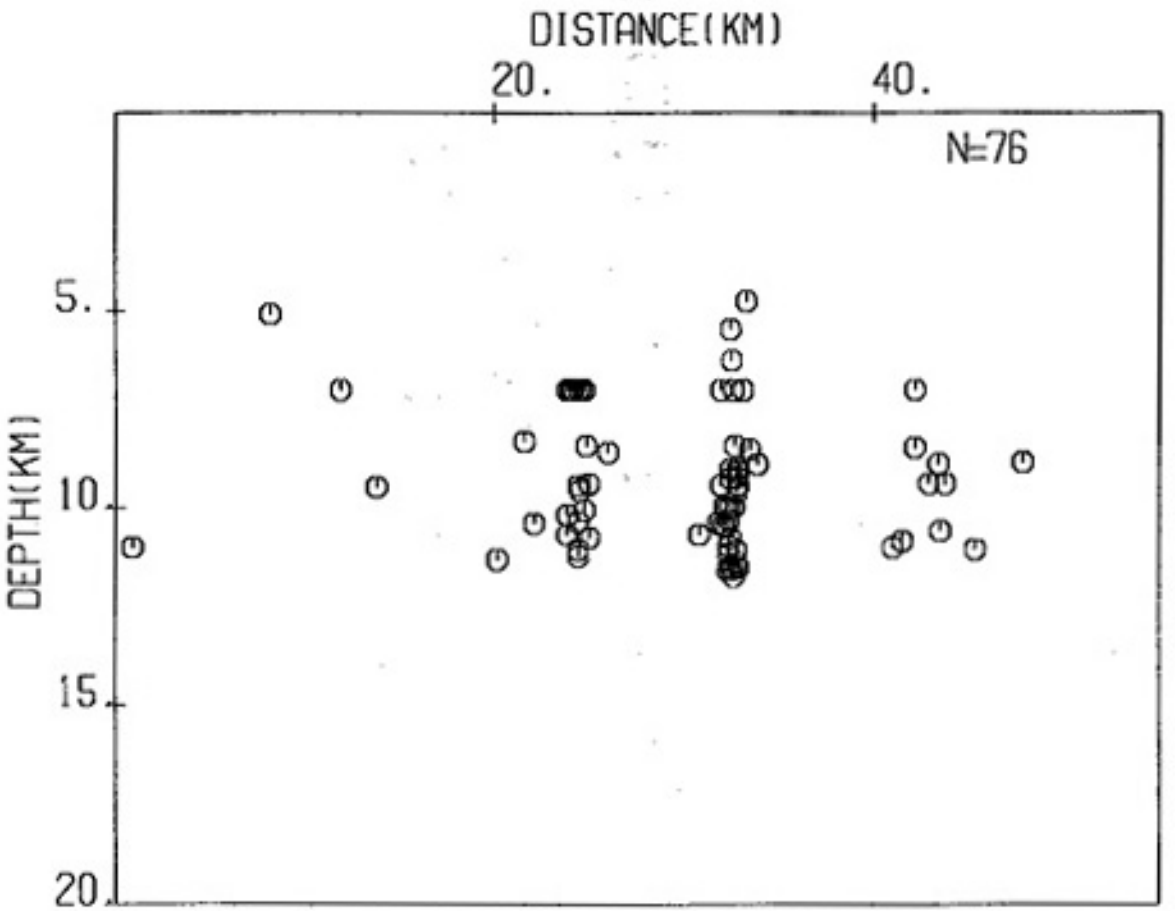

Figure 34(a). Cross section profile (XS2 in Figure 27) of QS - A quality events with two times vertical exaggeration. Events within ±2.5 km of the profile were projected onto the cross-section.

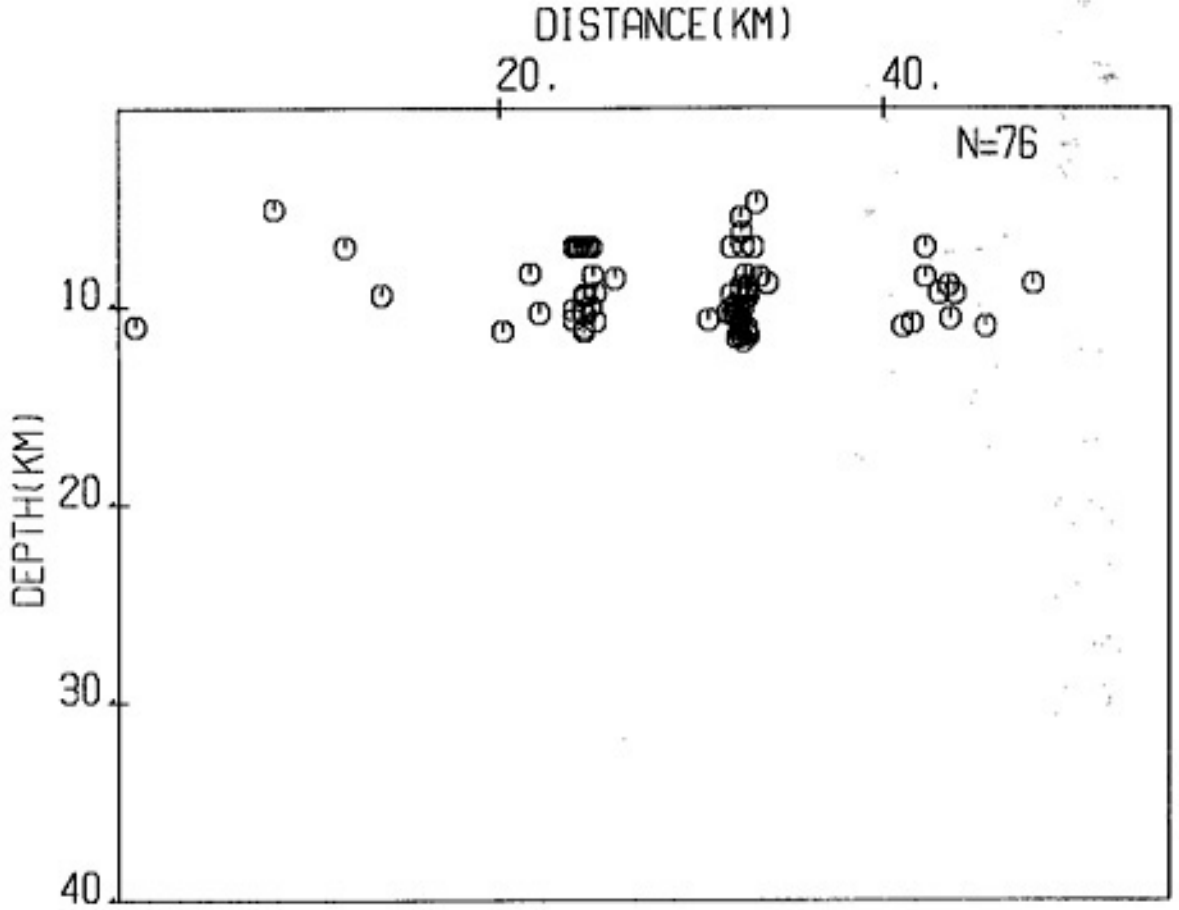

Figure 34(b). Cross section profile (XS2 in Figure 27) of QS = A quality events with no vertical exaggeration. Events within ±2.5 km of the profile were projected onto the cross-section.

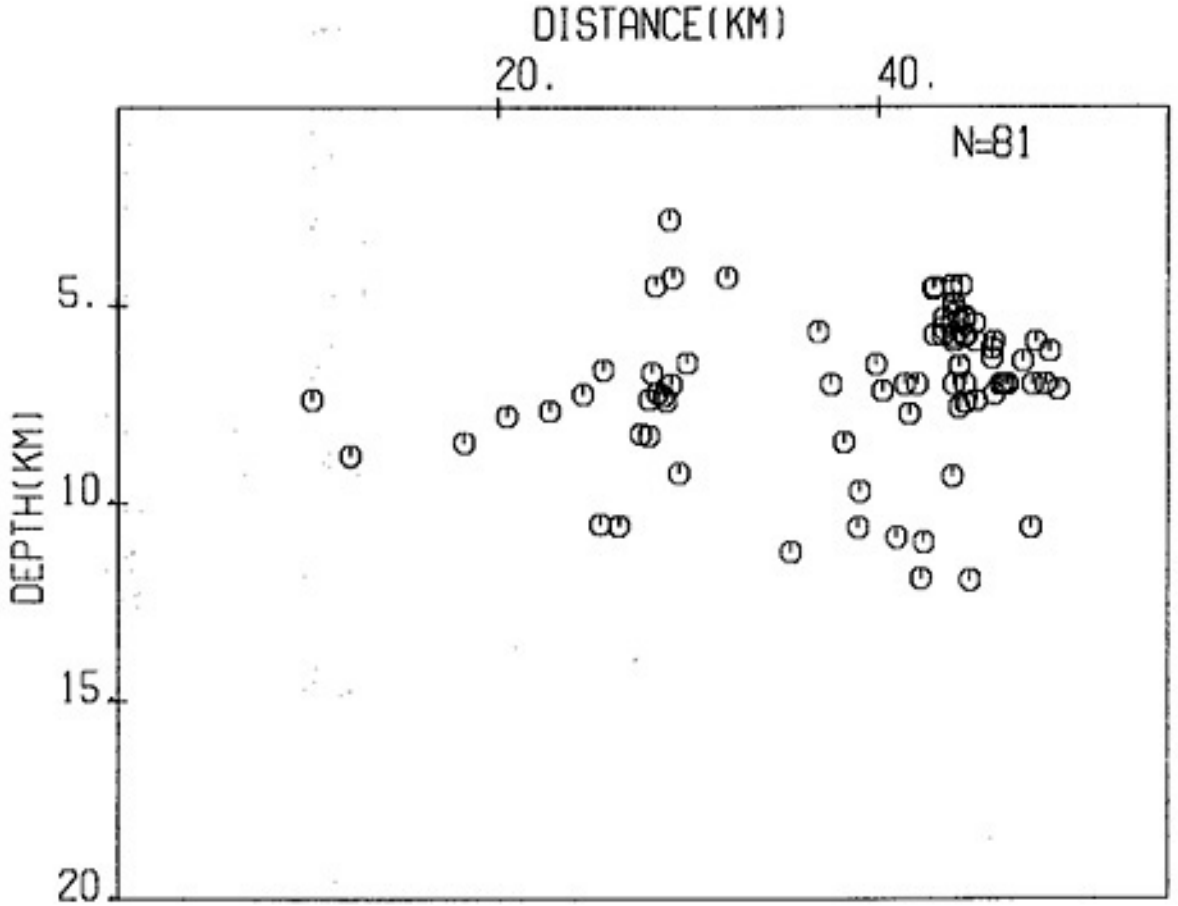

Figure 35(a). Cross section profile (XS3 in Figure 27) of QS = A quality events with two times vertical exaggeration. Events within ±2.5 km of the profile were projected onto the cross-section.

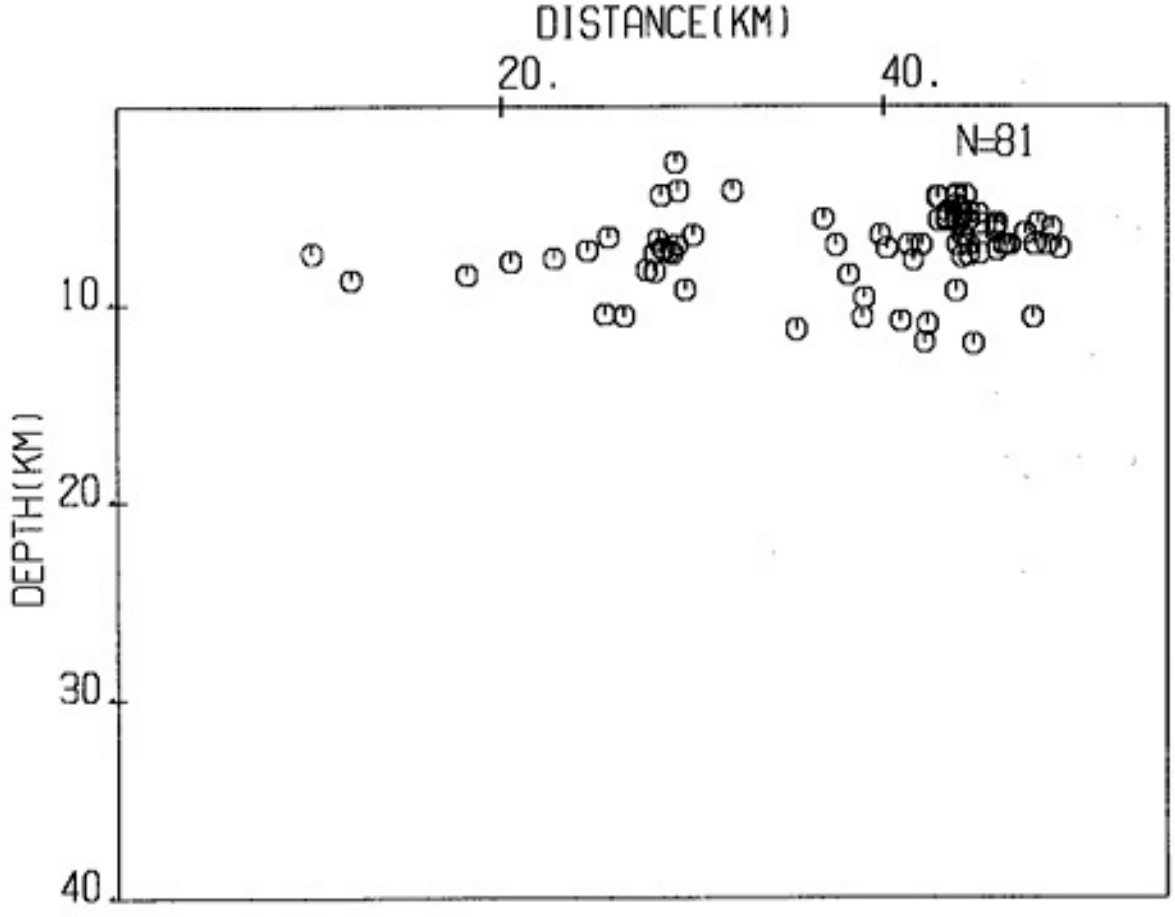

Figure 35(b). Cross section profile (XS3 in Figure 27) of QS = A quality events with no vertical exaggeration. Events within ±2.5 km of the profile were projected onto the cross-section.

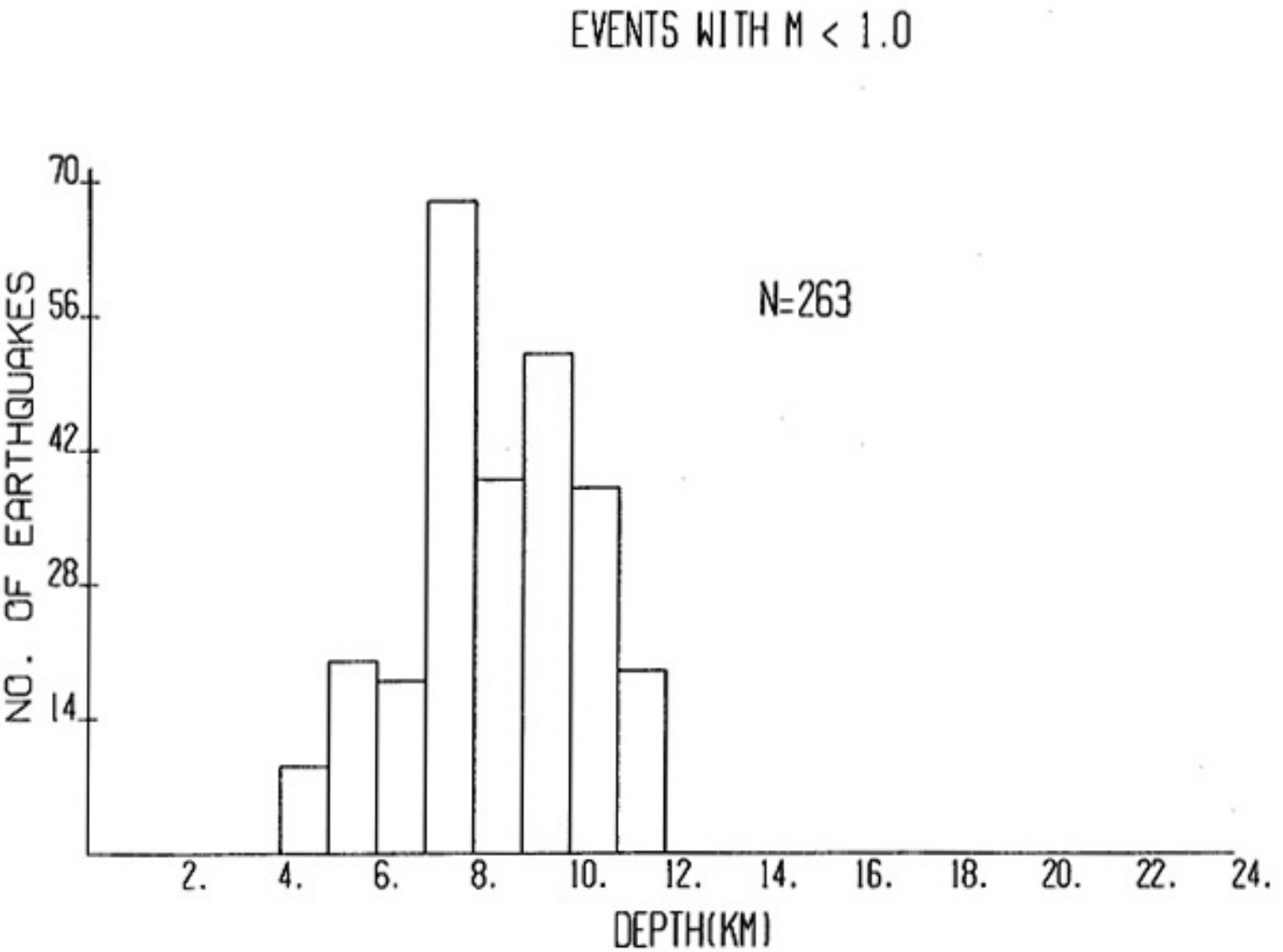

Figure 36. **Depth distribution of events with magnitudes < 1.0.**

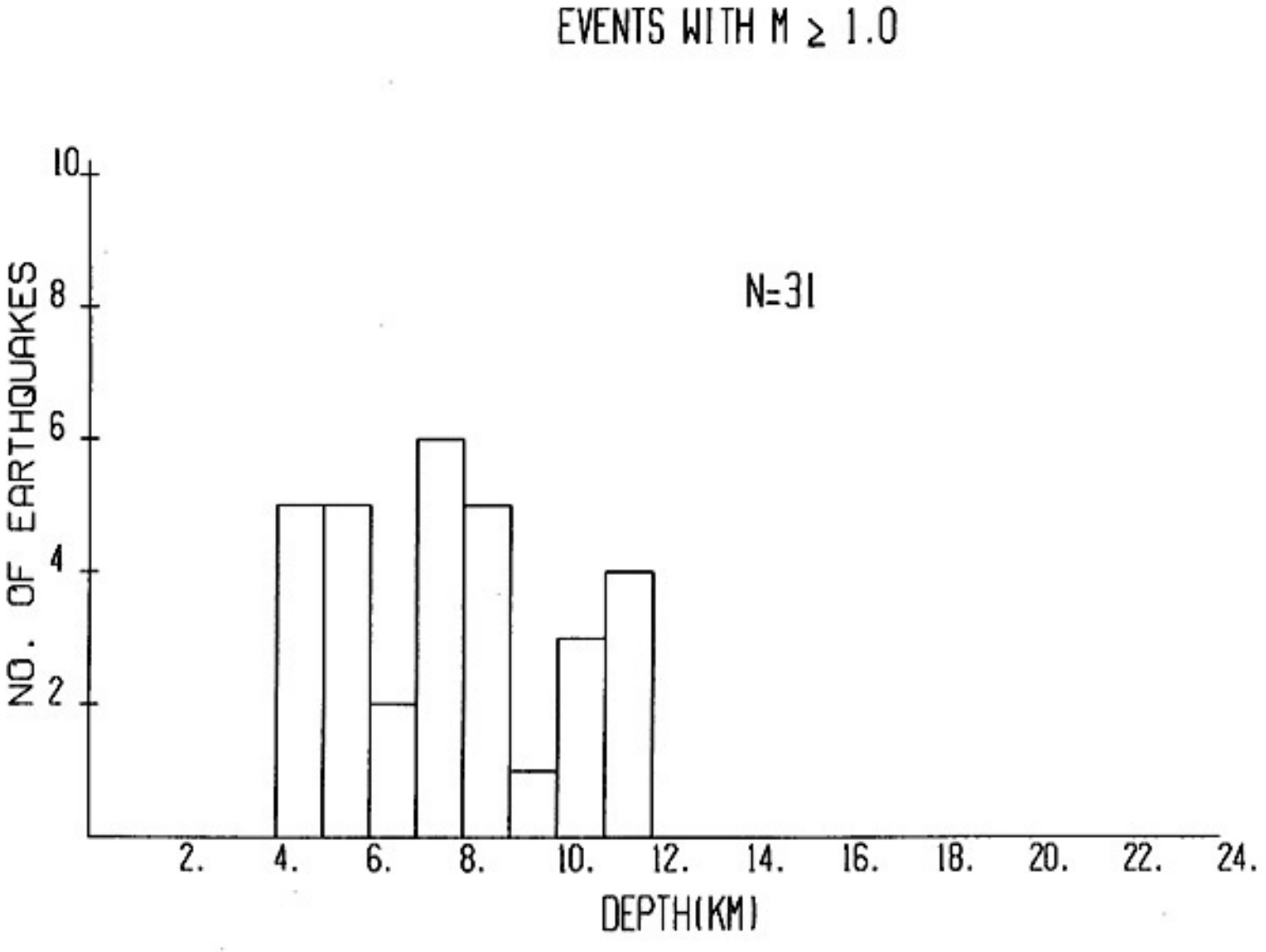

Figure 37. **Depth distribution of events with magnitudes ≥ 1.0.**

majority of events have magnitudes less than 1.0, and that almost 75 percent of these occur at depths from 7.0 to 11.0 km. Most events with magnitudes M > 1.0 are found in three intervals: (1) from 4.0 to 6.0 km; (2) from 7.0 to 9.0 km; and (3) from 10.0 to 12.0 km. There is no indication from these plots that stronger earthquakes have deeper foci as has been suggested by others (Byerlee and Brace, 1968).

DISCUSSION

How does the depth distribution for the Socorro area compare to those in other areas where microearthquakes occur? Figure 38 shows the location of six other regions in the western United States that provide depth distributions of microseismic activity (Figure 39). Regions of active subduction have been excluded. As Sibson (1982) points out, most of the activity in the six regions is confined to the upper 10 to 12 km, with the exception of the Transverse Ranges. The Socorro distribution also clearly agrees with this observation. Figure 40 shows earthquake depth distributions for regions in the southeastern United States. Although it can be argued that most of the activity is also confined to the upper 10 to 12 km, a significant percentage of earthquakes do occur at depths greater than 12 km, especially in the Valley Ridge-Blue Ridge (VRBR) region.

Seismically active (non-subducting) regions with high

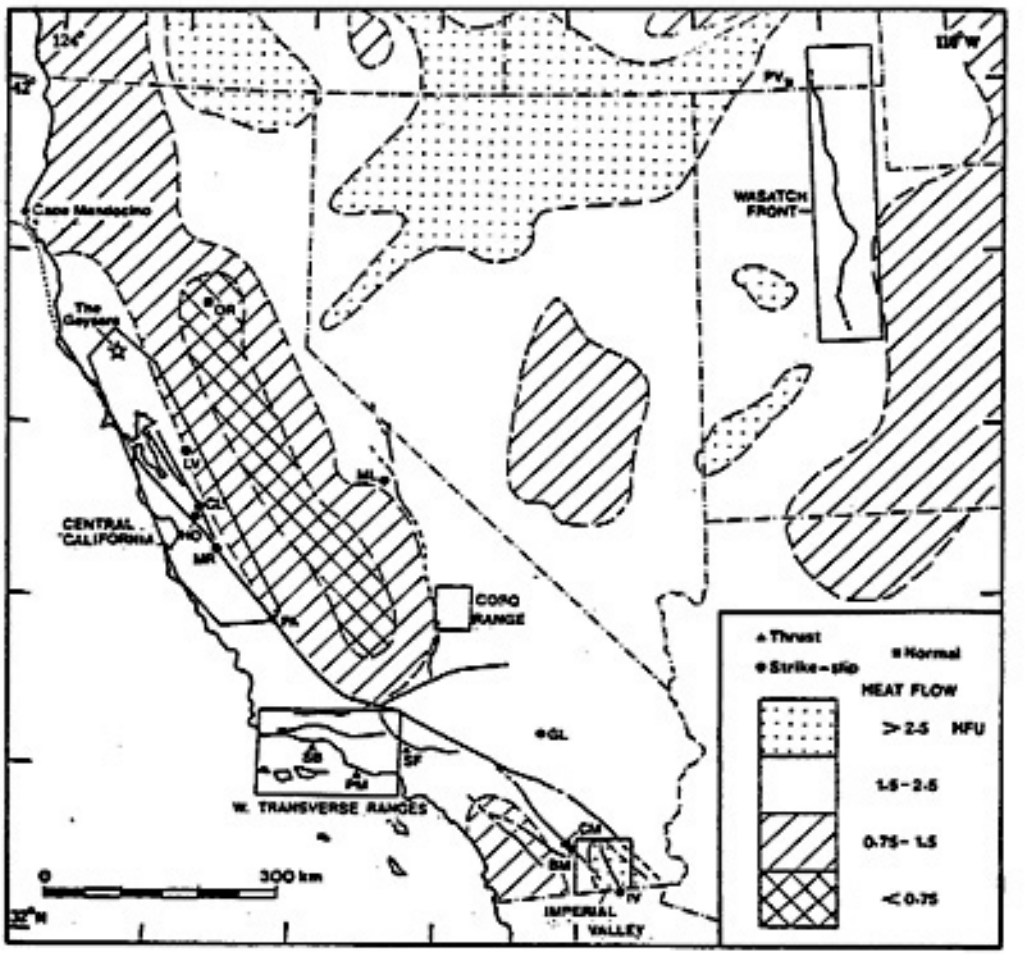

Figure 38. Microseismic sampling areas in relation to major heat flow provinces of the western United States (after Lachenbruch and Sass, 1980; and Sibson, 1982).

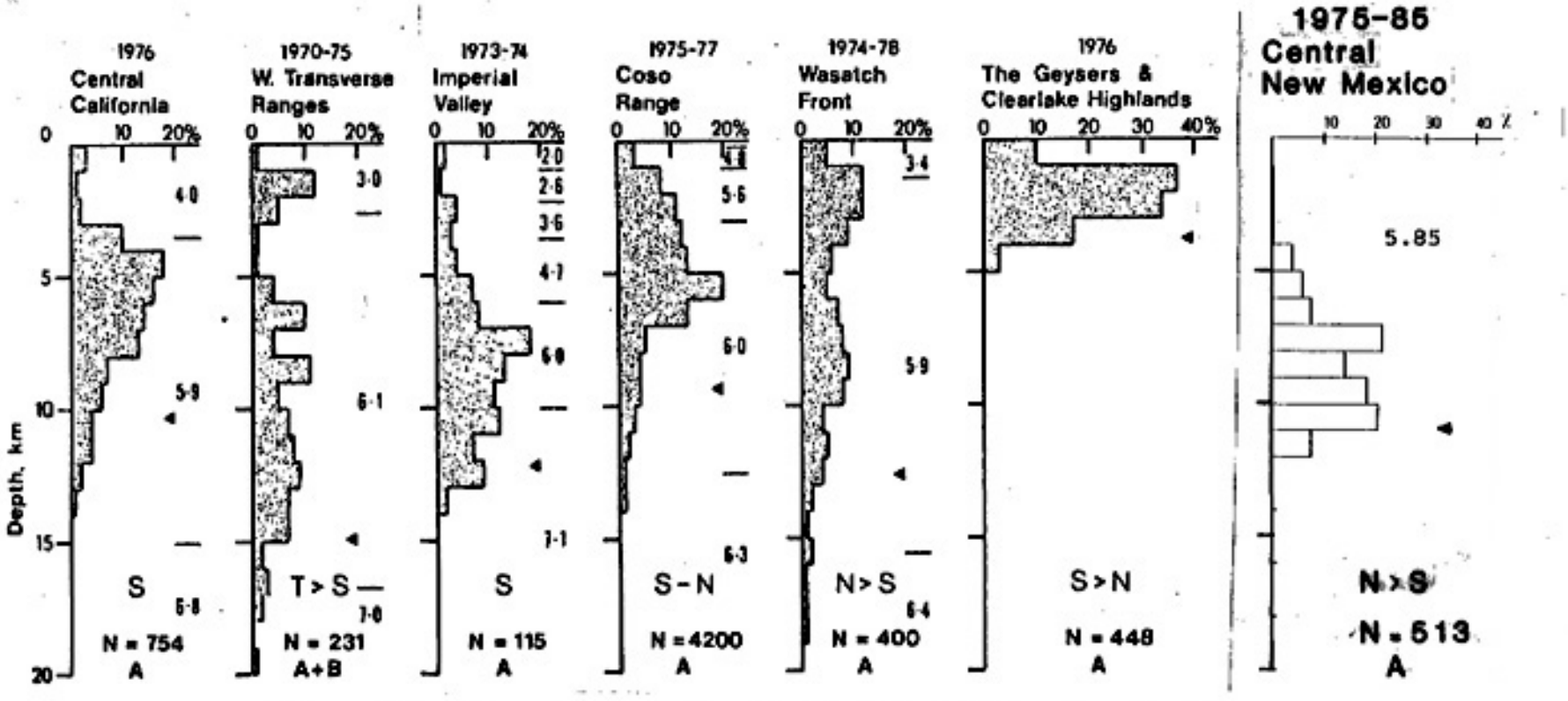

Figure 39. Comparison of the depth distribution for the Socorro area to some other areas with microseismic activity. P-wave velocities (km/sec) for the crustal models used in location are given on the right of the histograms and the depth above which 90 percent of the activity occurs is indicated by the solid triangles; the dominant faulting mode (T=thrust, S=strike-slip, N=normal), the number of microearthquakes in the sample, and the quality of the data are listed at the base (after Bollinger et al., 1985).

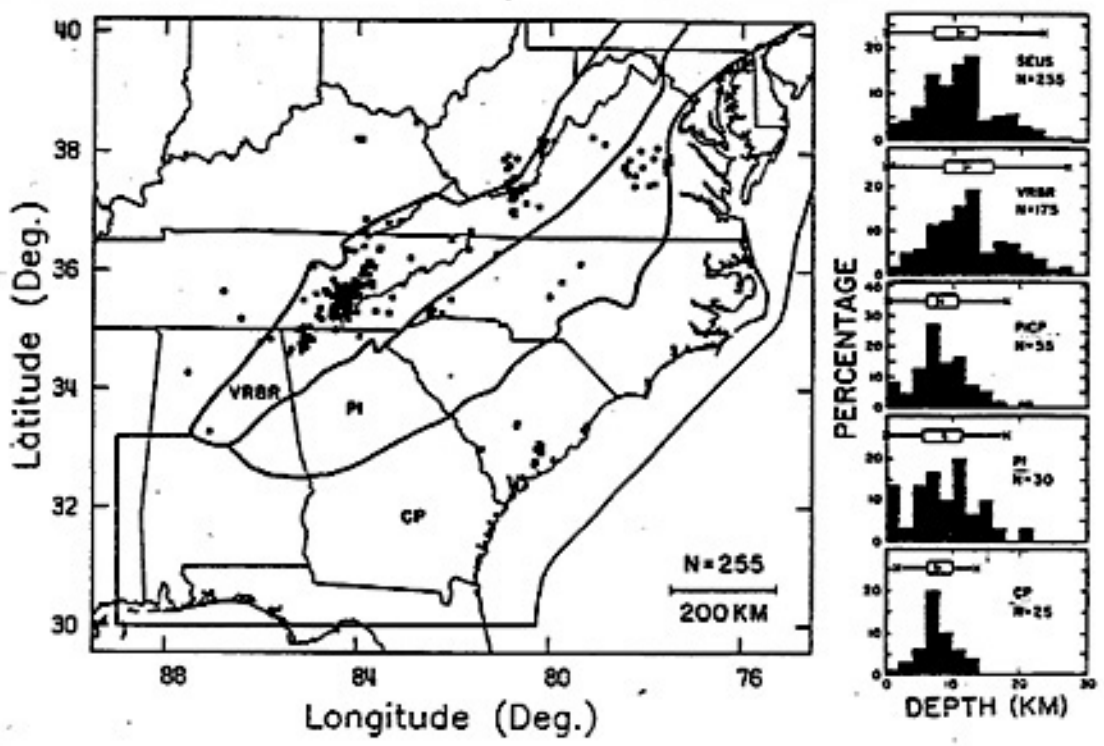

Figure 40. Left: Earthquake epicenters in the southeastern U. S. (SEUS; 0.0 ≤ magnitude ≤ 4.2 and ERZ ≤ 5.0 km). Major geologic provinces are also indicated: Valley and Ridge–Blue Ridge (VRBR), Piedmont (PI), and Coastal Plain (CP). Right: Histograms showing focal depth distributions for the various geologic provinces, as well as that for the entire region (after Bollinger et al., 1985).

heat flow typically have shallow seismogenic zones, as is witnessed in the histogram for the Geysers and Clearlake Highlands in Figure 39. The Socorro area and the Rio Grande rift in general are associated with heat flow values on the order of 2.5 HFU (Reiter et al., 1986). In terms of both heat flow values and depth of foci, then, the Socorro area is similar to the Imperial Valley region: both regions have high heat flow (> 2.0 HFU) and most of the seismic activity occurs between 7 and 12 km.

Assuming the geotherm for the southern Rio Grande rift (Figure 41) is also appropriate for the central Rio Grande rift and the Socorro area, it can be seen that the lower boundary of the seismogenic zone (~12 km) corresponds to a temperature near 425°C. This is within the estimated temperature range in which fractures and pore space for silicates may disappear and in which plastic flow begins. However, the geotherm in Figure 41 may not be applicable to the Socorro area. Some very anomalously high temperature gradients (33.8 to 286.9°C/km) measured near Socorro (Sanford, 1977) suggest temperatures from 400°C to greater than 2000°C at 12 km (assuming linear gradients). These extrapolations are brought into question, however, due to the possibility of shallow-source contamination from radiogenic heat production and convective heat transfer by moving ground water.

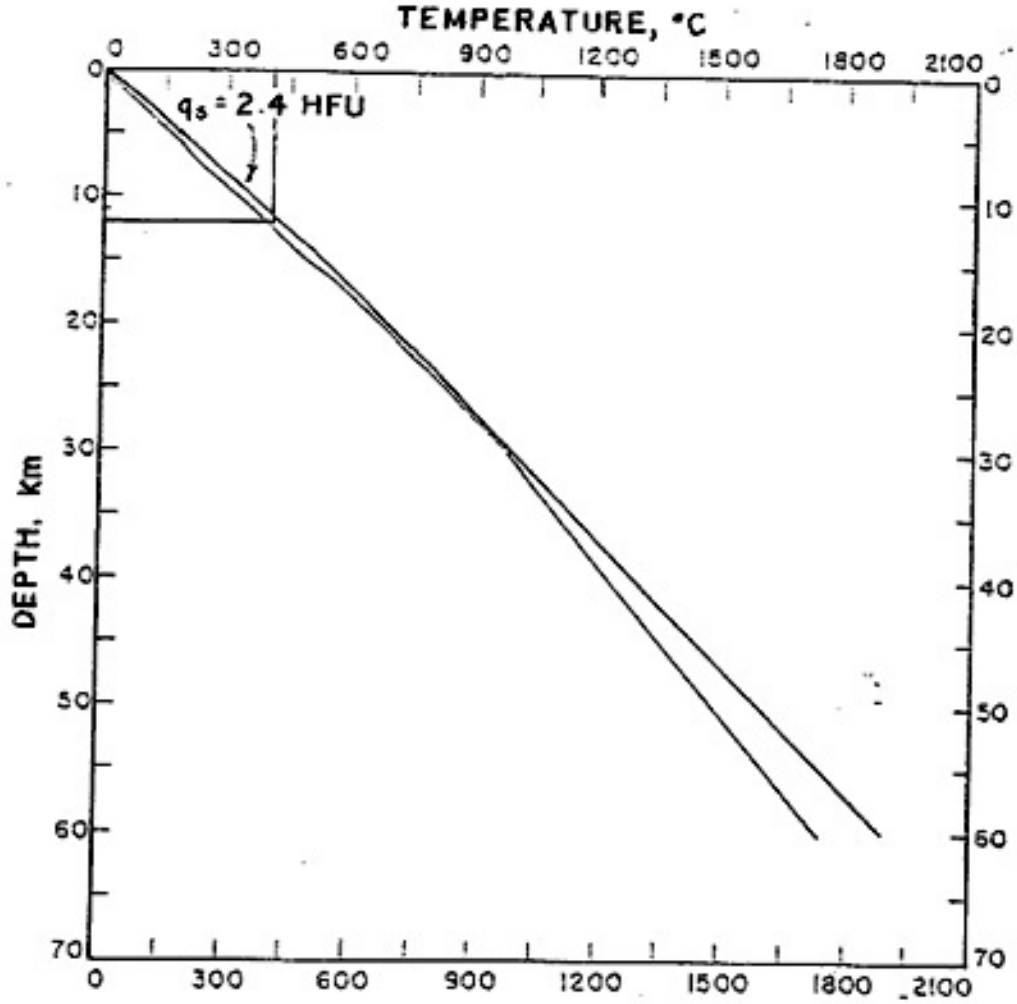

Figure 41. Steady state temperature as a function of depth with a surface flux (q_s) of 2.4 HFU for the southern Rio Grande rift (after Decker and Smithson, 1975).

SUMMARY AND CONCLUSIONS

Only well-constrained focal depths can be trusted in studies attempting to define boundaries of seismogenic zones. Errors in focal depth locations (ERZ) > 5 km are devastating if the seismogenic zone is as thin as it appears to be in the Socorro area. Although maximum errors of ±2 km are also not quite satisfactory, they were the best estimate that could be made with the Socorro data set.

An initial data set consisting of 717 B quality (ERZ can be greater than 5 km) events was compiled from events which occurred within two distinct time periods: data set A consists of 220 events which were recorded by an array of temporary stations between May 20, 1975 and January 20, 1978; data set B consists of 497 events recorded by a permanent network of stations between September 22, 1982 and December 31, 1985. The final data set, consisting of 513 good-quality events with average ERH=0.40 ±0.155 km and average ERZ=0.84 ±1.871 km, was reduced from the larger data set by retaining only those events with ERZ $\leq$ 2.0 km.

In the attempt to relate the seismicity of the Socorro area to major geological features, depth distributions were calculated for (1) regions north and south of the Morenci shear zone, (2) the region within the confines of the Socorro caldera and (3) the central Rio Grande valley. The depth distributions for the regions north and south of the shear zone and within the caldera are similar to the distribution found for the entire

Socorro area, which confined most of the activity between 6 and 12 km. In contrast, the depth distribution for a region centered in the rift north of Socorro shows that foci are located predominantly between 4 and 8 km. The activity in this region does not appear to be associated with any extensive planar fault surfaces.

Epicentral locations display a dense cluster of swarm events to the south and southwest of station WTX, with some additional swarms appearing to the north of Socorro in the rift. For the final data set, the depth distribution for the entire area shows that (1) most of the activity occurs between 6 and 12 km; (2) there is a significant drop in the number of events occurring deeper than 11.0 km; and (3) the lower boundary of the seismogenic zone is ~12.0 km. The interval from 11.0 to 12.0 km may be interpreted as the transition interval from brittle to ductile crust.

Bimodal focal depth distributions for several regions within the Socorro area reveal a decline in seismic activity between 8 and 10 km. This suggests a layer of less rigid material sandwiched between more rigid crust above and below. Another area was found to have a large number of events with focal depths between 4 and 8 km, with a peak number of hypocenters occurring between 5 and 6 km. Maximum surface uplift has been documented in this region (Reilinger, 1976; Reilinger and others, 1980) along with compressional first motions which Jarpe (1984) found to exist throughout the focal sphere.

Suggestions for Further Study

Many observations concerning the seismicity in the Socorro area warrant further investigation. Depth distributions indicate a rapid transition from brittle to ductile crust. Horizontal regions of low seismicity sandwiched between layers of higher activity are observed. Foci distributed in a pillar-like fashion are also observed. Relatively shallow seismicity occurs in a region of recorded uplift. All of these observations require further research in order to understand their meaning and nature.

Although a difficult undertaking, it would be valuable, in terms of a better focal depth constraint, to modify the HYPO71 algorithm to include S_zS phase information (Sanford, personal communication). A larger data set containing only A quality solutions will also be helpful in any further investigations of depth of foci in the area.

REFERENCES

Ake, J.P., An analysis of the May and July, 1983 Socorro Mountain microearthquake swarms, New Mex. Inst. of Mining and Technol., Geosc. Dept., Geophysics Open-File Report, , 1984.

Batzle, M.L. and G. Simmons, Geothermal systems: rocks, fluids, fractures, in Heacock J.G. ed., The Earth's Crust, Geophys. Monogr. Ser., AGU, Washington, D.C., 20, 265-273, 1977.

Bollinger, G.A., M.C. Chapman, M.S. Sibol, and J.K. Costain, An analysis of earthquake focal depths in the southeastern U.S., Geophys. Res. Let., 12, 785-788, 1985.

Brace, W.F., and J.D. Byerlee, Stick-slip as a mechanism for earthquakes, Science, 153 (3739), 990-992, 1966.

Brace, W.F., Pore pressure in geophysics, in H.C. Heard ed., Flow and Fracture of Rocks, Geophys. Monogr. Ser., AGU, Washington, D.C., 16, 265-273, 1972.

Brace, W.F., Permeability of crystalline and argillaceous rocks, Int. J. Rock Mech. Mining Sci., in press, 1980.

Brace, W.F. and D.L. Kohlstedt, Limits on lithospheric stress imposed by laboratory experiments, Jour. of Geophys. Res., 85, 6248-6252, 1980.

Brocher, T.M., Geometry and physical properties of the Socorro, New Mexico, magma bodies, Jour. of Geophys. Res., 86, 9420-9432, 1981.

Brown, L.D., C.E. Chapin, A.R. Sanford, and others, Deep structure of the Rio Grande rift from seismic reflection profiling, Jour. of Geophys. Res., 85, 4773-4800, 1980.

Brown, L.D., P.A. Krumhansl, C.E. Chapin, and others, COCORP seismic reflection studies of the Rio Grande rift, in Riecker, R.E., ed., Rio Grande Rift: Tectonics and Magmatism, A.G.U., Wash., D.C., 169-174, 1979.

Byerlee, J.D. and W.F. Brace, Stick-slip, stable sliding, and earthquakes--effect of rock type, pressure, strain rate, and stiffness, Jour. of Geophys. Res., 73, 6031-6037, 1968.

Byerlee, J.D., Brittle-ductile transition in rocks, Jour. of Geophys Res., 73, 4741-4750,1968.

Byerlee, J.D., Friction of rocks, Pure Appl. Geophys., 116, 615-

626, 1978.

Caravella, F.J., A study of Poisson's ratio in the upper crust of the Socorro, New Mexico area, N. Mex. Inst. of Mining and Technol., Geosc. Dept., Geophysics Open-File Report 11, Socorro, 1976.

Carpenter, P.J. and A.R. Sanford, Apparent Q for upper crustal rocks of the central Rio Grande rift, Jour. of Geophys. Res., 90, 8661-8674, 1985.

Chapin, C.E., R.M. Chamberlin, G.R. Osburn, A.R. Sanford, and D.W. White, Exploration framework of the Socorro geothermal area, New Mexico, New Mex. Geol. Soc. Sp. Pub. no. 7, 115-129, 1978.

Chen,W.P., and P. Molnar, Focal depths of intracontinental and intraplate earthquakes and their implications for the thermal and mechanical properties of the lithosphere, Jour. of Geophys. Res., 88, 4183-4214, 1983.

Decker, E.R. and S.B. Smithson, Heat flow and gravity interpretation across the Rio Grande rift in southern New Mexico and west Texas, Jour. of Geophys. Res., 80, 2542-2552, 1975.

Fender, J.J., A study of Poisson's ratio in the upper crust in the Socorro, New Mexico area, New Mex. Inst. of Mining and Technol. Geosc. Dept., Geophysics Open-File Report 25, Socorro, 1978.

Frishman, M.S., Use of linear inverse techniques to study Poisson's ratio in the upper crust in the Socorro, New Mexico area, New Mex. Inst. of Mining and Technol., Geosc. Dept., Geophysics Open-File Report 27, Socorro, 1979.

Goetze, C. and W.F. Brace, Laboratory observations of high-temperature rheology of rocks, Tectonophysics, 13, 583-600, 1972.

Jaksha, L.H., J. Locke, J.B. Thompson and A. Garcia, Reconnaissance seismology near Albuquerque, New Mexico: U.S. Geological Survey, Open-File Rep., 78-339, Albuquerque, N.M., 1978.

Jaksha, L. Earthquakes near Albuquerque, New Mexico, 1976-1981, EOS, Trans. Amer. Geophys. U., 64, No. 45, 753, 1983.

Jarpe, S.P., A.R. Sanford, and L.H. Jaksha, Evidence for magmatic intrusion during an earthquake swarm in the central Rio Grande rift (abstract), EOS, Trans. AGU, 65, 1001, 1984.

Johnston, J.A., Microearthquake frequency attenuation of S phases in the Rio Grande rift near Socorro, New Mexico, New Mex. Inst. of Mining and Technol., Geosc. Dept., Geophysics Open-Fil Report 24, Socorro, 1978.

Lee, W.H.K. and J.C. Lahr, HYPO71 (revised): A computer program for determining hypocenter, magnitude, and first motion pattern of local earthquakes: U.S. Geological Survey, Open-File Rep.,75-311, 1975.

Meissner, R. and J. Strehlau, Limits of stresses in continental crusts and their relation to the depth-frequency distribution of shallow earthquakes, Tectonics, 1, 73-89, 1982.

Paterson, M., Experimental Rock Deformation: The Brittle Field, 254 pp., Springer New York, 1978.

Richter, C.F., Elementary Seismology, W. H. Freeman and Co., San Fransisco, 1958.

Reilinger, R., J. Oliver, L. Brown, and others, New measurements of crustal doming over the Socorro magma body, New Mexico Geology, 8, 291-295, 1980.

Reiter, M. and R. Smith, Subsurface temperature data in the Socorro Peak KGRA New Mexico, Geothermal Mag., 5, 37-41, 1977.

Reiter, M., Eggleston R.E., Broadwell, B.R., and Minier J., Estimates of terrestrial heat flow from deep petroleum tests along the Rio Grande rift in central and southern New Mexico, Jour. of Geophys. Res., 91, 6225-6245, 1986.

Rinehart, E.J., A.R. Sanford and R.M. Ward, Geographic extent and shape of an extensive magma body at midcrustal depths in the Rio Grande rift near Socorro, New Mexico, in Riecker, R.E., ed., Rio Grande Rift: Tectonics and Magmatism, A.G.U., Wash., D.C., 237-251, 1979.

Sanford, A.R., O.S. Alptekin and T.R. Toppozada, Use of reflection phases on microearthquake seismograms to map an unusual discontinuity beneath the Rio Grande rift, Bull. Seism. Soc. Amer., 63, 2021-2034, 1973.

Sanford A.R., Temperature gradient and heat flow measurements in the Socorro, New Mexico area, N. Mex. Inst. of Mining and Technol., Geosc. Dept., Geophysics Open-File Report 15, 1977.

Sanford, A.R., R.P. Mott, P.J. Shuleski, and others, Geophysical evidence for a magma body in the crust in te vicinity of Socorr New Mixico, in Heacock, J.G., ed., The Earth's Crust, A.G.U., Monograph 20, 385-403, 1977.

Sanford A.R., Magma bodies in the Rio Grande rift in central New Mexico, New Mex. Geol. Soc. Guidebook, 34 Field Conference, Socorro Region II, 123-125, 1983.

Sanford, A.R., K.H. Olsen and L.H. Jaksha, Seismicity of the Rio Grande rift, in Riecker, R.E., ed., Rio Grande Rift: Tectonics

and Magmatism, A.G.U., Wash., D.C., 145-168, 1979.

Sanford, A.R. and P. Einarsson, Magma chambers in rifts, in Palmason G., ed., Continental and Oceanic Rifts, A.G.U., Geodynamics series, 8, 147-168, 1982.

Shuleski, P.J., Seismic fault motion and SV wave screening by shallow magma bodies in the vicinity of Socorro, New Mexico, N. Mex. Inst. of Mining and Technol., Geosc. Dept., Geophys Open-File Report no. 8, Socorro, 1976.

Sibson, R.H., Frictional constraints on thrust, wrench and normal faults, Nature, 249, 542-545, 1974.

Sibson, R.H., Fault rocks and fault mechanisms, Jour. Geol. Soc. Lond.,133, 191-213, 1977a.

Sibson R.H., Fault zone models, heat flow and depth distribution of earthquakes in the continental crust of the United States, Bull. Seism. Soc. Amer.0, 72, 151-163, 1982.

Tullis, J., and R.A. Yund, Experimental deformation of dry Westerly granite, Jour. of Geophys. Res., 82, 5705-5718, 1977.

Ward, R.M., Determination of three dimensional velocity anomalies within the upper crust in the vicinity of Socorro, New Mexico using first P-arrivals from local earthquakes, Ph.D. dissertation, N. Mex. Inst. of Mining and Technol., Socorro, 1980.

Wieder, D.P., Tectonic significance of microearthquake activity from composite fault-plane solutions in the Rio Grande rift near Socorro, New Mexico, N. Mex. Inst. of Mining and Technol., Geophys. Open-File Rep. no. 37, 159, 1981.

APPENDIX 1

Algorithm HYPO71 parameters.

Most outputs of HYPO71 are printed by the line-printer. Cards are punched only when the data must be read back into the computer for subsequent running of other computer programs. The printer outputs are generally self-explanatory; the following explanations may be helpful to the users. Results of the test run (listed in Appendix 2) is given in Appendix 3 (p. 90-96).

3.1 Iteration Output (optional).

If IPRN = 1 on the control card, a one-line output appears for each iteration. This information shows what happened in each adjustment from the trial hypocenter to the final hypocenter.

Heading	Explanation
I	Iteration step number. If a particular step is repeated, I is also repeated.
ORIG	Origin time in sec. Date, hour and minute are given in HYPOCENTER OUTPUT (Section 3.2).
LAT LONG Depth	Hypocenter location at Step I. See Section 3.2 for details.
DM	Epicentral distance in km to the nearest station.
RMS	Root mean square error of time residuals in sec. corrected for average P & S residual (AVRPS).
SKD	For S and D explanation, see Section 3.2. K denotes the status of the critical F-value (CF) in the iteration step. See Section 4 for more details. For K = 0, CF = TEST(03). For K = 1, CF = TEST(03)/TEST(06). For K = 2, F-test is skipped in order to calculate error estimates. For K = 3, On this step no variable met the F-test entrance criterion and termination will occur. For K = 4, F-test is skipped, and the most significant variable is found. This step is taken only if the adjustment is greater than TEST(06) times its standard error.

3.1 Iteration Output (optional). -- Continued

Heading	Explanation
CF	Critical F-value. Its value is controlled by K as described above.
ADJUSTMENTS (km)	Under these three columns, adjustments in km for the latitude (DLAT), longitude (DLON), and focal depth (DZ) from the multiple regression analysis are given.
PARTIAL F-VALUES	Under these three columns, the partial F-values for the hypocentral adjustments are given. Values not calculated are set equal to -1.00.
STANDARD ERRORS	Under these three columns, the standard errors for the hypocenter adjustments are given in km.
ADJUSTMENTS TAKEN	Under these three columns, the actual adjustments taken to reach the next trial hypocenter are given in km.

3.2 Hypocenter Output.

Heading	Example	Explanation
DATE	700630	Date of earthquake: Year, month, and day. In this case, it is June 30, 1970.
ORIGIN	1659 24.05	Origin time: hour, minute, and second (Greenwich civil time). In this case, it is 16 hr, 59 mn, and 24.05 sec.
LAT	37-48.64	Latitude of epicenter in degrees and minutes: 37° 48.64'.
LONG	121-57.59	Longitude of epicenter in degrees and minutes: 121° 57.59'
DEPTH	3.62	Focal depth in km: 3.62 km. A '*' may follow the DEPTH to indicate a fixed focal depth solution.
MAG	1.35	Magnitude of the earthquake. User specifies its choice from XMAG and/or FMAG.
NO	15	Number of station readings used in locating the earthquake. P and S arrivals for the same station are regarded as 2 readings. If NO = 3, a fixed depth solution is given. If NO<3, no solution is given.

3.2 Hypocenter Output. -- Continued

Heading	Example	Explanation
DM	2	Epicentral distance in km to the nearest station.
GAP	110	Largest azimuthal separation in degrees between stations.
M	1	Crustal model number. M is used for the Variable First-Layer Model only.
RMS	0.09	Root mean square error of time residuals in sec. RMS = $\sqrt{\Sigma R_i^2/NO}$, where R_i is the time residual for the i^{th} station.
ERH	0.4	Standard error of the epicenter in km.* ERH = $\sqrt{SDX^2 + SDY^2}$, where SDX and SDY are the standard errors in latitude and longitude, respectively, of the epicenter. If ERH = blank, this means that ERH cannot be computed because of insufficient data.
ERZ	1.2	Standard error of the focal depth in km.* If ERZ is blank, this means that ERZ cannot be computed either because focal depth is fixed in the solution or because of insufficient data.
Q	B	Solution quality of the hypocenter. This measure is intended to indicate the general reliability of the solution:

Q	Epicenter	Focal Depth
A	Excellent	good
B	good	fair
C	fair	poor
D	poor	poor

Q is taken as the average of QS and QD (defined below). For example, an A and a C yield a B, and two B's yield a B. When QS and QD are only one level apart, the lower one is used, i.e., an A and a B yield a B.

SQD	A|B	QS and QD rating, In this case, QS = A, and QD = B. QS is rated by the statistical measure of the solution as follows:

* Statistical interpretation of standard errors involves assumptions which may not be met in earthquake locations. Therefore the standard errors may not represent actual error limits.

3.2 Hypocenter Output. -- Continued

QS	RMS (sec)	ERH (km)	ERZ (km)
A	< 0.15	≤ 1.0	≤ 2.0
B	< 0.30	≤ 2.5	≤ 5.0
C	< 0.50	≤ 5.0	
D	Others		

QD is rated according to the station distribution as follows:

QD	NO	GAP	DMIN
A	≥ 6	≤ 90°	≤ DEPTH or 5 km
B	≥ 6	≤ 135°	≤ 2x DEPTH or 10 km
C	≥ 6	≤ 180°	≤ 50 km
D	Others		

Heading	Example	Explanation
ADJ	0.0	Last adjustment of hypocenter in km. Normally this is 0 or less than 0.05.
IN	0	Instruction code (KNST and INST in input)
NR	17	Number of station readings available. This includes readings which are not used in determining hypocenter.
AVR	0.00	Average of time residuals in sec. AVR ≡ $\Sigma_i R_i/NO.$ Normally this is 0.
AAR	0.07	Average of the absolute time residuals in sec. AAR ≡ $\Sigma_i \lvert R_i \rvert /NO.$
NM	5	Number of station readings available for computing maximum amplitude magnitude (XMAG).
AVXM	1.4	Average of XMAG of available stations.
SDXM	0.1	Standard deviation of XMAG of available stations.
NF	3	Number of station readings available for computing F-P magnitude (FMAG).
AVFM	1.3	Average of FMAG of available stations.
SDFM	0.2	Standard deviation of FMAG of available stations.
I	4	Number of iterations to reach the final hypocenter.

Items from DATE to Q inclusive are repeated at the head of every first-motion plot. If summary cards are punched, these items occupy from column 1 to 80.* However, order for M, GAP, and DMIN are changed. A heading card is punched preceding the summary cards, if IPUN $\geq$ 1 on the control card.

3.3 Station Output.

After each hypocenter output of 2 lines, station output follows for each station.

Heading	Example	Explanation
STN	BOL	Station name.
DIST	1.3	Epicentral distance in km.
AZM	202	Azimuthal angle between epicenter to station measured from north in degrees.
AIN	94	Angle of incidence measured with respect to downward vertical.
PRMK	IPUO	This is PRMX from input data.
HRMN	1659	Hour and minute of arrival time from input data.
P-SEC	25.30	The second's portion of P-arrival time from input data.
TPOBS	1.25	Observed P-travel time in sec. TPOBS ≡ T + DT - ORG where T is the P-arrival time, ORG is the origin time, and DT is the time correction from input data.
TPCAL	1.09	Calculated travel time in sec.
DLY/H1	0.05 or 3.12	If the Station Delay Model is used, then DLY means the station delay in sec from the input station list. If the Variable First-Layer Model is used, then H1 means the thickness of the first-layer in km at this station.
P-RES	0.16	Residual of P-arrival in sec. If the Station Delay Model is used, then P-RES ≡ TPOBS - (TPCAL + DLY). If '**' follows P-RES, it means that in the Jeffreys' weighting, this P-arrival is not reliable. If the Variable First-Layer Model is used, then P-RES ≡ TPOBS - TPCAL.

* The punch format is given on p.61 (773-775) & is used on p.64 (934-935).

3.3 Station Output. -- Continued

Heading	Example	Explanation
P-WT	1.06	Weight used in hypocenter solution for P-arrival. This weight is a combination of quality weight specified in the data and other selected weightings. WT's are always normalized so that the sum is equal to NO. Normalization is necessary so as to avoid distortion in computing standard errors.
AMX	15.0	Maximum amplitude in mm from input data.
PRX	0.10	Period of maximum amplitude in sec. from input data. If PRX is not given on the phase card, then PRR from the corresponding station card is used in the computation of XMAG, but is not printed here.
CALX	2.20	Calibration in mm used in computing XMAG. If CALX is blank in the phase card, then CALR from the corresponding station card is used and is printed here as CALX.
K	5	System number for the station from input data.
XMAG	1.60	Maximum amplitude magnitude computed from AMX, PRX, CALX and K. A * follows XMAG if XMAG - AVXM $\geq$ 0.5.
RMK	Q05	Remark from input data.
FMP	10.0	F-P in sec from input data.
FMAG	1.02	F-P magnitude computed from F-P and DIST. A * follows FMAG if FMAG - AVFM $\geq$ 0.5.
SRMK	$ES_{\Delta}2$	This is SRMK from input data.
S-SEC	26.50	The second's portion of S-arrival time from input data.
TSOBS	2.45	Observed S-travel time in sec. TSOBS $\equiv$ T + DT - ORG, where T is the S-arrival time, ORG is the origin time, and DT is the time correction from input data.
S-RES	-0.22	Residual of S-arrival in sec. If the Station Delay Model is used, then S-RES $\equiv$ TSOBS - POS* (TPCAL + DLY). If the Variable First-Layer Model is used, then S-RES $\equiv$ TSOBS - POS*TPCAL.
S-WT	0.5	Weight used in hypocenter solution for S-arrival. See explanation of P-WT for additional information.
DT	blank	Station time correction in sec. from input data. DT is used to correct all stations to the same time base.

If S-P interval data are used, the meanings of some of the above headings are changed as follows.

Heading	Explanation
P-RES	S-P residual in sec. It is defined by P-RES ≡ TSOBS - TPOBS - (POS - 1) (DLY + TPCAL) for the Station Delay Model. DLY is multiplied by zero for computing P-RES as above for the Variable First-Layer Model.
S-RES	Same as P-RES
P-WT	Weight used in hypocenter solution for S-P interval data.
S-WT	Will always be **** to denote S-P interval data.
TSOBS	Observed S-P interval in sec.

3.4 Map of Auxiliary RMS Values.

This is an optional output for which KTEST is set to 1 on the Control Card (see p. 14). RMS values are computed at 10 points on a sphere centered on the final hypocenter. Each RMS value corresponds to an origin time which has been corrected for the average residual of the P and S arrivals (AVRPS) given at that point. A 3-dimensional view of the auxiliary RMS value minus the final hypocenter RMS value is printed (DRMS). An example is shown below; the view is looking down to the northwest. It is necessary by NOT sufficient for all DRMS values to be positive for a good solution. If any DRMS value is negative, then the solution has not converged to a minimum. It is important to set the radius of the sphere appropriately for a given application (see p.9, TEST(13)).

LAT	LON	Z	AVRPS	RMS
8.17	14.76	0.0	-0.39	0.63
8.17	8.02	0.0	-1.42	0.23
8.17	14.76	9.62	-0.31	0.81
8.17	8.02	9.62	-1.19	0.30
5.47	11.39	0.0	-0.26	0.34
				0.11
5.47	11.39	13.28	-0.56	0.48
2.77	14.76	0.0	0.50	0.27
2.77	8.02	0.0	-0.88	0.60
2.77	14.76	9.62	0.37	0.63
2.77	8.02	9.62	-0.74	0.70

DRMS

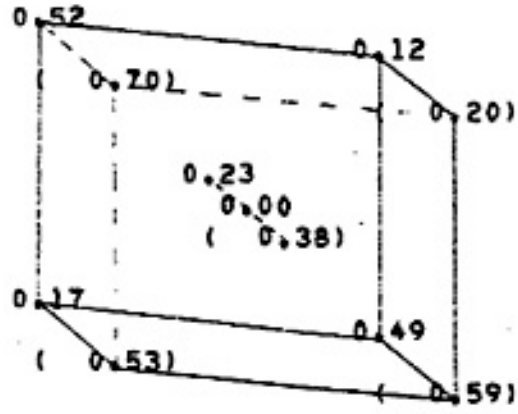

APPENDIX 2

Derivation of the hypocentral depth equation in which arrival times of S, P and S_zS phases are used, and examples of S_zS reflections off the Socorro magma body.

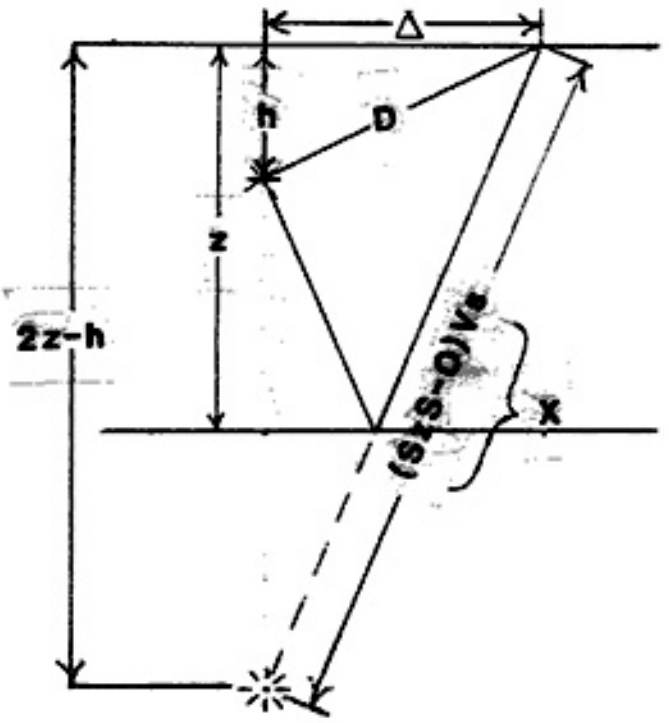

$$\Delta^2 = D^2 - h^2$$

$$X^2 = \Delta^2 + (2z - h)^2$$

$$= (D^2 - h^2) + 4z^2 - 4zh + h^2$$

$$h = \frac{D^2 + 4z^2 - X^2}{4z} \quad \text{where}$$

h = depth of focus

z = depth to magma body = 19.2 km

$D = t_t \; Vp = 1.37\,(S - P) \; 5.85$ km/sec

$X = (S_zS - 0) \; Vs = (S_zS - 0) \frac{5.85}{\sqrt{3}}$ km/sec

O = origin time

Examples of P, $\overline{S}$ and $\overline{S_zS}$ Phases

Date: Sep. 22 1984
Station: MAG
Time (Hr:Mn): 05:15

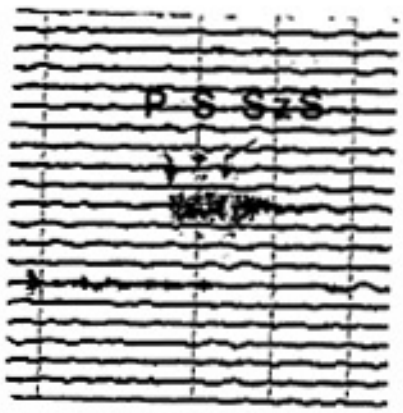

Date: Oct. 13,1984
Station: MAG
Time (Hr:Mn): 20:55

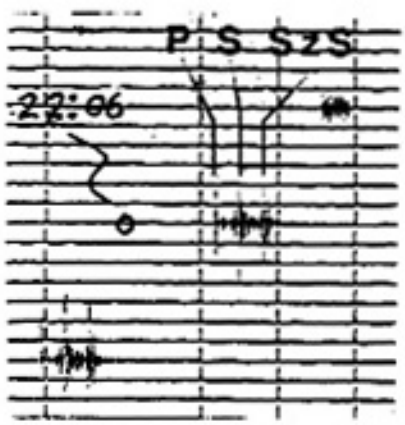

Date: Mar. 1 1985
Station: MAG
Time (Hr:Mn): 22:06

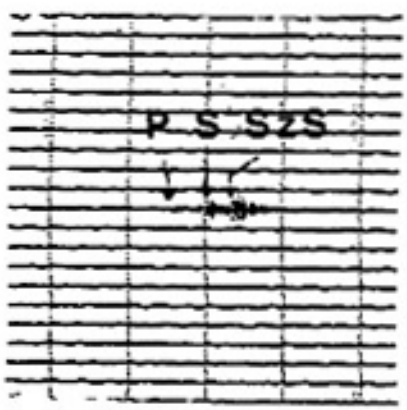

Date: July 8, 1985
Station: LAZ
Time (Hr:Mn): 04:34

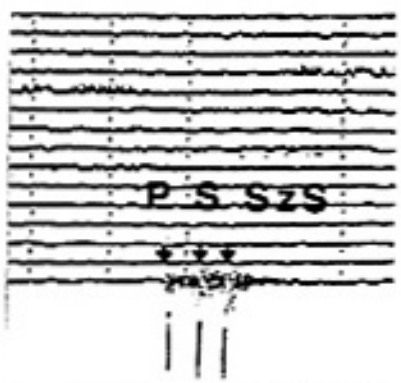

Date: May 15, 1985
Station: MAG
Time (Hr:Mn): 14:21

APPENDIX 3

* Temporal distribution of B quality for each year for preliminary data set B (497 events).

* Annual epicenter distributions (data set B).

* Epicentral distributions for given depth intervals (data set B).

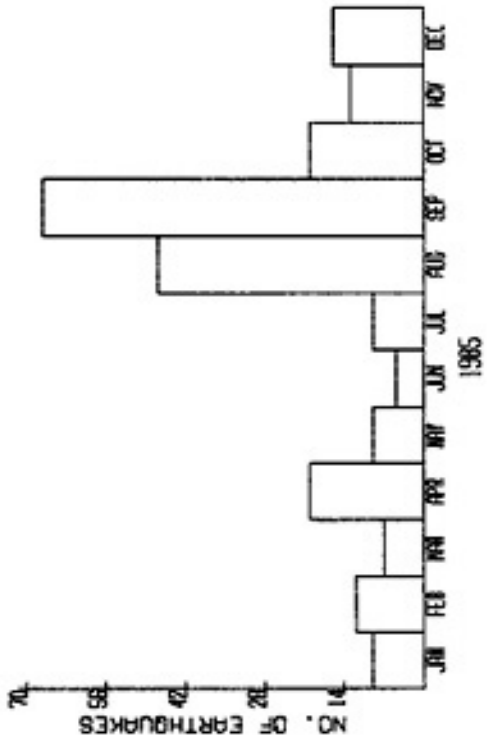
1985
NO. OF EARTHQUAKES
14
28
42
56
70
JAN
FEB
MAR
APR
MAY
JUN
JUL
AUG
SEP
OCT
NOV
DEC

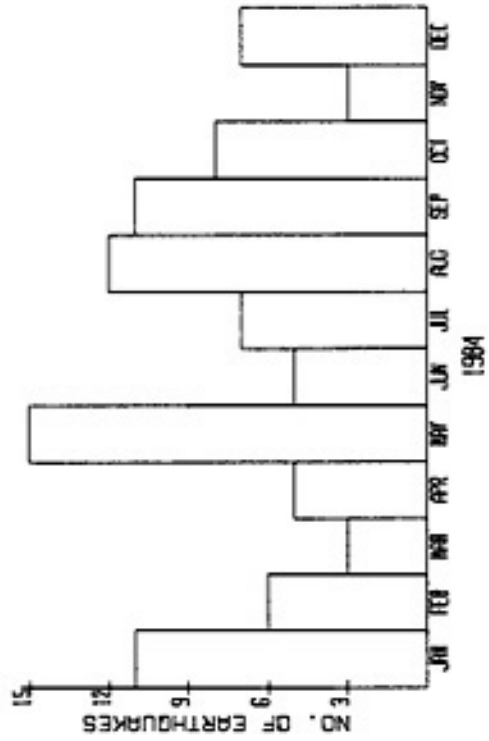
1984
NO. OF EARTHQUAKES
3
6
9
12
15
JAN
FEB
MAR
APR
MAY
JUN
JUL
AUG
SEP
OCT
NOV
DEC

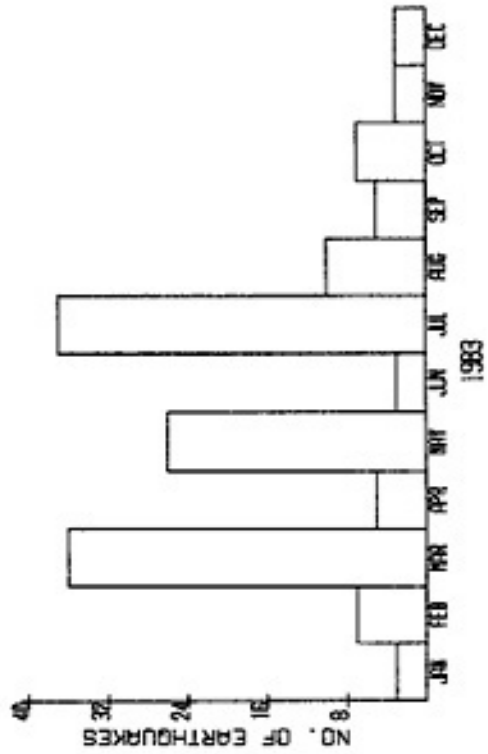
1983
NO. OF EARTHQUAKES
8
16
24
32
40
JAN
FEB
MAR
APR
MAY
JUN
JUL
AUG
SEP
OCT
NOV
DEC

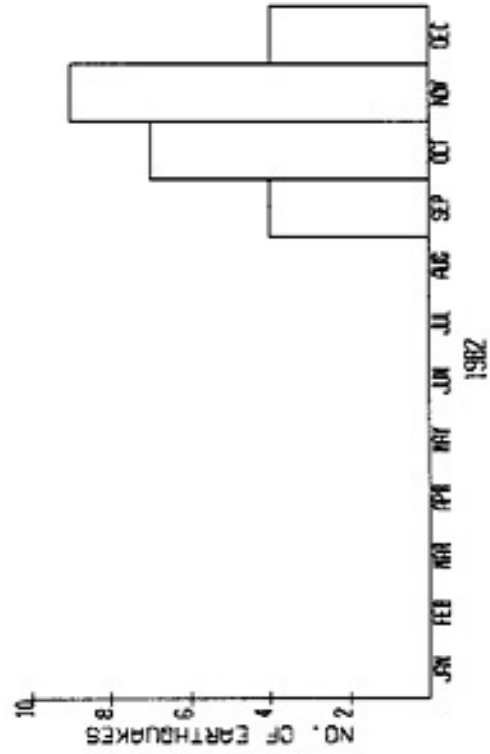
1982
NO. OF EARTHQUAKES
2
4
6
8
10
JAN
FEB
MAR
APR
MAY
JUN
JUL
AUG
SEP
OCT
NOV
DEC

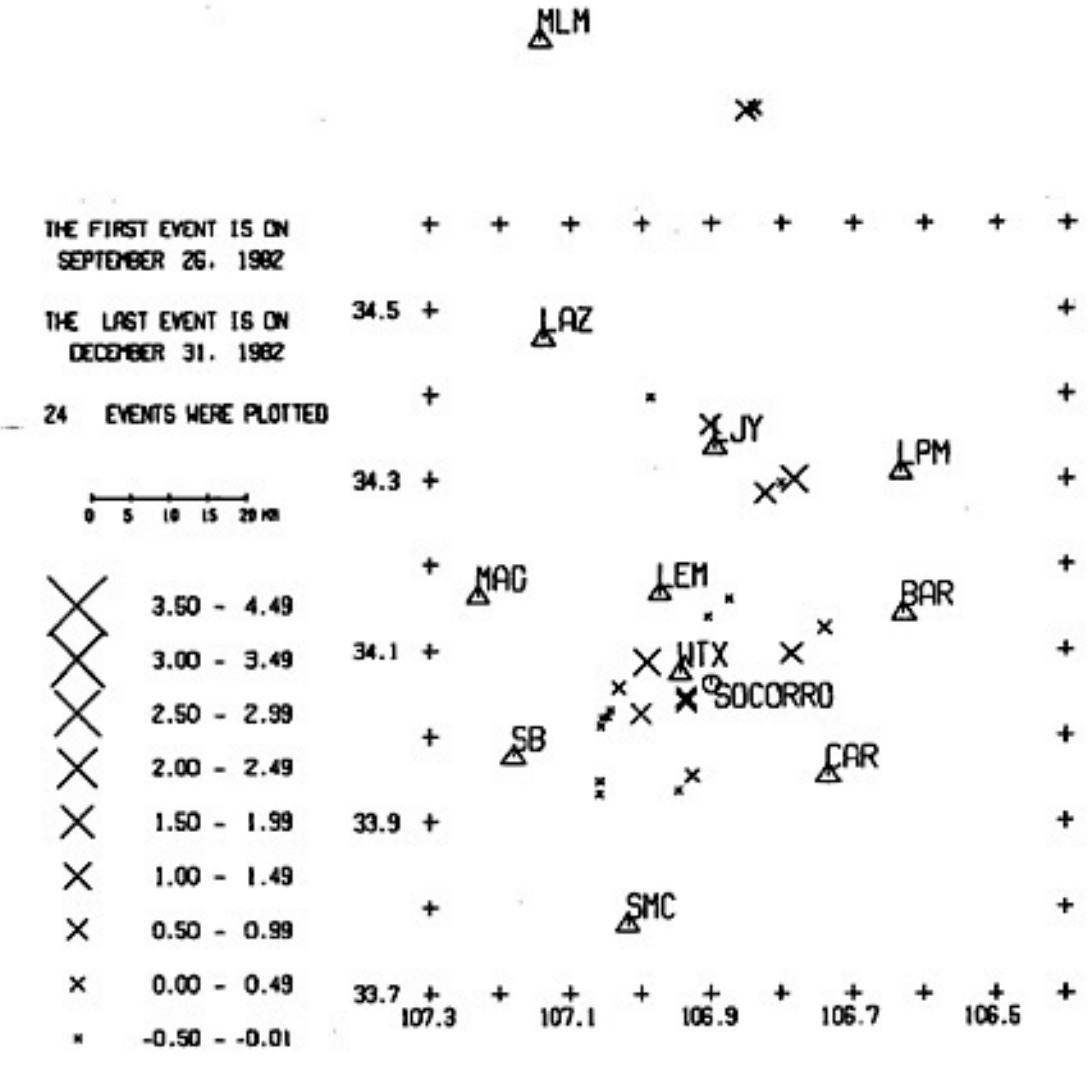
MLM
THE FIRST EVENT IS ON
SEPTEMBER 26, 1982
THE LAST EVENT IS ON
DECEMBER 31, 1982
24 EVENTS WERE PLOTTED
0 5 10 15 20 KM
3.50 - 4.49
3.00 - 3.49
2.50 - 2.99
2.00 - 2.49
1.50 - 1.99
1.00 - 1.49
0.50 - 0.99
0.00 - 0.49
-0.50 - -0.01
34.5
34.3
34.1
33.9
33.7
107.3
107.1
106.9
106.7
106.5
LAZ
JY
PM
MAC
LEM
BAR
WTX
SOCORRO
SB
CAR
SMC

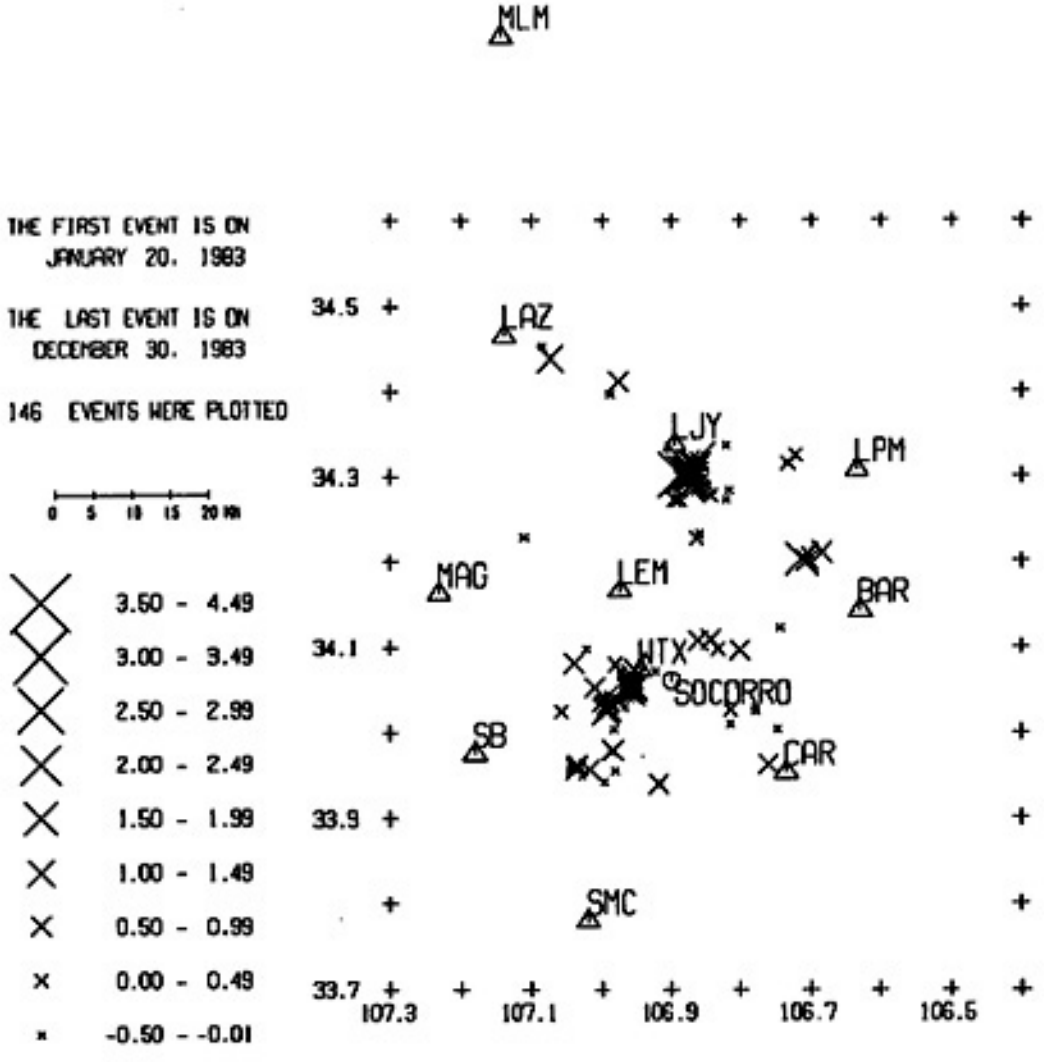
MLM
THE FIRST EVENT IS ON
JANUARY 20. 1983
THE LAST EVENT IS ON
DECEMBER 30. 1983
146 EVENTS WERE PLOTTED
0 5 10 15 20 km
3.50 - 4.49
3.00 - 3.49
2.50 - 2.99
2.00 - 2.49
1.50 - 1.99
1.00 - 1.49
0.50 - 0.99
0.00 - 0.49
-0.50 - -0.01
34.5
34.3
34.1
33.9
33.7
107.3
107.1
106.9
106.7
106.5
LAZ
LJY
LPM
MAG
LEM
BAR
WTX
SOCORRO
SB
CAR
SMC

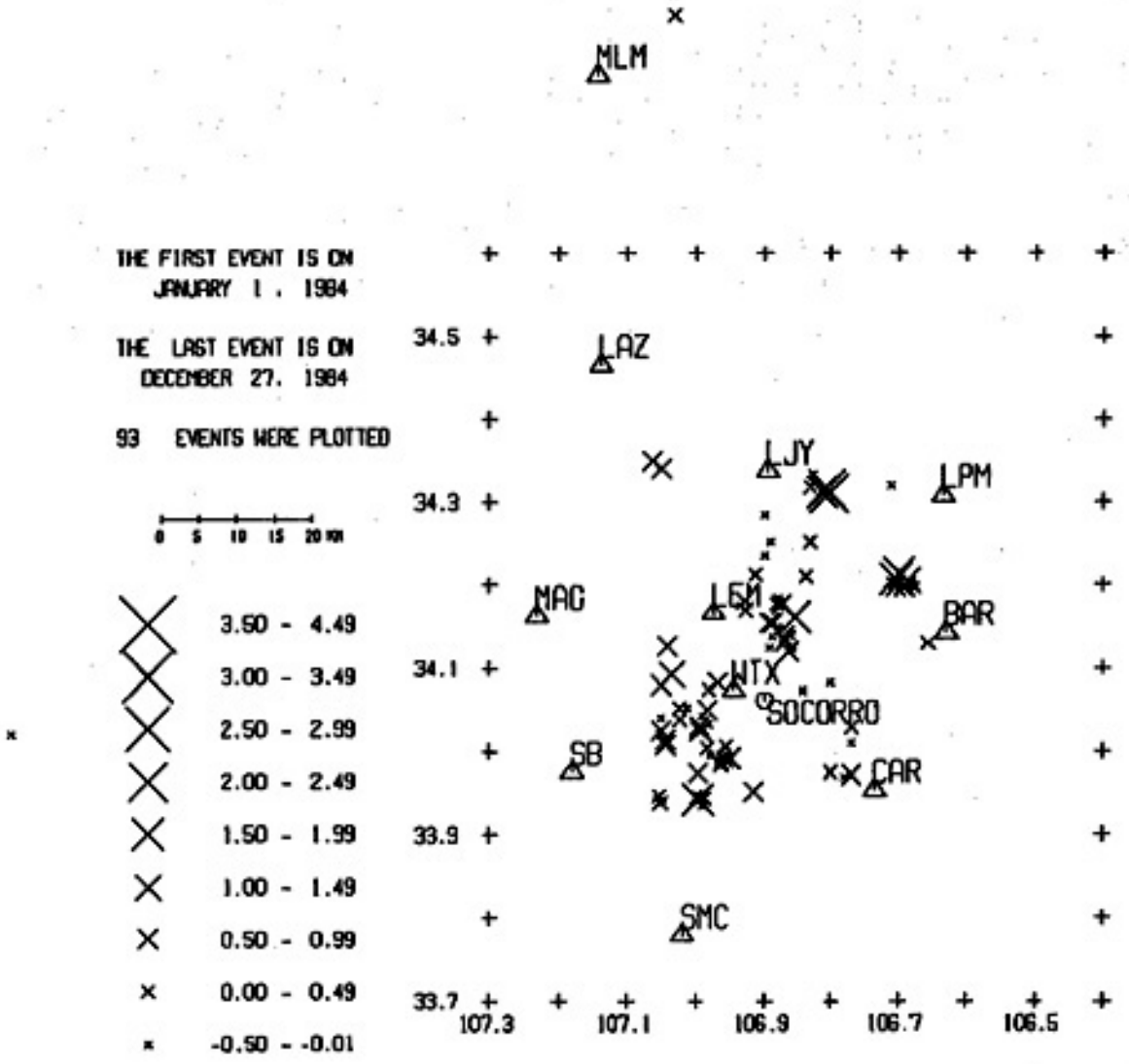
THE FIRST EVENT IS ON
JANUARY 1 , 1984
THE LAST EVENT IS ON
DECEMBER 27, 1984
93 EVENTS WERE PLOTTED
0 5 10 15 20 KM
3.50 - 4.49
3.00 - 3.49
2.50 - 2.99
2.00 - 2.49
1.50 - 1.99
1.00 - 1.49
0.50 - 0.99
0.00 - 0.49
-0.50 - -0.01
MLM
LAZ
JY
LPM
MAC
LEM
BAR
WTX
SOCORRO
SB
CAR
SMC
34.5
34.3
34.1
33.9
33.7
107.3
107.1
106.9
106.7
106.5

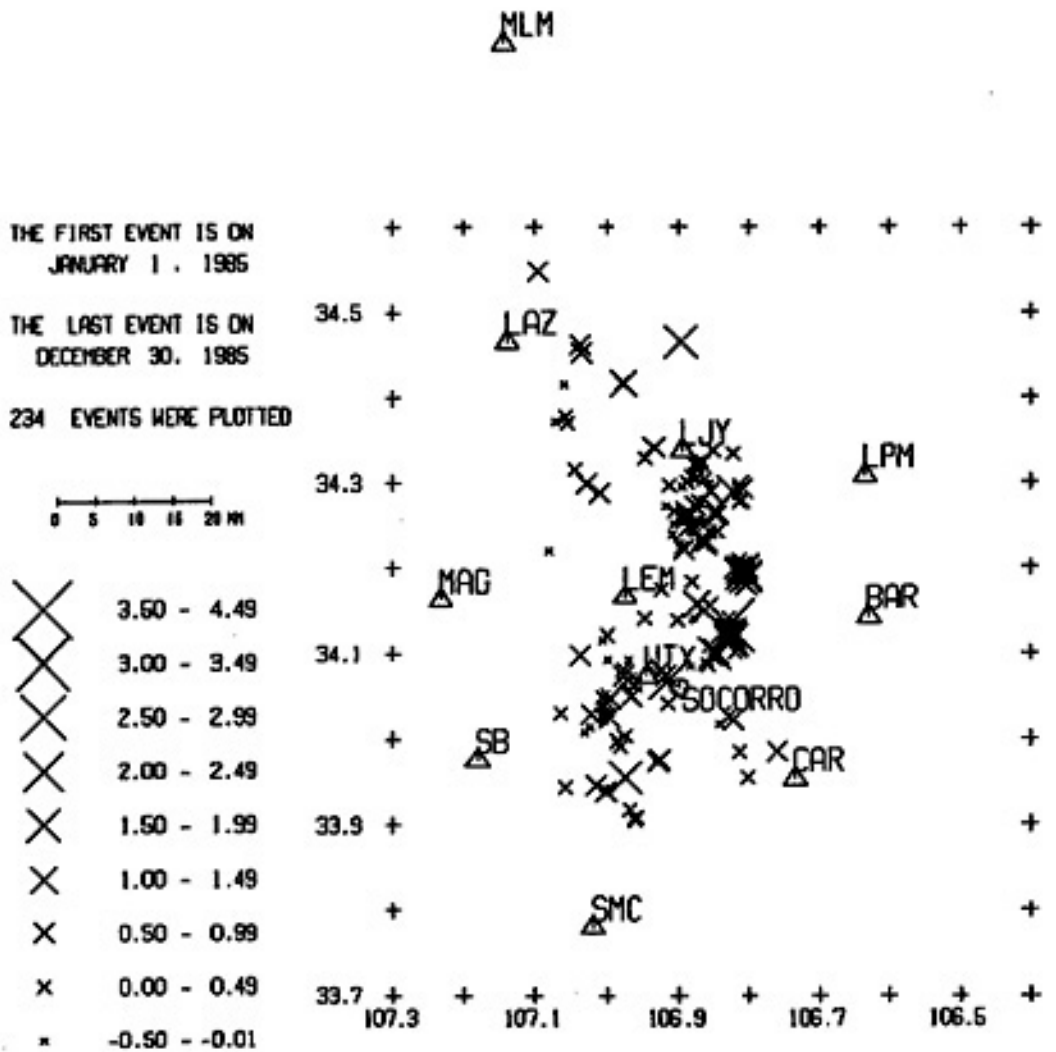
MLM
THE FIRST EVENT IS ON
JANUARY 1 . 1985
THE LAST EVENT IS ON
DECEMBER 30. 1985
234 EVENTS WERE PLOTTED
0 5 10 15 20 MM
3.50 - 4.49
3.00 - 3.49
2.50 - 2.99
2.00 - 2.49
1.50 - 1.99
1.00 - 1.49
0.50 - 0.99
0.00 - 0.49
-0.50 - -0.01
34.5
34.3
34.1
33.9
33.7
107.3
107.1
106.9
106.7
106.5
LAZ
JV
LPM
MAG
LEM
BAR
WTX
SOCORRO
SB
CAR
SMC

FOCAL DEPTHS < 4 KM

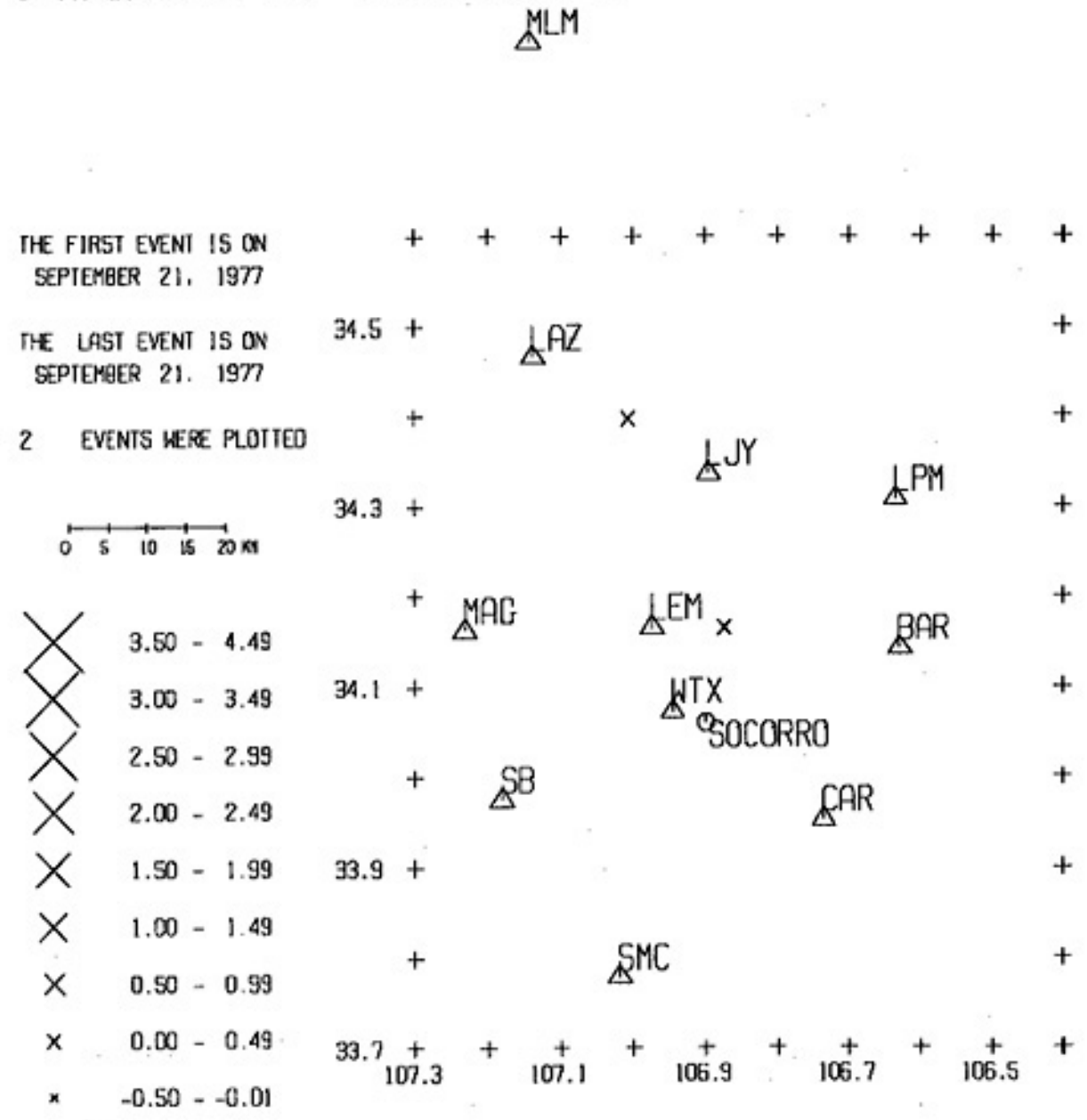

FOCAL DEPTHS 4-6 KM

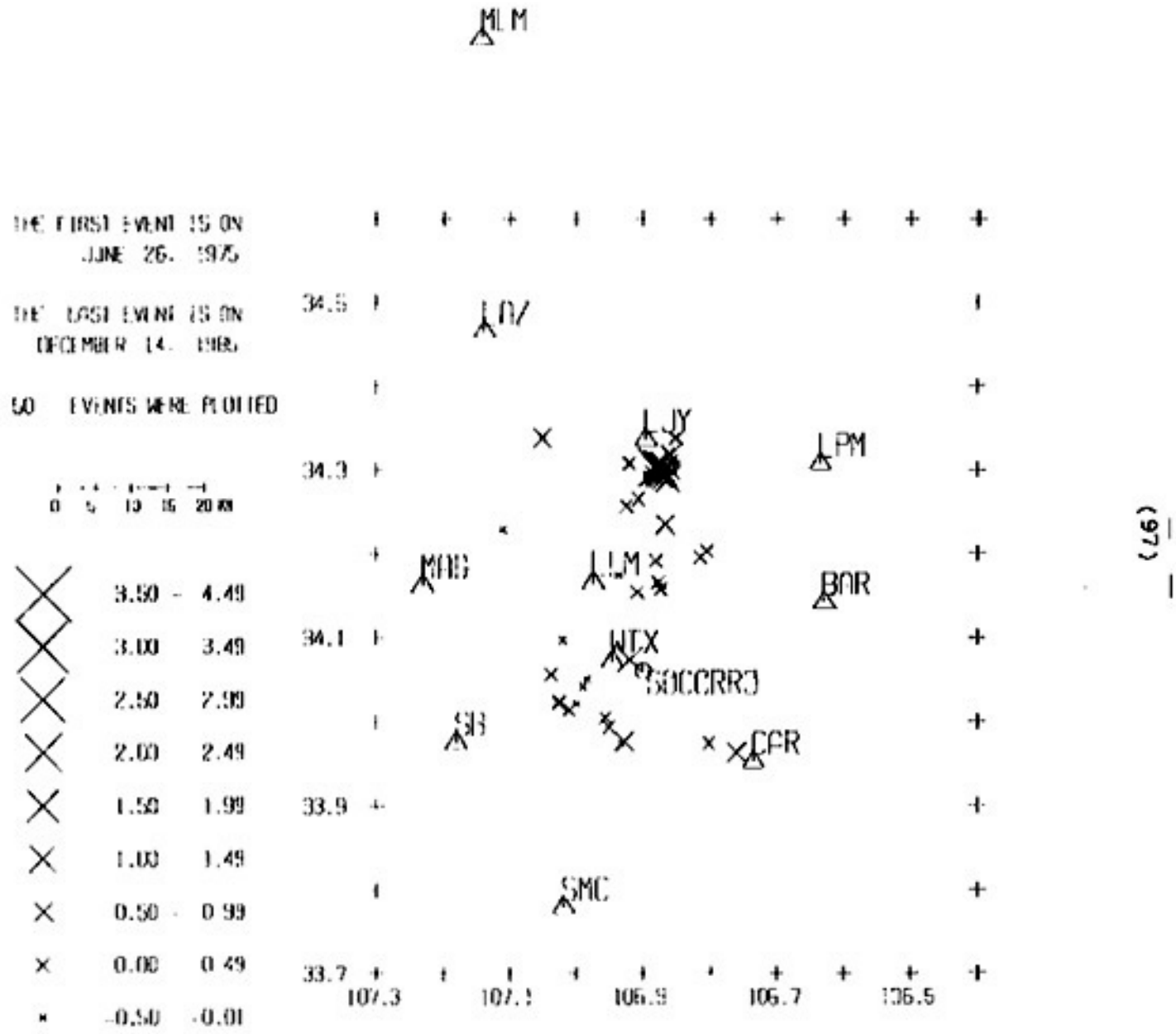

(97)

FOCAL DEPTHS 6-8 KM

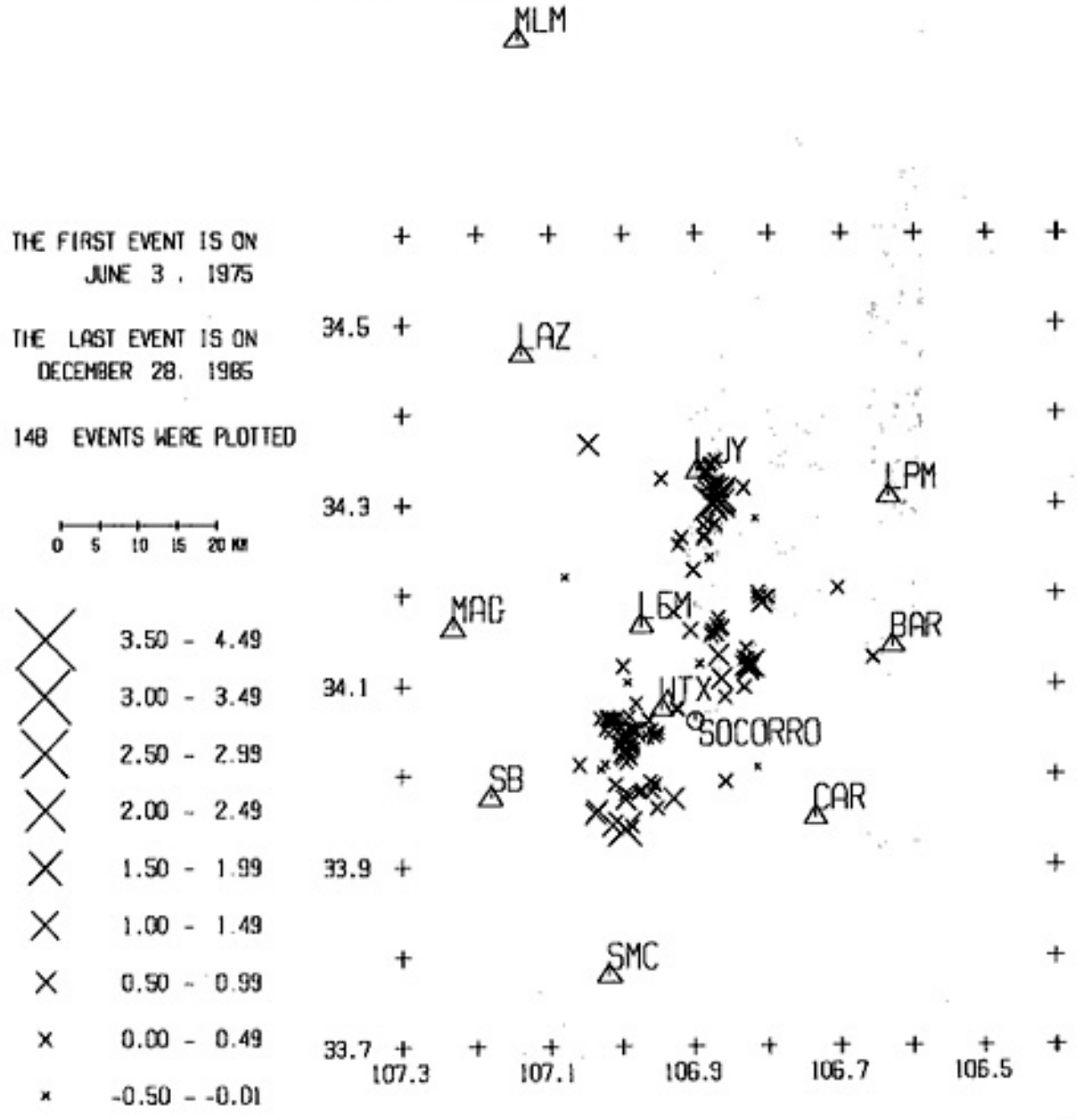

FOCAL DEPTHS 8-10 KM

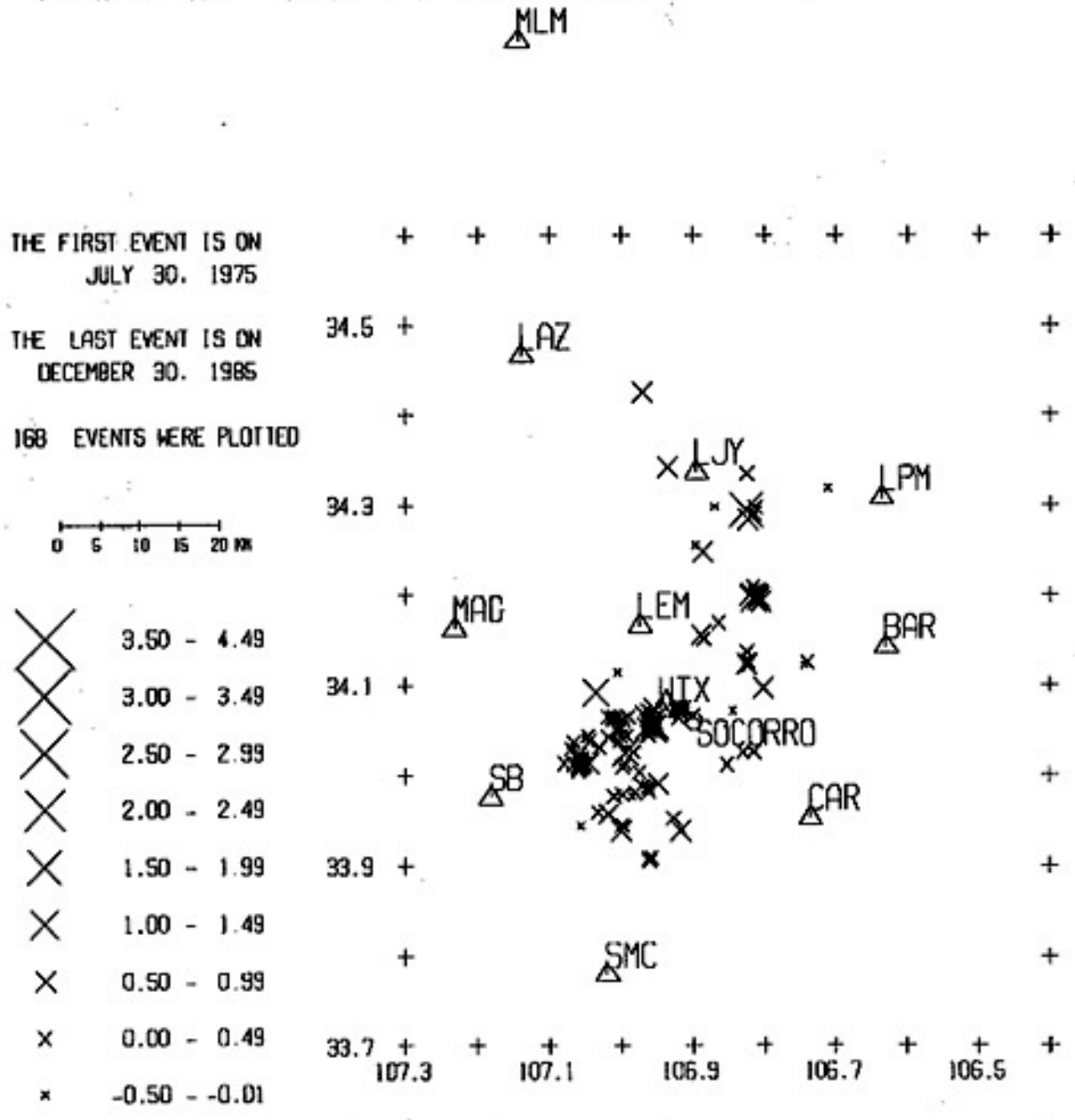

FOCAL DEPTHS 10-12 KM

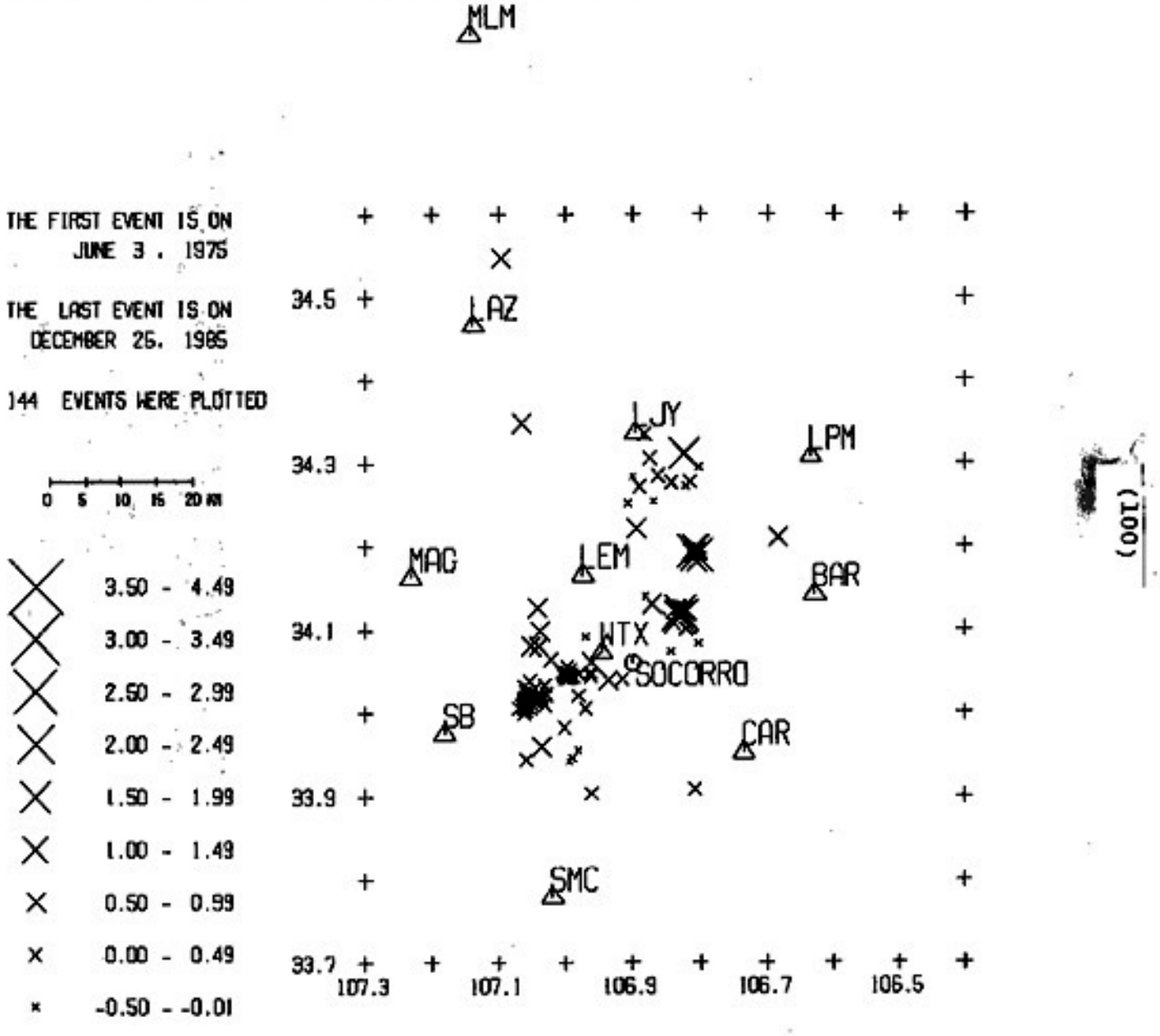

FOCAL DEPTHS > 12 KM

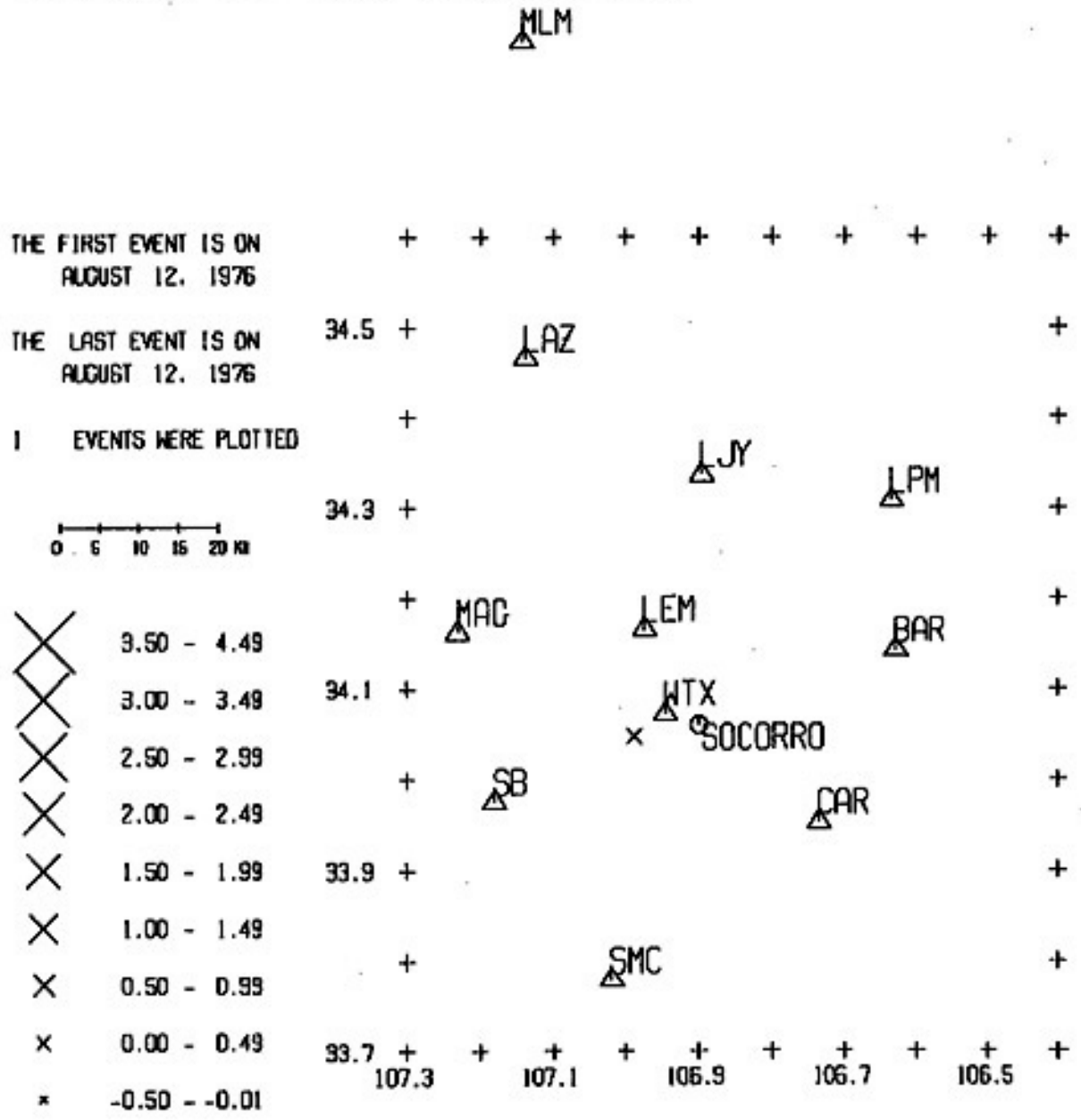

APPENDIX 4

Main program and subroutines used for the majority of data processing and plots.

```
      PROGRAM BQUAL
      CHARACTER FILNM*10,ZNM*10
      INTEGER K,TNO,M1,M2,M3,M4,MD,COUNT
      REAL TDEP,TERH,TERZ,MIN,MAX,AVED,AVEH,AVEZ,XD,XH,XZ,SDD,SDH,SDZ,
     *     P,R,LGI,LGF,LTI,LTF,D,E,F,G,S,T,V,W,S1,T1,V1
      DIMENSION IYR(1000),IMO(1000),IDY(1000),IHR(1000),IMN(1000),
     *    SEC(1000),LATD(1000),FLATM(1000),LONGD(1000),FLONGM(1000),
     *    DEPTH(1000),FMAG(1000),NO(1000),IDM(1000),IGAP(1000),
     *    RMS(1000),ERH(1000),ERZ(1000),IQ(1000),IQS(1000),IQD(1000),
     *    SUBD(1000),SUBH(1000),SUBZ(1000),FLAT(1000),FLONG(1000),
     *    DD(1000),CD(1000),IDATE(1000),MYR(1000),BLT(1000),BLG(1000)
      REAL X1(50),Y1(50),X(7),Y(7),Z(7,7),M(2,7,7),SA(6)
C
2     FORMAT(A10)
3     FORMAT(' DESIGNATE INPUT FILE:',$)
4     FORMAT(' NUMBER OF EVENTS IN INPUT FILE?:')
5     FORMAT(I)
6     FORMAT(5x,i6,2X,f9.2,2X,f6.3,2X,f7.3,2X,f5.2,2X,f4.1,2(2X,i2),
     *  2x,i3,2x,f4.2,2(2x,f4.1),3(2x,i1))
7     FORMAT(/T6,' DATE',T16,' O.T.',T26,' LAT',T34,' LONG',T41,
     *' DEPTH',T49,' MAG',T54,' NO',T58,' DM',T62,' GAP',T67,' RMS',
     *T74,' ERH',T80,' ERZ',T85,' Q',T87,' QS',T90,' QD'//)
8     FORMAT(' AVERAGE DEPTH= ',F5.2,' km +/- ',F5.3,'(1 s.d.)')
9     FORMAT(' AVERAGE ERROR IN EPICENTRAL LOCATION= ',F4.1,' km +/- ',
     *      F5.3,'(1 s.d.)')
10    FORMAT(' AVERAGE ERROR IN FOCAL DEPTH= ',F4.2,' km +/- ',F5.3,
     *      '(1 s.d.)')
11    FORMAT(' NUMBER OF EVENTS ',I3)
12    FORMAT(' NUMBER OF READINGS= ',I4)
13    FORMAT(' THE GREATEST FOCAL DEPTH= ',F5.2,'km')
14    FORMAT(' THE SHALLOWEST FOCAL DEPTH= ',F5.2,'km')
15    FORMAT(' SPECIFY THE INCREMENT OF LATITUDE: ')
16    FORMAT(' SPECIFY THE INCREMENT OF LONGITUDE: ')
17    FORMAT(//' FOR LATITUDES BETWEEN ',F7.3,' AND ',F7.3,
     *      ' AND LONGITUDES BETWEEN ',F7.3,' AND ',F7.3,' : '/)
18    FORMAT(//' NUMBER OF MEQS B/B OR BETTER= ',F5.1)
19    FORMAT(' % OF EVENTS WITH DEPTH OF FOCI < 4.0km= ',F5.1,'%')
20    FORMAT(' 4.0km < % OF EVENTS WITH DEPTH OF FOCI < 12.0km= ',F5.1,
     *      '%')
21    FORMAT(' % OF EVENTS WITH DEPTH OF FOCI > 12.0km= ',F5.1,'%')
22    FORMAT(' NO. OF EVENTS OF MAGNITUDE>2.0 AT DEPTHS>12.0= ',I3)
23    FORMAT(' NO. OF EVENTS OF MAGNITUDE<1.0= ',I3)
24    FORMAT(' NO. OF EVENTS OF MAGNITUDE>1.0 AND <2.0= ',I3)
25    FORMAT(' NO. OF EVENTS OF MAGNITUDE>2.0 AND <3.0= ',I3)
26    FORMAT(' NO. OF EVENTS OF MAGNITUDE>3.0= ',I3)
C
C     INITIALIZATION OF VARIABLES
C
      K=0
      J=0
      N=0
      TDEP=0.0
      TERH=0.0
      TERZ=0.0
      TNO=0
      MIN=30.0
      MAX=0.0
      XD=0.0
      XH=0.0
      XZ=0.0
```

```
      WRITE(5,*)'LAT AND LON COORDS. FOR ENTIRE NETWORK(Y OR N)?'
      READ(5,'A')LLAN
      IF((LLAN.EQ.'Y').OR.(LLAN.EQ.'y'))THEN
       LGI=106.400
       LGF=107.300
       LTI=33.700
       LTF=34.600
      END IF
      IF((LLAN.EQ.'N').OR.(LLAN.EQ.'n'))THEN
       WRITE(5,*)'SPECIFY INITIAL LONG., FINAL LONG., INITIAL LAT.,
     *  FINAL LAT.--IN THAT ORDER'
       READ(5,*)LGI,LGF,LTI,LTF
      END IF
      S=0
      T=0
      V=0
      M1=0
      M2=0
      M3=0
      M4=0
      MD=0
      SLT=33.85
      SLN=107.25
      A=1.539798
      B=1.848673
      CLT=33.978
      CLG=106.979
      LTCOR=60.*1.848673
      LGCOR=60.*1.539798
C
CC    INITIALIZATION OF ARRAYS
C
      DO 80 I=1,1000
       DEPTH(I)=0.0
       ERH(I)=0.0
       ERZ(I)=0.0
       NO(I)=0
       FLAT(I)=0.0
       FLONG(I)=0.0
       SUBD(I)=0.0
       SUBH(I)=0.0
       SUBZ(I)=0.0
80    CONTINUE
      WRITE(5,3)
      READ(5,2) FILNM
      OPEN(UNIT=22,DEVICE='DSK',ACCESS='SEQIN',FILE=FILNM)
C
CC    INPUT DATA FILE
C
1     FORMAT(3I2,1X,2I2,F5.2,1X,I2,F5.2,1X,I3,F5.2,1X,F5.2,1X,F5.2,
     *  1X,I2,1X,I2,1X,I3,1X,F4.2,1X,F3.1,1X,F3.1,1X,I1,1X,I1,1X,I1)
211   FORMAT(5x,i2,i2,i2,2X,i2,i2,f5.2,2X,f6.3,2X,f7.3,2X,f5.2,2X,f4.1,
     *  2(2X,i2),2x,i3,2x,f4.2,2(2x,f4.1),3(2x,i1))
      count=0
      WRITE(5,*)'PRINT OUT DATA? (Y OR N)?'
      READ(5,'A')PD
      IF((PD.EQ.'N').OR.(PD.EQ.'n'))GO TO 81
C     WRITE(3,7)
81    DO 100 I=1,1000
      READ(22,1,end=150)IYR(I),IMO(I),IDY(I),IHR(I),IMN(I),SEC(I),
```

```
*   LATD(i),FLATM(I),LONGD(i),FLONGM(I),DEPTH(i),FMAG(i),
*   NO(i),IDM(i),IGAP(i),RMS(i),ERH(i),ERZ(i),IQ(i),IQS(i),IQD(i)
    FLAT(I)=LATD(I)+FLATM(I)/60.
    FLONG(I)=LONGD(I)+FLONGM(I)/60.
    COUNT=count+1
    IF((PD.EQ.'N').OR.(PD.EQ.'n'))GO TO 100
C   IF((FLAT(I).LE.34.25).AND.(FLAT(I).GE.34.15))THEN
C    IF((FLONG(I).LE.106.85).AND.(FLONG(I).GE.106.8))THEN
C     IF((DEPTH(I).GT.2.).AND.(DEPTH(I).LE.12.))THEN
      WRITE(3,211)IYR(I),IMO(I),IDY(I),IHR(I),IMN(I),SEC(I),
*     FLAT(I),FLONG(I),DEPTH(I),FMAG(I),
*     NO(I),IDM(I),IGAP(I),RMS(I),ERH(I),ERZ(I),IQ(I),IQS(I),IQD(I)
C     END IF
C    END IF
C   END IF
100 CONTINUE
150 WRITE(5,*)'NUMBER OF EVENTS IN DATA FILE= ',COUNT
    WRITE(5,*)'          MENU:
*
*                                        '
    WRITE(5,*)'   MEAN DEPTHS AND S.DEVS.=1'
    WRITE(5,*)'   NO. OF EVENTS VS. DEPTH=2'
    WRITE(5,*)'   X-SECTION--X VS. HYPO. DEPTH=3'
    WRITE(5,*)'   RADIAL CONSTRAINT=4'
    READ(5,*)MNO
    IF(MNO.EQ.1)GO TO 82
    IF(MNO.EQ.2)CALL DEEP(DEPTH,IYR,COUNT,FLAT,FLONG)
    IF(MNO.EQ.3)CALL XSEX(FLAT,FLONG,DEPTH,COUNT)
    IF(MNO.EQ.4)CALL RAD(COUNT,FLAT,FLONG,DEPTH)
    GO TO 161
C
C   SPECIFICATION OF LAT. AND LONG. INCREMENTS
C
82  WRITE(5,15)
    READ(5,*)D
    WRITE(5,16)
    READ(5,*)E
C
C   CALCULATION OF AVERAGES,S.D.'S,MAX AND MINS
C
    WRITE(5,*)'DO YOU WANT OUTPUT SENT TO DATA FILE (Y OR N)?'
    READ(5,'A')SEND
    IF((SEND.EQ.'N').OR.(SEND.EQ.'n'))GO TO 38
    WRITE(5,37)
37  FORMAT(' DESIGNATE DEPTH FILE: ',$)
    READ(5,2)ZNM
    OPEN(UNIT=23,DEVICE='DSK',ACCESS='SEQOUT',FILE=ZNM)
C   LTI=34.005
C   LTF=34.025
C   LGI=107.05
C   LGF=107.0617
38  DO 110 P=LTI,LTF,D
     F=P+D
     J=J+1
     DO 115 R=LGI,LGF,E
      G=R+E
      DO 120 I=1,COUNT
       IF((FLAT(I).GE.P).AND.(FLAT(I).LT.F))THEN
        IF((FLONG(I).GE.R).AND.(FLONG(I).LT.G))THEN
C
```

```
C       OPTIONAL CONDITIONS                (106)
C
C           IF((FMAG(I).GT.1.).AND.(IQS(I).EQ.1))THEN
C           IF(IQS(I).EQ.1)THEN
C           IF((IQS(I).EQ.1).AND.(DEPTH(I).NE.7))THEN
C           IF(DEPTH(I).EQ.7.)WRITE(3,*)IQS(I),'/',IQD(I)
            IF(DEPTH(I).EQ.7.)THEN
          IF((SEND.EQ.'N').OR.(SEND.EQ.'n'))GO TO 39
          WRITE(23,1)IYR(I),IMO(I),IDY(I),IHR(I),IMN(I),SEC(I),
     *    LATD(I),FLATM(I),LONGD(I),FLONGM(I),DEPTH(I),FMAG(I),
     *    NO(I),IDM(I),IGAP(I),RMS(I),ERH(I),ERZ(I),IQ(I),IQS(I),IQD(I)
39            K=K+1
              DD(K)=DEPTH(I)
              MYR(K)=IYR(I)
              BLT(K)=FLAT(I)
              BLG(K)=FLONG(I)
              XD=DEPTH(I)**2.+XD
              XH=ERH(I)**2.+XH
              XZ=ERZ(I)**2.+XZ
              TDEP=TDEP+DEPTH(I)
              TERH=TERH+ERH(I)
              TERZ=TERZ+ERZ(I)
              TNO=TNO+NO(I)
              IF(MIN.GT.DEPTH(I))THEN
               MIN=DEPTH(I)
              END IF
              IF(MAX.LT.DEPTH(I))THEN
               MAX=DEPTH(I)
              END IF
             END IF
            END IF
            END IF
120         CONTINUE
          WRITE(5,*)'K=',K
            N=N+1
            IF((K.EQ.0).OR.(K.EQ.1))GO TO 115
C
C       OPTION TO CALL DEEP
C
          WRITE(5,*)'DO YOU WANT TO SEE A DEPTH DISTRIBUTION (Y OR N)?'
          READ(5,'A')YEN
          IF((YEN.EQ.'N').OR.(YEN.EQ.'n'))GO TO 114
            CALL DEEP(DD,MYR,K,BLT,BLG)
            GO TO 161
C
            WRITE(3,17)P,F,R,G
            CALL MEAN(TDEP,XD,K,SM,SD)
            WRITE(3,8)SM,SD
114         CALL MEAN(TERH,XH,K,SM,SD)
            WRITE(3,9)SM,SD
            CALL MEAN(TERZ,XZ,K,SM,SD)
            WRITE(3,10)SM,SD
            WRITE(3,11)K
            WRITE(3,12)TNO
            WRITE(3,13)MAX
            WRITE(3,14)MIN
            K=0
            TDEP=0.0
            TERH=0.0
            TERZ=0.0
```

```
          TNO=0
          MIN=30.00
          MAX=0.0
          XD=0.0
          XH=0.0
          XZ=0.0
115       CONTINUE
          N=0
110       CONTINUE
          CLOSE(UNIT=23)
          DO 160 I=1,COUNT
           IF ((DEPTH(I).LE.4.0).AND.(DEPTH(I).NE.0.0))THEN
            S=S+1
           ELSE IF((DEPTH(I).GT.4.0).AND.(DEPTH(I).LE.12.0))THEN
            T=T+1
           ELSE
            V=V+1
           END IF
          IF (DEPTH(I).GE.12.0)THEN
           IF(FMAG(I).GE.2.0)THEN
            MD=MD+1
           END IF
          END IF
          IF(FMAG(I).LE.1.0)THEN
           M1=M1+1
          ELSE IF((FMAG(I).LE.2.0).AND.(FMAG(I).GT.1.0))THEN
           M2=M2+1
          ELSE IF((FMAG(I).LE.3.0).AND.(FMAG(I).GT.2.0))THEN
           M3=M3+1
          ELSE
           M4=M4+1
          END IF
160       CONTINUE
          W=S+T+V
          S1=S/W*100.
          T1=T/W*100.
          V1=V/W*100.
          WRITE(3,18)W
          WRITE(3,19)S1
          WRITE(3,20)T1
          WRITE(3,21)V1
          WRITE(3,22)MD
          WRITE(3,23)M1
          WRITE(3,24)M2
          WRITE(3,25)M3
          WRITE(3,26)M4
          CLOSE(UNIT=22)
          GO TO 161
161       STOP
          END
C
C         MEAN CALCULATES THE >MEAN AND S.D.
C
          SUBROUTINE MEAN(X,X2,N,SSM,SSD)
          SSM=0.
          SSD=0.
          SSM=X/N
          SSD=SQRT(((N*X2)-(X**2.))/(N*(N-1)))
          END
C
```

```
C       SUBROUTINE DEEP PLOTS NUMBER OF EVENTS VS DEPTH
C
        SUBROUTINE DEEP(Z,NYR,C,GLAT,GLONG)
        DIMENSION Z(1000),NYR(1000),sum(1000),GLAT(1000),GLONG(1000)
        REAL GT1,GT2,GN1,GN2
        INTEGER C
        CHARACTER YL5*18,YL3*9,YL6*30,YORN,PN*5,RET*20
        np=1
        DZ=2.
        WRITE(5,*)'ENTER PLOT NAME: '
        READ(5,'A')PN
        CALL INITAL(-1,PN)
169     WRITE(5,*)'DO YOU WANT LAT. AND LONG. RESTRICTIONS?(Y OR N)'
        READ(5,'A')YORN
        IF((YORN.EQ.'N').or.(YORN.EQ.'n'))GO TO 171
        WRITE(5,*)'ENTER INITIAL LATITUDE COORDINATE'
        READ(5,*)GT1
        WRITE(5,*)'ENTER FINAL LATITUDE COORDINATE'
        READ(5,*)GT2
        WRITE(5,*)'ENTER INITIAL LONGITUDE COORDINATE'
        READ(5,*)GN1
        WRITE(5,*)'ENTER FINAL LONGITUDE COORDINATE'
        READ(5,*)GN2
171     WRITE(5,*)'ENTER THE CORRECT YEAR (19--) '
        READ(5,*)NY
        L=0
        DO 172 K=1,12
         SUM(K)=0.
172     CONTINUE
        FM=-1.
        ENUM=0.
        KK=0
        SUM(0)=0.
        DO 30 DK=0.,24.,DZ
         L=L+1
         DO 40 I=1,C
C         IF(NYR(I).NE.NY)GO TO 40
C         IF(NYR(I).EQ.NY)THEN
          IF((YORN.EQ.'N').or.(YORN.EQ.'n'))GO TO 31
           IF((GLAT(I).GE.GT1).AND.(GLAT(I).LE.GT2))THEN
            IF((GLONG(I).GE.GN1).AND.(GLONG(I).LE.GN2))THEN
             IF((Z(I).GE.DK).AND.(Z(I).LT.DK+DZ))THEN
              SUM(L)=SUM(L)+1.
              ENUM=ENUM+1.
              IF (FM.LT.SUM(L))FM=SUM(L)
             END IF
            END IF
           END IF
          GO TO 40
31           IF((Z(I).GE.DK).AND.(Z(I).LT.DK+DZ))THEN
              SUM(L)=SUM(L)+1.
              ENUM=ENUM+1.
              IF (FM.LT.SUM(L))FM=SUM(L)
             END IF
C         END IF
40       CONTINUE
        IF(SUM(L).NE.0.)KK=KK+1
        IF((SUM(L).EQ.0.).AND.(((SUM(L-1)).AND.(SUM(L+1))).NE.0.))
     *  KK=KK+1
30      CONTINUE
```

```
C
C       OPTION TO CALL HIST--% OF EVENTS VS DEPTH
C
        WRITE(5,*)'CALL HIST(Y OR N)?'
        READ(5,'A')HST
        IF((HST.EQ.'N').OR.(HST.EQ.'n'))GO TO 83
        CALL HIST(NP,SUM,ENUM)
        GO TO 72
C
C       OPTION TO CALL AVE
C
C       CALL AVE(KK,ENUM,SUM)
83      WRITE(5,*)'FM= ',FM
        CALL SCALE(FM,SF)
        WRITE(5,*)'SF= ',SF
        IF(NP.EQ.1)CALL PLOT(1.,1.,-3)
        IF(NP.EQ.2)CALL PLOT(0.,9.,-3)
        IF(NP.EQ.3)CALL PLOT(14.,-9.,-3)
        IF(NP.EQ.4)CALL PLOT(0.,9.,-3)
        CALL PLOT(12.,0.,2)
        CALL PLOT(0.,0.,3)
        CALL PLOT(0.,5.,2)
        CALL PLOT(0.,0.,3)
        k=0
        DO 50 TI=1.,11.,1.
         K=K+1
         X=TI-1.
         Y=SUM(K)/SF
         CALL PLOT(X,Y,2)
         X=X+1.
         CALL PLOT(X,Y,2)
         CALL PLOT(X,0.,2)
50      CONTINUE
        DO 60 TK=1.,12.,1.
         YL4=2.*TK
         CALL NUMBER(TK,-.25,.2,YL4,0.,0)
60      CONTINUE
        YL3='DEPTH(KM)'
        CALL SYMBOL(5.5,-.7,.25,YL3,0.,9)
        YL5='NO. OF EARTHQUAKES'
        CALL SYMBOL(-.6,1.,.25,YL5,90.,18)
        WRITE(5,*)'ENTER THE HEADING WITHIN TICKS '
        READ(5,*)YL6
        CALL SYMBOL(5.0,6.,.25,YL6,0.,25)
        CALL SYMBOL(7.0,4.,.25,'N=',0.,4)
        CALL NUMBER(7.4,4.,.25,ENUM,0.,-1)
        DO 70 S=1.,5.
         YIN=S
         YLB=SF*S
         CALL NUMBER(-.4,YIN,.2,YLB,0.,-1)
         CALL SYMBOL(0.,YIN,.2,3,0.,-1)
70      CONTINUE
72      WRITE(5,*)'ANOTHER PLOT ON SAME PAGE(Y OR N)?'
        READ(5,'A')RET
        NP=NP+1
        IF((RET.EQ.'Y').OR.(RET.EQ.'y'))GO TO 169
        END
C
C       SCALE SCALES THE NUMBER OF EVENTS TO FIT ON A Y-AXIS
C       5.0 INCHES IN LENGTH
```

```
C
      SUBROUTINE SCALE(FMS,SFS)
      DT=5.
      S=0.
      DO 170 T=10.,400.,DT
       S=S+1.
       T1=T+DT
       IF((FMS.GT.T).AND.(FMS.LE.T1))SFS=2.+S
       IF(FMS.LE.10)SFS=2.
170   CONTINUE
      END
C
C     AVE CALCULATES AVERAGE NUMBER OF EVENTS/DEPTH INTERVAL
C     AND IS CALLED FROM SUBROUTINE DEEP
C
      SUBROUTINE AVE(N,EN,SUM1)
      DIMENSION SUM1(1000)
      API=EN/N
      DO 32 L=1,12
      IF(SUM1(L).NE.0.)THEN
      V1=SUM1(L)/API
      IF(V1.LE.1.)THEN
      V2=(1.-V1)*100.
      WRITE(3,*)'INTERVAL ',L,' = ',V2,'% < ',API
      END IF
      IF(V1.GT.1.)THEN
      V2=(V1-1.)*100.
      WRITE(3,*)'INTERVAL ',L,' = ',V2,'% > ',API
      END IF
      END IF
32    CONTINUE
      END
C
C     HIST PLOTS NORMALIZED PERCENTAGE OF EVENTS VS.DEPTH AND
C     IS CALLED FROM SUBROUTINE DEEP
C

      SUBROUTINE HIST(NP,SUM,ENUM)
      DIMENSION SUM(1000)
      CHARACTER XLAB*30,YLAB*30,HD*30,YON*30
      IF(NP.EQ.1)CALL PLOT(1.,14.,-3)
      IF(NP.GT.1)CALL PLOT(7.,0.,-3)
      CALL PLOT(0.,-12.,2)
      CALL PLOT(0.,0.,3)
      CALL PLOT(6.5,0.,2)
      CALL PLOT(0.,0.,3)
      K=0
      DO 51 TI=-1.,-11.,-1
       K=K+1
       X=SUM(K)/ENUM*10.
       Y=TI+1.
       CALL PLOT(X,Y,2)
       Y=Y-1.
       CALL PLOT(X,Y,2)
       CALL PLOT(0.,Y,2)
51    CONTINUE
C
C     LABEL Y-AXIS
C
```

```
      DO 61 TK=1.,12.,1.
      YNO=2.*TK
      CALL NUMBER(-.28,-TK,.2,YNO,0.,0)
61    CONTINUE
      YLAB='DEPTH(KM)'
      IF(NP.EQ.1)CALL SYMBOL(-.7,-5.5,.25,YLAB,90.,9)
C
CC    LABEL X-AXIS
C
      DO 71S=1.,6.,1.
      XIN=S
      XNO=10.*XIN
      CALL NUMBER(XIN,.2,.2,XNO,0.,-1)
      CALL SYMBOL(XIN,0.,.2,3,0.,-1)
71    CONTINUE
      XLAB='% OF EARTHQUAKES'
      CALL SYMBOL(1.,.6,.25,XLAB,0.,20)
C
CC    PLOT HEADING AND OTHER LABELS
C
      WRITE(5,*)'ENTER THE DESIRED HEADING: '
      READ(5,'A')HD
      CALL SYMBOL(2.,-8.,.25,HD,0.,20)
      CALL SYMBOL(2.,-8.5,.25,'N=',0.,4)
      CALL NUMBER(2.4,-8.5,.25,ENUM,0.,-1)
      CALL NUMBER(2.4,-8.5,.25,ENUM,0.,-1)
C     CALL RSTR
      END
C
CC    SUBROUTINE XSEX PLOTS HYPOCENTRAL DEPTHS AGAINST X-SECTION
CC    DISTANCES.  ENDPOINT COORDINATES IN DEGREES OF LAT. AND LONG.
CC    ARE SUPPLIED BY THE USER ALONG WITH A WIDTH OF X-SECTION
CC    PROJECTION.  EVENTS ARE PROJECTED PERPENDICULAR TO THE X-
CC    SECTION
C
      SUBROUTINE XSEX(FLAT,FLONG,Z,C)
      DIMENSION FLAT(1000),FLONG(1000),Z(1000),TD(1000),ZN(1000)
      DATA PI/3.141592654/,LTC/110.92038/,LGC/92.38788/,K/0/
      INTEGER C
      CHARACTER NM*20,YLAB*20,XLAB*20
      PIFO=PI/4.
      WRITE(5,*)'IS X-SECTION SKEWED(1), PARALLEL TO LINES OF'
      WRITE(5,*)'LONGITUDE(2), OR PARALLEL TO LINES OF LATITUDE(3)?'
      READ(5,*)LQ
      IF(LQ.EQ.1)GO TO 1
      IF(LQ.EQ.2)GO TO 2
      IF(LQ.EQ.3)GO TO 3
1     WRITE(5,*)'ENTER ENDPTS. OF X-SECTION (X1,Y1) AND (X2,Y2)
     *  WHERE X1>X2 (IN DEG. OF LON/LAT)'
      READ(5,*)X1,Y1,X2,Y2
      S=ABS((Y2-Y1)/(X2-X1))*LTC/LGC
      A=ATAN(S)
      WRITE(5,*)'S= ',S
      WRITE(5,*)'A= ',A
      WRITE(5,*)'ENTER X-SECTION HALF-WIDTH(KM)'
      READ(5,*)XW
C
C
      IF(A.LE.PIFO)THEN
      DO 5 I=1,C
```

```
      IF((Z(I).GT.2.).AND.(Z(I).LE.12.))THEN
      IF((FLONG(I).GT.X1).OR.(FLONG(I).LT.X2))GO TO 5
      R=XW/COS(A)
      XS=(X1-FLONG(I))*LGC
      YS=S*XS
      FLAKM=((FLAT(I)-Y1)*LTC)-YS
      IF (ABS(FLAKM).LT.R)THEN
      FS=SQRT(XS**2.+YS**2.)
      K=K+1
      ZN(K)=Z(I)
      D=FLAKM
      DS=D*SIN(A)
      TD(K)=FS+DS
      END IF
      END IF
5     CONTINUE
      END IF
C
C
      IF(A.LE.PIFO)GO TO 6
      IF(A.GT.PIFO)THEN
      DO 7 I=1,C
      IF((Z(I).GT.2.).AND.(Z(I).LE.12.))THEN
      IF((FLAT(I).GT.Y2).OR.(FLAT(I).LT.Y1))GO TO 7
      R=XW/COS(A)
      XS=(X1-FLONG(I))*LGC
      YS=S*XS
      FLAKM=((FLAT(I)-Y1)*LTC)-YS
      IF (ABS(FLAKM).LT.R)THEN
      FS=SQRT(XS**2.+YS**2.)
      K=K+1
      ZN(K)=Z(I)
      D=FLAKM
      DS=D*SIN(A)
      TD(K)=FS+DS
      END IF
      END IF
7     CONTINUE
      END IF
      GO TO 6
C
C
2     WRITE(5,*)'ENTER ENDPTS. OF X-SECTION (X1,Y1) AND (X2,Y2)
     *  WHERE Y2>Y1 (IN DEG. OF LON/LAT)'
      READ(5,*)X1,Y1,X2,Y2
      WRITE(5,*)'ENTER X-SECTION WIDTH (KM)'
      READ(5,*)R
      DO 20 I=1,C
      IF((Z(I).GT.2.).AND.(Z(I).LE.12.))THEN
      IF((FLAT(I).GT.Y1).AND.(FLAT(I).LT.Y2))THEN
      FLOKM=ABS(FLONG(I)-X1)*LGC
      IF(FLOKM.LT.R)THEN
      K=K+1
      TD(K)=(FLAT(I)-Y1)*LTC
      ZN(K)=Z(I)
      END IF
      END IF
      END IF
20    CONTINUE
      GO TO 6
```

```
C
C
3       WRITE(5,*)'ENTER ENDPTS. OF X-SECTION (X1,Y1) AND (X2,Y2)
     *  WHERE X1>X2 (IN DEG. OF LON/LAT)'
        READ(5,*)X1,Y1,X2,Y2
        WRITE(5,*)'ENTER X-SECTION WIDTH (KM)'
        READ(5,*)R
        DO 25 I=1,C
        IF((Z(I).GT.2.).AND.(Z(I).LE.12.))THEN
        IF((FLONG(I).GT.X2).AND.(FLONG(I).LT.X1))THEN
        FLAKM=ABS(FLAT(I)-Y1)*LTC
        IF(FLAKM.LE.R)THEN
        K=K+1
        TD(K)=(X1-FLONG(I))*LGC
        ZN(K)=Z(I)
        END IF
        END IF
        END IF
25      CONTINUE
6       XT=SQRT(((X2-X1)*LGC)**2.+((Y2-Y1)*LTC)**2.)
        SFXT=XT/10.
        WRITE(5,*)'K= ',K
        WRITE(5,*)'ENTER PLOT NAME'
        READ(5,'A')NM
        CALL INITAL(-1,NM)
        CALL PLOT(1.,5.,-3)
C       SCALE FACTORS : X=10 KM/INCH,Z=5KM/INCH
        SFX=10.
        SFZ=5.
        CALL PLOT(0.,-4.,2)
        CALL PLOT(0.,-4.,-3)
        CALL PLOT(SFXT,0.,2)
        CALL PLOT(SFXT,0.,-3)
        CALL PLOT(0.,4.,2)
        CALL PLOT(0.,4.,-3)
        CALL PLOT(-SFXT,0.,2)
        CALL PLOT(-SFXT,0.,-3)
        WRITE(5,*)'DO YOU WANT VERTICAL EXAGERATION(Y OR N)?'
        READ(5,'A')VE
        IF((VE.EQ.'N').OR.(VE.EQ.'n'))SFZ=SFX
        DO 10 I=1,K
        X=TD(I)/SFX
        Y=-ZN(I)/SFZ
        CALL SYMBOL(X,Y,.10,1,0.,-1)
10      CONTINUE
        DO 15 D=1.,6.,1.
        ZNO=D*SFZ
        IF(D.LE.(SFXT/2.))THEN
        D2=D*2.
        XNO=D*2.*SFX
        CALL NUMBER(D2,.1,.15,XNO,0.,0)
        CALL SYMBOL(D2,0.,.1,13,0.,-1)
        END IF
        IF(D.LE.4.)CALL NUMBER(-.3,-D,.15,ZNO,0.,0)
        IF(D.LE.4.)CALL SYMBOL(0.,-D,.1,13,90.,-1)
15      CONTINUE
        SX2=SFXT/2.5
        FK=FLOAT(K)
        SCL=1.1*SFXT
        SCL2=SCL+.2
```

```
      XLAB='DISTANCE(KM)'
      CALL SYMBOL(SX2,.35,.15,XLAB,0.,15)
      YLAB='DEPTH(KM)'
      CALL SYMBOL(-.4,-2.5,.15,YLAB,90.,9)
      CALL SYMBOL(SCL,-.25,.15,'N=',0.,4)
      CALL SYMBOL(SCL,-.25,.15,'N=',0.,4)
      CALL NUMBER(SCL2,-.25,.15,FK,0.,-1)
      CALL NUMBER(SCL2,-.25,.15,FK,0.,-1)
      CALL RSTR
      END

      SUBROUTINE RAD(COUNT,FLAT,FLONG,DEPTH)
      DIMENSION FLAT(1000),FLONG(1000),DEPTH(1000),CD(1000)
      INTEGER COUNT
      LTCOR=60.*1.848673
      LGCOR=60.*1.539798
      CLT=33.978
      CLG=106.979
125   WRITE(5,*)'SPECIFY CALDERA RADIUS: '
      READ(5,*)RL
      KD=0
      CD2=0.
      CDS=0.
      DO 126 I=1,COUNT
       LTY=(FLAT(I)-CLT)*LTCOR
       LGX=(FLONG(I)-CLG)*LGCOR
       RDS=SQRT(LTY**2.+LGX**2.)
       IF(RDS.LE.RL)THEN
        KD=KD+1
        CD(KD)=DEPTH(I)
        CD2=DEPTH(I)**2.+CD2
        CDS=DEPTH(I)+CDS
       END IF
126   CONTINUE
      CALL MEAN(CDS,CD2,KD,SM,SD)
      WRITE(3,*)'NUMBER OF EVENTS W/I RADIUS= ',KD
      WRITE(3,*)'RADIUS= ',RL
      WRITE(3,*)'MEAN= ',SM,'   S.D.= ',SD
      CALL DEEP(CD,IYR,KD,FLAT,FLONG)
      WRITE(5,*)'AGAIN(Y OR N)? '
      READ(5,'A')ANSR
      IF((ANSR.EQ.'Y').OR.(ANSR.EQ.'y'))GO TO 125
      END
```

APPENDIX 5

Final data set used in study, containing only A/A, A/B and A/C quality events.

DATE	ORIGIN	LAT N	LONG W	DEPTH	MAG	NO	DM	GAP	RMS	ERH	ERZ	Q/QS/QD
75 6 3	44818.08	34 4.34	10655.48	7.00	0.00	9	2	117	0.08	0.4	1.0	2 1 2
75 6 3	151015.48	34 1.07	107 2.23	10.51	0.00	9	5	124	0.08	0.6	0.7	2 1 2
75 616	234320.82	34 1.34	107 2.24	10.64	0.00	9	5	127	0.08	0.6	0.7	2 1 2
75 626	25645.25	34 3.36	107 2.29	5.73	0.00	7	7	166	0.03	0.4	0.8	2 1 3
75 724	42314.23	34 3.13	10659.43	6.40	0.00	8	5	122	0.05	0.3	0.5	2 1 2
75 730	214442.06	34 4.52	10655.16	9.60	0.00	8	2	122	0.02	0.2	0.2	2 1 2
75 8 5	226 2.30	34 1.51	10659.02	9.70	0.00	8	6	101	0.07	0.5	1.0	2 1 2
75 8 5	41720.58	34 1.27	10658.85	10.44	0.00	10	7	98	0.06	0.3	0.5	2 1 2
75 8 5	141922.36	34 0.97	107 2.55	10.06	0.00	8	4	128	0.04	0.4	0.5	2 1 2
75 8 8	105357.82	34 3.84	10655.26	8.67	0.00	8	2	116	0.10	0.8	0.9	2 1 2
75 8 8	105722.32	34 4.35	10655.31	8.54	0.00	8	2	119	0.03	0.3	0.3	2 1 2
75 812	152528.56	34 2.31	10659.66	7.10	0.00	11	6	116	0.08	0.4	0.6	2 1 2
75 813	33851.07	34 4.43	10655.38	8.95	0.00	11	2	110	0.03	0.2	0.2	2 1 2
75 813	346 5.84	34 4.27	10655.34	8.52	0.00	11	2	110	0.03	0.2	0.2	2 1 2
75 813	73918.43	34 4.35	10655.53	8.86	0.00	9	2	108	0.03	0.2	0.2	2 1 2
75 813	112226.70	34 0.33	10658.22	10.13	0.00	10	6	108	0.05	0.3	0.4	2 1 2
75 819	81146.74	34 2.87	10657.71	10.08	0.00	8	3	103	0.04	0.4	0.4	2 1 2
75 819	81244.76	34 2.78	10657.81	9.97	0.00	8	3	103	0.05	0.4	0.4	2 1 2
75 818	10 0 7.19	3358.95	107 0.08	10.51	0.00	9	5	159	0.03	0.2	0.3	2 1 3
75 819	201022.97	34 4.27	10655.11	8.18	0.00	8	3	119	0.05	0.4	0.5	2 1 2
75 820	51640.25	34 3.97	10654.03	8.46	0.00	10	4	124	0.10	0.5	0.8	2 1 2
75 820	52219.90	34 4.43	10655.30	9.26	0.00	10	2	120	0.09	0.5	0.6	2 1 2
75 820	122052.20	34 4.43	10654.81	8.18	0.00	9	3	123	0.09	0.5	0.7	2 1 2
75 820	124919.27	34 4.21	10655.02	8.57	0.00	10	3	118	0.04	0.2	0.3	2 1 2
75 820	152836.29	34 4.53	10655.41	9.47	0.00	10	2	121	0.04	0.2	0.3	2 1 2
75 821	04022.93	34 4.43	10655.47	7.45	0.00	10	2	119	0.06	0.3	0.5	2 1 2
75 821	34448.60	34 1.06	107 2.49	10.08	0.00	8	4	125	0.02	0.2	0.3	2 1 2
75 821	7 351.48	34 4.32	10655.11	8.03	0.00	10	3	119	0.04	0.2	0.3	2 1 2
75 821	19 4 6.18	34 2.65	10657.74	10.05	0.00	9	3	104	0.03	0.2	0.2	2 1 2
75 821	19 911.54	34 2.77	10657.89	10.67	0.00	9	3	102	0.05	0.3	0.4	2 1 2
75 821	191842.12	34 2.65	10657.77	9.82	0.00	9	3	104	0.04	0.3	0.3	2 1 2
75 825	193740.85	34 4.12	10654.91	9.03	0.00	9	3	117	0.03	0.2	0.2	2 1 2
75 919	84257.01	34 0.70	10651.12	8.78	0.00	7	11	148	0.04	0.4	0.6	2 1 3
751029	205049.26	3359.39	107 0.62	6.91	0.00	8	7	155	0.04	0.3	0.5	2 1 3
7511 4	163011.68	34 2.20	107 4.02	9.77	0.00	9	4	179	0.05	0.4	0.4	2 1 3
7511 6	11 548.39	3359.57	10651.49	7.38	0.00	9	10	153	0.05	0.3	0.8	2 1 3
76 123	25333.03	34 1.81	107 1.82	8.98	0.00	10	6	171	0.08	0.5	0.7	2 1 3
76 129	15 640.19	3358.99	10658.47	7.00	0.00	9	4	129	0.05	0.3	0.6	2 1 2
76 129	182427.51	3358.88	10658.70	7.52	0.00	9	4	136	0.04	0.2	0.3	2 1 3
76 130	91635.44	3358.83	10658.88	8.35	0.00	8	4	141	0.03	0.2	0.3	2 1 3
76 218	54455.92	34 0.70	107 3.04	10.27	0.00	8	4	148	0.04	0.5	0.4	2 1 3
76 218	91330.75	34 0.82	107 0.70	4.15	0.00	8	2	112	0.08	0.7	0.8	2 1 2
76 218	232535.24	34 1.73	107 4.17	9.99	0.00	9	3	171	0.03	0.3	0.3	2 1 3
76 219	0 836.81	34 0.95	107 3.30	9.92	0.00	12	3	130	0.05	0.3	0.3	2 1 2
76 220	125145.11	34 0.82	107 2.67	11.11	0.00	8	4	150	0.01	0.1	0.1	2 1 3
76 413	94540.75	34 3.88	107 0.70	8.59	0.00	10	6	148	0.05	0.4	0.6	2 1 3
76 413	955 8.11	34 3.69	107 0.83	7.02	0.00	10	6	147	0.05	0.4	0.5	2 1 3
76 413	1117 5.09	34 3.70	107 0.67	8.04	0.00	10	6	145	0.02	0.1	0.2	2 1 3
76 413	114125.36	34 1.88	107 3.66	10.52	0.00	9	4	163	0.05	0.4	0.5	2 1 3
76 413	115834.64	3358.95	10657.57	6.41	0.00	11	3	170	0.07	0.4	0.4	2 1 3
76 413	185213.76	34 3.69	10659.92	9.03	0.00	10	5	134	0.08	0.6	0.7	2 1 2
76 413	231515.04	34 1.36	107 1.60	4.71	0.00	9	3	121	0.07	0.4	0.7	2 1 2
76 414	15028.88	3358.67	10659.90	9.80	0.00	10	1	164	0.05	0.4	0.3	2 1 3
76 414	9 525.63	3358.58	107 0.60	8.96	0.00	9	2	176	0.04	0.4	0.4	2 1 3
76 415	34148.76	34 3.78	107 0.29	9.40	0.00	10	6	141	0.09	0.7	0.8	2 1 3
76 415	6 840.08	34 3.73	107 1.03	7.80	0.00	10	6	151	0.05	0.3	0.5	2 1 3
76 415	7 359.12	34 3.69	107 0.65	7.44	0.00	10	6	145	0.07	0.5	0.7	2 1 3
76 415	84552.51	34 3.75	107 0.75	8.58	0.00	11	6	147	0.05	0.3	0.4	2 1 3

DATE	ORIGIN	LAT N	LONG W	DEPTH	MAG	NO	DM	GAP	RMS	ERH	ERZ	Q/QS/QD
76 415	85150.64	34 3.70	107 0.92	7.72	0.00	10	6	149	0.06	0.4	0.6	2 1 3
76 415	102412.82	34 3.81	107 0.86	7.69	0.00	12	6	150	0.06	0.3	0.4	2 1 3
76 415	115520.07	34 3.69	107 0.74	7.69	0.00	11	6	146	0.06	0.4	0.5	2 1 3
76 415	144316.16	34 0.80	107 4.79	9.78	0.00	9	1	145	0.03	0.4	0.3	2 1 3
76 415	153027.48	34 3.85	107 1.06	8.07	0.00	10	6	153	0.10	0.6	1.0	2 1 3
76 415	182837.23	34 2.78	10657.21	7.95	0.00	10	3	168	0.04	0.3	0.3	2 1 3
76 415	224820.64	34 2.96	10657.31	8.28	0.00	10	3	162	0.10	0.8	0.7	2 1 3
76 415	231611.87	34 3.81	107 0.61	7.56	0.00	10	6	146	0.08	0.6	0.8	2 1 3
76 416	12022.71	34 3.79	107 1.07	7.90	0.00	12	6	152	0.09	0.5	0.7	2 1 3
76 416	93342.88	34 3.58	107 0.56	7.58	0.00	12	6	142	0.06	0.3	0.5	2 1 3
76 416	936 7.88	34 3.80	107 1.31	6.65	0.00	10	6	156	0.09	0.5	0.9	2 1 3
76 416	14 733.22	34 3.91	10659.44	8.97	0.00	11	4	130	0.07	0.4	0.6	2 1 2
76 416	14 954.14	34 3.79	107 1.26	7.95	0.00	10	6	155	0.09	0.6	0.8	2 1 3
76 416	142411.60	34 3.82	107 1.24	7.17	0.00	10	6	155	0.09	0.5	0.9	2 1 3
76 416	15 436.66	34 3.69	107 1.19	7.73	0.00	10	6	153	0.09	0.6	1.0	2 1 3
76 526	195418.91	3354.48	10648.43	11.01	0.00	7	8	172	0.03	0.3	0.6	2 1 3
76 6 8	61612.41	34 2.64	10659.81	10.37	0.00	10	4	121	0.05	0.4	0.4	2 1 2
76 6 8	61626.16	34 2.74	10659.52	10.28	0.00	10	4	125	0.05	0.4	0.4	2 1 2
76 6 8	62440.91	34 2.83	10658.81	10.46	0.00	10	4	139	0.04	0.4	0.4	2 1 3
76 6 8	636 9.95	34 2.57	10659.80	10.56	0.00	10	3	120	0.06	0.5	0.5	2 1 2
76 6 8	64114.28	34 2.59	10659.60	9.68	0.00	10	3	125	0.06	0.4	0.5	2 1 2
76 6 8	64251.00	34 3.13	10659.03	6.61	0.00	10	4	127	0.04	0.2	0.3	2 1 2
76 6 8	7 418.63	34 2.63	10659.29	10.23	0.00	10	4	132	0.03	0.2	0.2	2 1 2
76 6 8	72219.08	34 2.62	10659.57	10.13	0.00	10	4	126	0.05	0.4	0.4	2 1 2
76 6 8	75039.72	34 2.64	10659.31	10.38	0.00	10	4	131	0.02	0.2	0.2	2 1 2
76 6 8	113148.87	34 2.76	10659.77	10.34	0.00	10	4	122	0.03	0.2	0.2	2 1 2
76 630	844 1.50	34 0.62	107 1.83	10.61	0.00	10	5	124	0.07	0.4	0.5	2 1 2
76 715	105834.21	34 1.05	107 3.80	10.02	0.00	12	3	119	0.03	0.2	0.2	2 1 2
76 715	1643 7.66	34 1.25	107 3.35	11.08	0.00	9	3	112	0.06	0.5	0.5	2 1 2
76 8 5	219 6.48	34 3.14	10659.98	9.92	0.00	10	5	131	0.05	0.3	0.4	2 1 2
76 810	25311.52	34 2.91	107 0.30	10.26	0.00	10	6	149	0.05	0.3	0.4	2 1 3
76 810	121841.77	34 3.09	10659.59	11.09	0.00	10	5	148	0.09	0.6	0.7	2 1 3
76 811	6 343.56	34 3.62	10659.86	9.17	0.00	9	5	163	0.07	0.5	0.7	2 1 3
76 811	10 037.81	34 2.99	107 0.15	10.00	0.00	10	6	150	0.04	0.2	0.3	2 1 3
76 8 5	91935.32	34 2.14	107 0.25	6.71	0.00	10	7	120	0.05	0.3	0.5	2 1 2
76 8 9	184017.60	34 2.88	107 0.30	9.58	0.00	9	6	130	0.06	0.4	0.5	2 1 2
76 811	18 827.25	34 2.82	107 0.07	10.16	0.00	10	6	134	0.07	0.4	0.5	2 1 2
7612 8	05636.11	34 2.64	10659.56	11.18	0.00	11	5	126	0.04	0.2	0.3	2 1 2
76 812	059 8.01	34 2.53	10659.81	11.33	0.00	11	6	123	0.04	0.3	0.3	2 1 2
76 812	1 314.26	34 2.84	107 0.23	10.13	0.00	10	6	126	0.06	0.4	0.5	2 1 2
76 812	12436.46	34 2.85	10659.33	12.40	0.00	12	5	127	0.10	0.6	0.7	2 1 2
76 812	14541.49	34 2.70	10659.53	11.12	0.00	12	5	126	0.06	0.3	0.4	2 1 2
7612 8	154 4.77	34 2.60	107 0.10	9.74	0.00	11	6	120	0.04	0.2	0.3	2 1 2
76 812	23425.87	34 2.66	10659.78	10.37	0.00	12	6	122	0.05	0.3	0.4	2 1 2
76 812	318 5.67	34 2.51	107 0.04	11.07	0.00	10	6	119	0.07	0.5	0.6	2 1 2
76 812	456 5.06	34 2.70	10659.71	11.67	0.00	12	5	122	0.07	0.4	0.5	2 1 2
76 812	5 859.07	34 2.72	107 0.12	10.63	0.00	12	6	123	0.08	0.4	0.6	2 1 2
76 812	52048.69	34 2.87	10659.83	10.24	0.00	12	5	124	0.06	0.3	0.4	2 1 2
76 812	752 6.31	34 3.11	107 0.22	9.75	0.00	12	6	131	0.07	0.3	0.5	2 1 2
76 812	112551.57	34 2.48	10659.92	10.00	0.00	12	6	122	0.04	0.2	0.3	2 1 2
76 812	115750.35	34 2.56	10659.87	10.24	0.00	10	6	122	0.03	0.2	0.3	2 1 2
76 812	23 712.52	34 2.79	10659.77	10.60	0.00	10	5	122	0.04	0.3	0.4	2 1 2
76 813	02246.93	34 2.48	10659.68	10.49	0.00	10	6	126	0.09	0.6	0.8	2 1 2
76 824	13113.62	34 2.54	107 1.08	8.47	0.00	12	7	124	0.10	0.4	0.7	2 1 2
76 825	21 4 9.33	34 3.30	10659.81	10.85	0.00	8	5	133	0.04	0.4	0.4	2 1 2
76 825	223223.10	34 2.85	10659.79	11.57	0.00	9	5	123	0.05	0.4	0.5	2 1 2
76 827	14439.52	34 2.57	10659.89	11.26	0.00	9	6	121	0.05	0.4	0.5	2 1 2
76 827	81528.15	34 0.48	107 3.54	10.81	0.00	8	3	146	0.07	0.6	0.6	2 1 3

DATE	ORIGIN	LAT N	LONG W	DEPTH	MAG	NO	DM	GAP	RMS	ERH	ERZ	Q/QS/QD
7610 7	223549.40	34 1.29	107 1.72	11.16	0.00	9	5	115	0.08	0.7	0.8	2 1 2
7610 7	223737.66	34 1.97	107 1.84	10.36	0.00	10	6	117	0.05	0.3	0.4	2 1 2
7610 7	2321 9.59	34 1.40	107 1.76	10.24	0.00	10	5	112	0.06	0.4	0.5	2 1 2
77 121	0 616.26	3359.96	107 3.66	11.40	0.00	8	3	175	0.08	0.8	0.7	2 1 3
77 121	164228.36	34 0.56	107 3.50	11.03	0.00	10	3	147	0.09	0.5	0.7	2 1 3
77 122	424 5.02	34 0.70	107 3.10	9.64	0.00	10	3	139	0.07	0.4	0.5	2 1 3
77 2 9	13616.12	34 1.37	107 2.51	10.70	0.00	9	5	131	0.07	0.5	0.6	2 1 2
77 2 9	83847.31	3359.32	10658.25	8.03	0.00	9	3	115	0.05	0.4	0.5	2 1 2
77 2 9	105958.84	34 0.90	10659.70	7.04	0.00	10	6	99	0.04	0.2	0.4	2 1 2
77 2 9	11 713.69	34 0.54	10659.90	9.80	0.00	8	5	96	0.05	0.4	0.6	2 1 2
77 2 9	113852.84	34 0.72	10659.70	8.55	0.00	7	5	96	0.07	0.7	1.2	2 1 2
77 216	85116.69	34 1.14	107 3.11	10.30	0.00	12	4	131	0.04	0.2	0.2	2 1 2
77 216	144449.47	34 0.70	107 3.02	9.91	0.00	11	4	138	0.06	0.4	0.5	2 1 3
77 225	0 7 8.07	34 0.87	107 2.83	10.27	0.00	10	4	132	0.05	0.4	0.4	2 1 2
77 3 8	43041.64	34 0.14	107 3.61	10.40	0.00	8	3	166	0.04	0.4	0.4	2 1 3
77 3 8	455 6.07	34 0.70	107 3.27	9.71	0.00	8	3	139	0.06	0.6	0.6	2 1 3
77 3 9	112544.37	34 0.52	107 3.29	9.87	0.00	10	3	147	0.05	0.3	0.3	2 1 3
77 3 9	1149 2.43	34 0.70	107 3.33	9.59	0.00	10	3	140	0.04	0.3	0.3	2 1 3
77 3 9	115015.93	34 0.70	107 3.32	9.39	0.00	10	3	140	0.05	0.3	0.3	2 1 3
77 3 9	122755.97	34 0.70	107 3.01	10.00	0.00	10	4	138	0.06	0.4	0.5	2 1 3
77 3 9	123319.15	34 0.70	107 3.21	9.35	0.00	10	3	139	0.05	0.3	0.4	2 1 3
77 3 9	1239 0.20	34 0.62	107 3.29	9.71	0.00	10	3	143	0.03	0.2	0.3	2 1 3
77 310	2 342.59	34 0.19	107 3.46	10.18	0.00	9	3	162	0.02	0.2	0.2	2 1 3
77 413	191523.72	34 3.79	107 1.86	6.80	0.00	12	8	74	0.09	0.3	0.7	2 1 2
77 419	164020.11	3359.64	10657.04	4.23	0.00	9	5	141	0.02	0.2	0.5	2 1 3
77 426	2 820.40	34 3.83	107 1.32	10.20	0.00	9	7	140	0.08	0.5	0.8	2 1 3
77 427	8 440.27	34 1.46	107 1.56	5.65	0.00	10	6	112	0.08	0.4	0.8	2 1 2
77 427	121556.25	34 0.88	107 3.25	9.81	0.00	10	3	132	0.05	0.3	0.4	2 1 2
77 427	122327.19	34 1.01	107 3.36	10.20	0.00	12	3	127	0.04	0.2	0.3	2 1 2
77 428	105910.49	34 2.64	107 2.80	9.68	0.00	9	5	154	0.04	0.3	0.4	2 1 3
77 428	11 330.92	34 2.28	107 2.64	9.76	0.00	9	5	163	0.04	0.3	0.4	2 1 3
77 6 2	64816.35	34 1.07	107 3.46	8.43	0.00	11	3	125	0.07	0.4	0.5	2 1 2
77 6 2	65024.36	34 0.44	107 3.66	9.00	0.00	10	3	153	0.05	0.3	0.3	2 1 3
77 6 2	65521.42	34 0.70	107 3.52	8.22	0.00	10	3	140	0.07	0.4	0.5	2 1 3
77 6 2	81147.68	34 0.70	107 3.63	7.00	0.00	8	3	140	0.08	0.8	0.9	2 1 3
77 6 2	1142 0.47	34 0.70	107 3.62	7.73	0.00	8	3	140	0.09	0.9	0.9	2 1 3
77 6 2	12 7 4.04	34 0.70	107 3.61	7.83	0.00	9	3	140	0.07	0.5	0.5	2 1 3
77 6 2	1730 8.17	34 0.53	107 3.45	8.24	0.00	8	3	147	0.03	0.2	0.2	2 1 3
77 6 3	349 1.56	34 0.82	107 3.46	8.77	0.00	10	3	135	0.03	0.2	0.2	2 1 2
77 6 3	2045 3.28	3413.60	10654.15	7.00	0.00	8	16	172	0.04	0.3	0.9	2 1 3
77 610	4 444.84	34 1.04	107 3.43	9.96	0.00	8	3	126	0.04	0.3	0.3	2 1 2
77 714	234 1.96	34 9.52	10652.50	7.20	0.00	9	7	136	0.08	0.6	1.0	2 1 3
77 714	10 032.71	34 9.66	10651.92	7.30	0.00	10	7	99	0.07	0.4	0.6	2 1 2
77 714	113151.10	34 9.29	10652.67	7.38	0.00	10	8	87	0.10	0.6	0.9	2 1 2
77 714	202416.65	34 2.28	107 3.18	10.44	0.00	12	5	89	0.08	0.4	0.6	1 1 1
77 715	122625.70	34 0.43	107 3.69	10.04	0.00	11	3	153	0.03	0.2	0.2	2 1 3
77 722	719 0.58	3410.36	10652.12	6.46	0.00	9	6	149	0.05	0.3	0.5	2 1 3
77 727	155315.04	34 0.33	107 3.59	10.93	0.00	7	3	157	0.02	0.3	0.3	2 1 3
77 727	18 820.12	34 9.58	10654.39	6.94	0.00	9	7	169	0.08	0.5	0.6	2 1 3
77 728	1847 3.77	34 9.22	10654.52	5.68	0.00	7	7	146	0.08	0.6	1.4	2 1 3
77 817	6 319.88	34 9.78	10651.78	7.40	0.00	9	6	161	0.08	0.6	1.0	2 1 3
77 817	153722.04	3415.77	10655.14	6.34	0.00	9	11	151	0.08	0.5	1.2	2 1 3
77 817	155258.71	3415.41	10655.49	5.08	0.00	8	11	145	0.07	0.5	1.7	2 1 3
77 818	53113.72	34 0.70	107 4.06	9.62	0.00	9	2	141	0.10	0.7	0.8	2 1 3
77 818	73324.48	34 9.93	10652.16	6.98	0.00	10	6	138	0.06	0.4	0.7	2 1 3
77 818	93013.62	34 9.47	10652.44	4.50	0.00	7	7	135	0.06	0.6	1.6	2 1 2
77 818	103814.82	34 1.09	107 3.56	9.21	0.00	11	3	123	0.08	0.5	0.8	2 1 2
77 818	103847.51	34 0.70	107 3.68	10.31	0.00	10	3	140	0.09	0.6	0.6	2 1 3

DATE	ORIGIN	LAT N	LONG W	DEPTH	MAG	NO	DM	GAP	RMS	ERH	ERZ	Q/QS/QD
77 818	1039 9.87	34 0.58	107 3.89	10.57	0.00	12	2	147	0.05	0.3	0.3	2 1 3
77 818	121645.02	34 0.50	107 3.81	10.33	0.00	10	2	151	0.04	0.3	0.3	2 1 3
77 818	123247.68	3410.13	10651.83	9.26	0.00	8	6	138	0.09	0.9	1.3	2 1 3
77 818	1542 6.77	34 0.67	107 3.80	10.32	0.00	10	2	142	0.07	0.5	0.5	2 1 3
77 819	351 0.22	34 1.01	107 3.62	8.52	0.00	14	3	126	0.10	0.5	0.6	2 1 2
77 819	9 548.23	34 0.70	107 3.86	10.40	0.00	10	2	141	0.05	0.4	0.4	2 1 3
77 819	922 4.93	34 0.45	107 3.78	10.18	0.00	9	2	153	0.07	0.6	0.6	2 1 3
77 819	92822.66	34 0.38	107 4.16	11.39	0.00	9	2	161	0.04	0.3	0.3	2 1 3
77 819	94951.09	34 0.75	107 3.55	10.04	0.00	9	3	138	0.04	0.3	0.4	2 1 3
77 819	102442.59	34 0.50	107 3.71	10.22	0.00	10	3	150	0.05	0.3	0.4	2 1 3
77 824	112134.69	34 0.70	107 3.43	9.58	0.00	12	3	135	0.08	0.4	0.5	2 1 3
7724 8	112235.67	34 0.46	107 3.31	10.57	0.00	12	3	145	0.06	0.3	0.4	2 1 3
77 825	62626.99	34 0.58	107 3.56	9.77	0.00	15	3	142	0.05	0.2	0.3	2 1 3
77 826	61259.57	34 0.70	107 3.59	9.59	0.00	10	3	136	0.07	0.4	0.5	2 1 3
77 826	102230.12	34 0.70	107 3.77	10.60	0.00	9	2	137	0.10	0.7	0.8	2 1 3
77 826	102544.17	34 0.38	107 3.55	9.82	0.00	11	3	151	0.06	0.3	0.4	2 1 3
77 826	103257.84	34 0.41	107 3.82	10.69	0.00	17	2	153	0.09	0.4	0.5	2 1 3
77 826	103327.50	34 0.35	107 3.75	10.34	0.00	12	3	155	0.10	0.5	0.7	2 1 3
77 826	103511.41	34 0.70	107 3.63	10.85	0.00	12	3	136	0.09	0.5	0.6	2 1 3
77 826	103546.64	3357.85	10657.17	6.61	0.00	13	2	171	0.08	0.5	0.5	2 1 3
77 826	103810.67	34 0.29	107 3.57	9.91	0.00	14	3	156	0.10	0.4	0.6	2 1 3
77 830	183728.74	34 2.19	107 0.22	7.55	0.00	12	8	114	0.09	0.4	0.8	2 1 2
77 9 1	31433.55	34 9.94	10652.64	4.29	0.00	6	7	148	0.05	0.8	1.9	2 1 3
77 9 1	215848.52	34 0.61	107 2.91	10.21	0.00	13	4	135	0.05	0.3	0.3	2 1 2
77 9 2	34918.72	34 0.42	107 3.13	10.36	0.00	12	3	145	0.09	0.5	0.6	2 1 3
77 9 2	74111.71	3358.82	10659.70	6.55	0.00	10	2	130	0.09	0.6	0.7	2 1 2
77 915	05335.23	34 1.54	107 3.55	10.06	0.00	10	3	176	0.07	0.5	0.5	2 1 3
77 915	1 134.42	3415.28	10655.42	6.10	0.00	14	11	119	0.08	0.3	0.9	2 1 2
77 915	64516.89	3420.70	10652.66	6.15	0.00	13	16	164	0.09	0.4	1.4	2 1 3
77 915	114334.43	3418.47	10655.25	4.86	0.00	9	15	137	0.07	0.3	1.8	2 1 3
77 915	1230 4.71	3420.55	10652.81	7.00	0.00	12	16	162	0.06	0.3	0.9	2 1 3
77 916	8 4 8.18	34 3.88	10659.46	7.00	0.00	8	9	173	0.05	0.3	0.5	2 1 3
77 920	81923.18	34 9.54	10652.38	7.21	0.00	10	7	89	0.10	0.5	0.8	1 1 1
77 921	6 9 8.76	34 9.88	10652.43	2.84	0.00	7	7	112	0.05	0.3	1.1	2 1 2
77 921	192155.18	3423.85	107 0.47	3.32	0.00	8	7	163	0.06	0.5	1.8	2 1 3
77 922	52027.98	3419.93	10653.10	6.41	0.00	12	15	156	0.06	0.3	1.0	2 1 3
77 922	63636.31	3420.18	10653.09	7.00	0.00	9	16	158	0.04	0.3	1.0	2 1 3
77 922	82218.16	34 9.35	10652.26	6.72	0.00	7	7	120	0.07	0.5	0.9	2 1 2
77 922	191916.66	3420.14	10652.95	10.64	0.00	12	15	158	0.08	0.4	0.8	2 1 3
771115	19 241.44	34 9.03	10653.13	8.24	0.00	8	9	138	0.07	0.6	1.0	2 1 3
771118	9 938.46	34 1.96	107 0.21	6.68	0.00	9	5	122	0.08	0.5	0.7	2 1 2
771214	205728.19	3417.42	10653.19	5.73	0.00	10	11	92	0.07	0.3	1.1	2 1 2
78 1 5	12 323.33	3416.56	10653.28	7.00	0.00	10	10	87	0.09	0.4	1.2	2 1 2
78 1 5	1445 8.50	3416.89	10652.90	7.00	0.00	9	10	132	0.09	0.5	1.4	2 1 2
78 117	231421.33	3420.90	10652.35	7.14	0.00	8	13	120	0.03	0.2	0.8	2 1 2
821013	943 6.75	34 1.36	107 2.98	9.01	-0.42	12	11	85	0.11	0.4	0.9	2 1 2
821015	194858.74	34 7.52	10644.33	9.34	0.24	9	10	99	0.10	0.6	1.6	2 1 2
8211 7	114345.84	34 2.38	10656.20	10.21	-1.22	10	4	77	0.12	0.5	1.0	1 1 1
821125	21019.99	3417.73	10648.06	10.59	-0.14	9	16	117	0.08	0.5	1.3	2 1 2
821125	34511.16	3357.16	10655.68	9.07	0.12	13	13	114	0.14	0.5	1.4	2 1 2
8212 8	215026.45	3416.98	10649.37	8.46	-0.55	9	18	145	0.08	0.6	1.9	2 1 3
83 120	1336 8.68	34 1.41	107 3.44	9.58	0.20	6	12	96	0.06	0.6	1.6	2 1 2
83 2 6	2011 0.94	34 2.94	10657.69	7.32	0.03	13	3	73	0.12	0.4	0.6	1 1 1
83 2 7	4 935.58	34 2.69	10658.08	7.00	-0.07	12	4	74	0.15	0.6	0.9	1 1 1
83 211	33634.68	34 2.66	10659.49	7.56	-0.11	9	5	92	0.13	0.6	1.1	2 1 2
83 211	214256.04	34 3.01	10659.06	4.38	-0.23	9	4	101	0.09	0.5	0.7	2 1 2
83 212	14 723.90	3417.00	10648.97	7.00	-0.24	9	17	145	0.08	0.3	1.7	2 1 3
83 3 3	1119 0.05	3418.29	10652.10	7.00	1.67	10	2	112	0.08	0.5	0.6	2 1 2

DATE	ORIGIN	LAT N	LONG W	DEPTH	MAG	NO	DM	GAP	RMS	ERH	ERZ	Q/QS/QD
83 3 3	16 7 0.04	3418.08	10651.78	7.57	1.00	10	2	106	0.07	0.5	0.6	2 1 2
83 3 3	1740 0.05	3418.59	10652.01	7.41	1.92	11	2	109	0.05	0.3	0.4	2 1 2
83 3 3	2235 0.02	3417.92	10652.58	4.51	1.02	11	1	94	0.05	0.3	0.4	2 1 2
83 3 4	0 0 0.02	3418.29	10652.54	5.35	1.99	13	1	67	0.10	0.5	0.6	1 1 1
83 3 4	147 0.00	3417.93	10652.33	4.61	1.87	12	1	67	0.06	0.3	0.5	1 1 1
83 3 4	149 0.01	3418.14	10652.52	6.55	1.30	12	1	66	0.04	0.2	0.3	1 1 1
83 3 4	326 0.05	3419.08	10652.34	7.25	0.73	10	2	78	0.04	0.2	0.3	1 1 1
83 3 4	52559.99	3418.08	10652.67	6.54	1.90	12	1	64	0.05	0.3	0.3	1 1 1
83 3 4	1353 0.02	3418.56	10652.67	5.45	0.57	9	1	126	0.04	0.3	0.4	2 1 2
83 3 4	181959.94	3417.67	10652.35	5.32	1.10	12	2	65	0.08	0.4	0.6	1 1 1
83 3 4	214859.99	3418.59	10652.52	5.90	0.84	10	1	70	0.08	0.5	0.7	1 1 1
83 3 5	11 5 0.00	3417.97	10651.57	5.93	0.93	10	3	76	0.09	0.6	0.9	1 1 1
83 3 6	01060.00	3418.29	10652.00	7.46	0.96	10	2	74	0.04	0.3	0.4	1 1 1
83 3 6	25960.00	3417.95	10651.93	7.00	0.51	10	2	72	0.05	0.3	0.5	1 1 1
83 3 6	2213 0.07	3417.65	10652.94	5.57	0.91	9	1	87	0.05	0.4	0.5	1 1 1
83 3 6	2326 0.04	3417.96	10652.26	4.97	0.60	9	5	99	0.04	0.3	0.6	2 1 2
83 3 8	6 6 0.05	3418.29	10652.79	5.79	1.24	11	1	93	0.04	0.2	0.3	2 1 2
83 3 8	619 0.01	3418.17	10652.80	4.48	2.03	12	1	92	0.07	0.4	0.5	2 1 2
83 3 8	827 0.13	3417.37	10651.80	4.57	1.42	11	3	99	0.05	0.3	0.5	2 1 2
83 3 8	16 4 0.04	3419.07	10651.60	5.92	0.90	10	3	123	0.06	0.4	0.5	2 1 2
83 3 9	9 460.00	3418.10	10652.74	5.43	1.69	11	1	95	0.05	0.3	0.4	2 1 2
83 3 9	15 3 0.00	3418.29	10652.58	5.75	0.84	9	1	98	0.05	0.3	0.4	2 1 2
83 3 9	23 3 0.02	3418.29	10652.72	5.30	0.72	10	1	97	0.05	0.3	0.4	2 1 2
83 3 9	2325 0.01	3418.05	10652.78	5.16	1.24	11	1	95	0.04	0.2	0.3	2 1 2
83 311	11 7 0.03	3417.41	10652.29	4.56	0.63	8	2	106	0.06	0.5	0.7	2 1 2
83 311	1146 0.02	3419.05	10652.03	6.09	0.61	8	2	110	0.08	0.7	1.0	2 1 2
83 411	143511.55	3416.62	10650.56	11.91	0.19	9	20	113	0.06	0.4	1.1	2 1 2
83 423	1426 5.05	34 5.81	10649.93	7.00	0.05	17	11	77	0.14	0.4	1.2	2 1 2
83 428	21021.38	34 6.39	10651.76	7.66	0.58	13	9	81	0.14	0.5	1.3	2 1 2
83 428	222926.38	3416.34	10653.39	10.87	0.16	11	13	137	0.13	0.7	1.4	2 1 3
83 5 1	945 5.79	34 5.84	107 1.28	5.56	-0.05	13	8	84	0.14	0.5	1.4	2 1 2
83 510	657 2.32	34 3.09	10657.39	8.90	0.23	15	2	73	0.12	0.4	0.6	1 1 1
83 510	163729.18	34 3.43	10657.67	9.28	0.48	14	2	71	0.08	0.3	0.6	1 1 1
83 511	611 0.00	34 3.81	10657.65	9.07	-0.09	8	0	124	0.10	0.8	0.5	2 1 2
83 511	616 0.00	34 3.38	10657.41	8.53	0.36	11	0	71	0.09	0.4	0.4	1 1 1
83 511	1359 0.00	34 3.58	10657.46	9.02	0.52	9	0	70	0.05	0.3	0.3	1 1 1
83 511	1433 0.00	34 3.64	10657.81	7.55	0.34	9	0	70	0.07	0.4	0.3	1 1 1
83 511	1452 0.00	34 2.61	10657.35	7.53	0.32	7	0	121	0.08	0.7	0.6	2 1 2
83 511	1525 0.00	34 3.10	10657.33	8.92	1.05	12	0	73	0.07	0.3	0.3	1 1 1
83 514	1 828.24	34 3.67	10657.70	8.32	0.14	15	2	70	0.13	0.4	0.7	1 1 1
83 514	144319.62	34 3.82	10657.59	9.19	-0.42	9	2	124	0.06	0.4	0.4	2 1 2
83 523	112138.33	3417.90	10652.20	9.32	-0.17	11	16	151	0.11	0.5	1.3	2 1 3
83 529	41634.15	34 2.00	10659.52	7.69	0.77	12	6	87	0.13	0.7	0.8	1 1 1
83 529	5 649.99	34 2.35	10659.75	7.42	1.03	13	6	91	0.13	0.5	0.8	2 1 2
83 529	55310.93	34 2.12	10659.35	7.96	0.31	11	6	88	0.07	0.3	0.7	1 1 1
83 528	55130.79	34 0.51	10648.87	7.00	-0.31	9	10	87	0.10	0.5	1.1	2 1 2
83 529	55310.90	34 1.99	10659.48	7.78	0.31	15	6	75	0.13	0.4	1.2	1 1 1
83 6 4	72250.49	3416.37	10649.30	10.98	-0.34	10	18	139	0.06	0.4	1.2	2 1 3
83 7 6	43820.18	3357.43	107 1.11	8.96	0.92	13	14	97	0.12	0.6	1.8	2 1 2
83 714	55225.16	34 4.00	10657.55	9.68	-0.54	10	1	122	0.07	0.5	0.3	2 1 2
83 714	113946.43	34 3.80	10657.88	9.85	0.10	8	2	97	0.09	0.7	0.8	2 1 2
83 714	1242 0.00	34 4.43	10657.29	8.67	-0.51	9	0	119	0.09	0.7	0.5	2 1 2
83 714	1613 0.00	34 3.15	10657.92	8.90	-0.67	10	0	129	0.14	0.9	0.7	2 1 2
83 714	161753.61	34 2.84	10656.85	7.87	-0.40	11	3	131	0.08	0.6	0.5	2 1 2
83 715	514 0.00	34 3.87	10657.64	8.99	-0.45	10	0	123	0.12	0.8	0.5	2 1 2
83 715	851 3.30	34 3.95	10657.75	9.45	-0.17	12	2	93	0.05	0.2	0.2	2 1 2
83 716	310 0.00	34 3.60	10657.68	10.81	0.56	8	0	96	0.08	0.6	0.5	2 1 2
83 716	435 0.00	34 3.30	10657.60	8.76	-0.43	10	0	128	0.06	0.4	0.3	2 1 2

DATE	ORIGIN	LAT N	LONG W	DEPTH	MAG	NO	DM	GAP	RMS	ERH	ERZ	Q/QS/QD
83 716	612 0.00	34 3.58	10657.92	8.14	0.16	14	0	122	0.10	0.5	0.3	2 1 2
83 716	85948.73	34 3.07	10657.70	8.62	0.00	10	3	72	0.14	0.8	0.7	1 1 1
83 716	1739 0.00	34 3.51	10657.61	9.31	0.16	10	0	71	0.09	0.5	0.4	1 1 1
83 716	2150 0.00	34 3.02	10657.81	9.20	-0.37	11	0	73	0.12	0.6	0.6	1 1 1
83 716	22 6 0.00	34 3.51	10657.50	8.92	1.77	10	0	71	0.09	0.5	0.4	1 1 1
83 716	2248 0.00	34 3.44	10657.11	9.11	0.15	12	0	71	0.07	0.4	0.3	1 1 1
83 717	1 126.77	34 3.55	10657.15	9.65	0.03	15	1	71	0.09	0.3	0.3	1 1 1
83 717	11 935.62	34 3.89	10657.59	9.73	-0.17	12	2	92	0.13	0.7	0.6	2 1 2
83 717	113256.38	34 3.66	10657.44	9.03	0.00	9	2	70	0.03	0.2	0.2	1 1 1
83 718	11 935.64	34 3.89	10657.56	9.49	-0.28	12	1	92	0.13	0.7	0.6	2 1 2
83 719	44028.61	34 3.43	10657.48	8.55	0.00	10	2	71	0.07	0.4	0.3	1 1 1
83 719	91254.40	34 3.34	10657.76	8.44	0.00	10	2	71	0.10	0.6	0.5	1 1 1
83 720	04154.39	34 3.54	10657.50	8.90	0.00	9	2	117	0.03	0.2	0.2	2 1 2
83 726	192429.25	34 2.79	10657.17	7.99	0.17	13	3	74	0.09	0.5	0.4	1 1 1
83 727	174915.90	34 2.59	10657.52	7.99	-0.14	12	3	75	0.08	0.5	0.4	1 1 1
83 727	1813 1.31	34 2.30	10657.67	7.20	-0.47	12	4	76	0.08	0.4	0.4	1 1 1
83 725	235133.82	3412.66	10641.00	10.49	0.52	9	9	124	0.11	0.9	1.8	2 1 2
83 8 1	1 116.69	34 7.35	10644.59	9.90	-0.13	8	11	132	0.09	0.7	1.2	2 1 2
83 8 3	32538.12	34 3.49	10657.53	8.49	-0.27	11	2	152	0.09	0.5	0.5	2 1 3
83 8 9	25357.59	3413.77	107 6.68	4.10	-0.10	14	15	97	0.07	0.3	1.6	2 1 3
83 817	63012.70	34 1.55	10648.86	9.44	0.05	11	11	85	0.13	0.6	1.1	2 1 2
83 818	152856.97	34 1.49	10659.69	8.37	1.01	13	7	76	0.10	0.4	0.8	1 1 1
83 818	1535 8.98	34 1.70	10659.86	6.82	0.34	14	7	75	0.06	0.3	0.4	2 1 2
83 820	53417.63	34 4.77	10658.90	7.19	0.28	13	3	124	0.13	0.6	0.6	2 1 2
83 827	103021.80	34 5.76	10648.05	8.31	0.61	13	13	134	0.13	0.5	1.3	2 1 2
83 913	228 9.01	3417.11	10651.75	10.99	0.11	12	21	145	0.09	0.4	1.3	2 1 3
83 919	1114 3.48	3357.32	10658.85	10.05	-0.25	15	13	99	0.14	0.5	1.3	2 1 2
83 922	11 852.56	3357.45	107 2.24	7.00	0.67	17	13	103	0.06	0.2	0.6	2 1 2
83 922	171229.07	3357.55	107 1.98	9.92	0.25	11	15	144	0.07	0.3	0.8	2 1 3
83 925	1 738.14	3358.62	10659.14	9.46	-0.42	13	11	91	0.09	0.3	0.6	2 1 2
8310 3	124534.56	34 4.80	107 2.40	10.28	-0.52	12	9	112	0.08	0.4	0.6	2 1 2
831013	1937 4.15	3356.41	10654.96	8.94	-0.38	17	15	123	0.12	0.4	1.0	2 1 2
831023	0 126.12	3357.69	107 2.11	7.00	-0.90	13	14	101	0.13	0.4	1.5	2 1 2
831031	223425.07	34 3.12	107 0.67	7.95	-0.65	13	6	112	0.10	0.5	0.6	2 1 2
831123	34653.02	3357.57	107 2.10	10.46	-0.68	12	14	102	0.14	0.5	1.3	2 1 2
831123	12 319.00	34 6.56	10650.56	11.42	-0.75	12	10	105	0.10	0.4	0.9	2 1 2
831225	1320 9.41	3356.35	10655.05	8.22	0.50	17	15	123	0.13	0.4	1.4	2 1 2
831230	43330.35	3357.77	10645.62	4.51	-0.72	10	3	114	0.14	0.8	1.1	2 1 2
84 1 1	225059.40	34 1.45	107 3.11	10.88	-1.29	11	11	111	0.08	0.4	0.8	2 1 2
84 1 5	8 059.35	34 4.77	107 3.12	10.66	-1.28	9	10	121	0.09	0.6	0.9	2 1 2
84 112	145354.85	34 9.27	10653.28	8.30	-0.56	12	11	93	0.09	0.4	1.0	2 1 2
84 126	823 9.77	3417.01	10654.02	11.91	-0.02	10	24	142	0.12	0.6	1.9	2 1 3
84 130	11929.89	34 2.40	107 3.02	9.59	-0.25	13	10	70	0.09	0.4	0.7	2 1 2
84 221	152417.00	3412.39	10642.22	7.72	0.25	8	10	107	0.06	0.5	1.1	2 1 2
84 226	205619.00	34 1.49	10659.61	7.81	0.34	13	7	82	0.10	0.4	1.0	1 1 1
84 227	1 2 6.73	34 1.42	10659.63	7.56	-0.65	13	7	81	0.08	0.3	0.5	1 1 1
84 227	53041.48	34 1.79	10659.70	6.74	-0.75	14	7	85	0.10	0.4	0.6	1 1 1
84 327	65627.07	3410.83	10655.78	7.00	0.09	15	11	134	0.14	0.5	1.6	2 1 2
84 329	330 8.58	3410.46	10656.17	5.49	-0.08	13	11	98	0.11	0.4	1.6	2 1 3
84 427	45545.75	3356.63	107 3.39	9.11	-0.07	10	12	118	0.07	0.3	0.9	2 1 2
84 521	175038.84	34 7.77	10639.31	6.13	0.04	8	3	139	0.08	0.7	1.2	2 1 3
84 523	238 0.25	34 7.87	10652.24	10.53	0.64	13	10	87	0.15	0.6	1.9	1 1 1
84 529	44944.27	34 7.96	10652.05	6.62	0.72	13	10	87	0.11	0.4	1.2	2 1 2
84 6 7	195155.16	34 1.28	10659.98	4.53	-0.07	9	8	122	0.05	0.3	0.7	2 1 2
84 614	125726.16	3419.12	10642.59	8.67	-0.21	10	7	172	0.10	0.7	1.2	2 1 3
84 615	056 9.00	3420.94	107 3.92	10.31	0.88	10	9	145	0.12	0.7	1.9	2 1 3
84 615	12726.72	3420.38	107 3.14	5.21	-0.52	9	11	168	0.07	0.4	1.7	2 1 3
84 7 5	161843.11	3358.41	10659.83	6.24	-0.82	14	12	90	0.12	0.4	1.4	2 1 2

DATE	ORIGIN	LAT N	LONG W	DEPTH	MAG	NO	DM	GAP	RMS	ERH	ERZ	Q/QS/QD
84 7 6	43533.96	34 7.37	10653.60	7.24	-0.13	9	7	121	0.10	0.6	1.3	2 1 2
84 713	114728.26	34 4.99	10648.11	11.28	-0.10	11	13	108	0.14	0.5	1.4	2 1 2
84 716	161215.44	34 4.28	10650.63	9.38	-0.09	13	9	74	0.14	0.5	1.0	2 1 2
84 716	161643.53	3358.46	10648.09	5.07	0.26	10	7	112	0.10	0.5	1.5	2 1 2
84 720	113158.91	34 0.80	107 2.66	9.22	-0.88	12	11	148	0.13	0.7	1.1	2 1 3
84 722	165537.90	34 4.43	10650.59	10.86	-0.21	12	9	74	0.13	0.5	1.4	1 1 1
84 8 4	153359.81	3359.36	10657.38	6.70	0.18	13	9	93	0.10	0.4	0.9	2 1 2
84 8 4	1826 0.49	3359.47	10657.01	8.02	-0.55	12	9	111	0.08	0.4	0.8	2 1 2
84 8 5	121431.97	3359.41	10657.29	6.88	-0.35	11	9	112	0.10	0.5	1.1	2 1 2
84 813	720 3.28	34 2.51	10659.41	5.60	-0.40	15	5	73	0.10	0.4	0.6	1 1 1
84 812	15152.33	34 2.87	10658.97	6.41	-0.77	11	4	72	0.08	0.4	0.6	1 1 1
84 827	21435.49	34 0.27	10657.39	5.86	0.10	14	7	87	0.09	0.3	0.7	2 1 2
84 9 2	02050.86	3356.49	10659.81	7.00	1.89	13	15	99	0.09	0.4	1.6	2 1 3
84 9 2	13 112.93	3356.75	10659.41	11.23	-0.22	14	14	129	0.11	0.4	0.9	2 1 2
84 9 2	151616.99	3356.66	10659.92	9.46	0.08	13	15	129	0.09	0.3	0.7	2 1 2
84 9 3	64046.78	3356.63	10659.25	7.00	0.15	9	15	133	0.09	0.5	1.5	2 1 3
84 910	630 3.37	3356.50	10659.65	11.34	-0.45	16	15	100	0.14	0.5	1.0	2 1 2
84 917	25359.64	3359.53	10657.72	6.49	0.01	13	9	115	0.12	0.5	0.9	2 1 2
84 919	327 4.74	3419.05	10649.95	7.55	0.06	11	6	163	0.10	0.6	0.8	2 1 3
8410 8	159 1.12	34 5.50	107 2.12	8.38	1.17	13	9	67	0.14	0.6	1.7	2 1 2
841013	2055 0.57	3411.49	10652.87	4.29	0.02	10	15	91	0.05	0.2	1.5	2 1 3
841019	11347.88	34 1.90	10658.87	7.61	-0.09	11	6	76	0.09	0.4	0.7	1 1 1
8411 5	846 0.26	3418.72	10649.40	11.04	1.70	11	17	118	0.10	0.5	1.7	2 1 2
8412 2	183041.04	3358.96	10657.77	8.96	0.05	12	10	169	0.07	0.4	0.6	2 1 3
8412 2	183413.38	3359.18	10657.83	8.54	0.28	16	10	93	0.06	0.2	0.4	2 1 2
8412 4	05353.22	34 7.58	107 2.48	10.48	0.68	13	11	65	0.10	0.4	0.9	2 1 2
8412 6	205150.11	34 3.05	107 1.50	6.85	0.19	12	8	67	0.10	0.4	1.3	2 1 2
841227	1816 9.92	3359.38	10657.97	9.41	-0.38	10	9	116	0.10	0.4	0.9	2 1 2
85 1 1	01211.79	34 0.42	107 1.80	7.00	-0.04	14	11	78	0.13	0.4	1.6	2 1 2
85 1 6	82549.73	34 1.78	10659.66	8.18	-0.43	13	7	75	0.10	0.3	0.6	1 1 1
85 112	164139.52	34 4.43	10657.84	9.97	-0.14	7	2	145	0.07	0.8	0.9	2 1 3
85 112	175132.71	34 5.48	10658.20	10.98	-0.12	8	3	152	0.05	0.3	0.6	2 1 3
85 115	03117.58	3419.70	10656.82	7.04	0.42	14	5	144	0.14	0.5	1.0	2 1 3
85 216	202022.44	3354.23	10657.67	11.11	0.05	12	15	126	0.10	0.5	1.2	2 1 2
85 216	175253.19	3354.31	10657.67	8.06	0.19	12	15	125	0.07	0.3	1.0	2 1 2
85 219	2 744.22	3425.49	10658.22	9.31	0.96	12	12	132	0.10	0.4	1.3	2 1 2
85 219	13 827.04	3354.50	10657.71	9.48	0.25	14	15	123	0.13	0.5	1.6	2 1 2
85 219	1417 4.63	3354.51	10657.51	8.80	0.44	15	15	125	0.12	0.5	1.4	2 1 2
85 223	141755.81	3358.38	10655.90	5.56	-0.44	10	11	104	0.05	0.2	0.9	2 1 2
85 224	11912.30	3358.53	10655.66	5.58	0.90	18	11	103	0.13	0.4	1.3	2 1 2
85 224	12645.96	3358.42	10655.78	7.00	0.91	17	11	104	0.13	0.4	1.2	2 1 2
85 226	2317 4.11	34 1.50	10659.86	6.01	0.78	15	7	76	0.11	0.4	0.9	2 1 2
85 3 1	22 6 7.71	34 6.18	10659.60	7.00	-0.11	8	22	106	0.03	0.2	1.2	2 1 3
85 320	2048 9.22	3419.03	10652.37	6.33	0.28	10	3	136	0.09	0.5	0.9	2 1 3
85 4 8	124515.93	3418.39	10652.52	11.97	0.15	12	4	118	0.14	0.7	1.5	2 1 2
85 4 9	55924.44	3414.83	10653.18	8.47	0.54	10	10	78	0.09	0.4	1.5	2 1 2
85 412	7 031.34	34 2.94	107 0.42	7.03	0.26	12	6	130	0.10	0.4	0.7	2 1 2
85 414	24449.18	34 2.84	10659.69	6.87	-0.58	9	5	118	0.08	0.4	0.7	2 1 2
85 414	2152 4.62	34 0.74	107 1.45	7.67	-0.47	11	10	96	0.07	0.3	0.7	2 1 2
85 415	150 6.62	34 2.47	10659.96	7.50	0.07	15	6	72	0.15	0.5	1.1	1 1 1
85 415	220 8.43	34 2.76	10659.81	7.86	0.00	12	6	77	0.08	0.3	0.6	1 1 1
85 423	101039.05	3420.29	10651.10	5.92	0.39	10	4	173	0.14	0.9	1.6	2 1 3
85 430	1943 6.07	34 4.43	10655.16	4.68	1.10	9	2	83	0.13	0.8	1.4	1 1 1
85 5 1	101217.44	3420.50	10656.10	9.85	0.60	14	4	167	0.13	0.6	0.8	2 1 3
85 524	62138.77	3415.25	10652.16	10.64	-0.03	7	9	93	0.04	0.5	1.2	2 1 2
85 524	81757.95	3414.45	10652.76	7.00	-0.21	7	11	140	0.04	0.4	1.5	2 1 3
85 527	14 5 1.30	3356.63	107 3.49	10.43	0.23	9	12	118	0.07	0.4	1.0	2 1 2
85 612	131752.03	3417.63	10653.73	5.76	-0.10	7	5	120	0.08	0.9	1.6	2 1 2

DATE	ORIGIN	LAT N	LONG W	DEPTH	MAG	NO	DM	GAP	RMS	ERH	ERZ	Q/QS/QD
85 716	35942.00	34 5.85	107 2.30	10.31	-1.01	11	7	104	0.09	0.4	0.8	2 1 2
85 717	162453.52	34 8.40	10652.85	10.59	-0.06	11	9	111	0.14	0.7	1.3	2 1 2
85 717	172815.24	3415.95	10654.44	4.77	0.17	8	8	104	0.05	0.3	1.3	2 1 2
85 8 8	215726.22	3415.29	10653.85	9.69	-0.19	8	9	116	0.12	0.7	1.4	2 1 2
85 810	44317.37	34 2.43	10654.92	11.71	0.37	11	5	175	0.08	0.5	0.6	2 1 3
85 814	52611.49	34 6.83	107 0.33	8.37	-0.14	13	6	96	0.08	0.3	0.5	2 1 2
85 815	11140.73	34 7.25	10660.00	7.30	0.45	12	5	89	0.11	0.5	0.7	1 1 1
85 816	12422.14	34 7.39	10649.48	7.00	0.76	15	13	83	0.14	0.5	1.7	2 1 2
85 816	153531.44	34 7.18	10649.48	7.00	0.87	12	12	162	0.12	0.6	2.0	2 1 3
85 816	154222.97	34 7.00	10649.55	7.00	0.82	14	12	124	0.11	0.4	1.8	2 1 2
85 816	1559 5.40	34 7.31	10649.42	11.21	0.88	12	13	122	0.11	0.5	1.3	2 1 2
85 816	16 025.54	34 7.30	10649.43	9.42	0.67	12	13	122	0.12	0.6	1.5	2 1 2
85 817	51446.30	34 6.85	10649.72	11.29	1.86	12	12	74	0.12	0.6	1.7	2 1 2
85 817	213410.84	34 7.33	10649.40	7.00	1.28	11	13	73	0.10	0.5	1.6	2 1 2
85 818	1029 8.53	34 7.30	10649.32	7.00	0.37	16	13	74	0.15	0.5	1.9	2 1 2
85 818	154815.37	34 7.27	10649.74	10.71	1.53	15	12	72	0.14	0.5	1.6	2 1 2
85 818	221427.54	34 7.11	10649.53	7.00	0.03	13	12	90	0.14	0.5	1.9	2 1 2
85 819	193533.76	34 7.00	10649.58	10.16	1.76	12	12	74	0.11	0.5	1.3	2 1 2
85 819	222350.50	3356.31	107 0.05	8.05	0.62	18	16	99	0.10	0.3	1.0	2 1 2
85 820	226 3.19	34 7.03	10649.77	10.73	-0.21	10	12	91	0.09	0.4	0.9	2 1 2
85 820	73611.67	34 7.70	10649.64	7.00	0.02	15	13	84	0.14	0.4	1.6	2 1 2
85 822	45748.63	3356.49	10659.75	9.72	-0.07	16	15	100	0.15	0.5	1.4	2 1 2
85 823	221656.74	34 7.02	10649.53	10.65	0.07	12	12	91	0.11	0.5	1.0	2 1 2
85 823	44011.87	34 7.15	10649.24	7.00	0.26	12	13	89	0.11	0.5	1.7	2 1 2
85 826	73959.67	34 7.30	10649.23	10.33	0.94	11	13	74	0.09	0.5	1.5	2 1 2
85 826	81622.75	34 7.53	10649.35	8.40	0.33	14	13	73	0.08	0.3	0.8	2 1 2
85 827	327 7.44	34 7.64	10649.51	9.36	-0.14	11	13	85	0.13	0.5	1.3	2 1 2
85 827	93314.56	34 7.51	10649.41	10.04	0.36	13	13	73	0.08	0.3	1.0	2 1 2
85 831	54130.38	34 7.35	10649.31	9.54	0.17	13	13	87	0.14	0.5	1.4	2 1 2
85 831	65624.73	34 7.40	10649.51	7.00	-0.14	10	12	90	0.12	0.5	2.0	2 1 2
85 910	82431.38	34 7.30	10649.56	11.06	-0.03	15	12	88	0.11	0.4	1.0	2 1 2
85 913	131212.45	34 7.54	10649.80	10.97	0.25	14	12	84	0.11	0.4	1.0	2 1 2
85 916	64922.88	3356.48	107 0.21	9.46	-0.05	14	15	135	0.10	0.4	1.0	2 1 2
85 917	103622.17	3411.79	10648.00	6.27	0.05	12	16	79	0.05	0.2	0.8	2 1 3
85 917	103910.50	3411.47	10648.48	9.41	-0.17	10	16	102	0.13	0.7	1.5	2 1 2
85 917	104126.01	3412.19	10648.29	4.77	0.20	16	16	82	0.12	0.3	1.9	2 1 3
85 917	11 548.25	3411.96	10649.21	9.09	0.78	16	15	77	0.09	0.3	1.0	2 1 2
85 917	11 625.10	3411.89	10648.68	9.60	0.04	14	15	105	0.07	0.2	0.6	2 1 2
85 917	1142 8.40	3411.74	10648.88	5.47	0.22	18	15	76	0.13	0.3	1.6	2 1 3
85 917	195050.85	3412.08	10648.81	7.00	0.11	13	15	90	0.10	0.4	1.9	2 1 3
85 917	22 638.39	3412.51	10648.92	8.86	0.33	14	15	110	0.12	0.4	1.2	2 1 2
85 918	111455.38	3411.74	10648.46	9.27	0.75	16	16	75	0.09	0.3	1.1	2 1 2
85 918	113722.70	3411.94	10648.62	11.50	-0.15	13	16	105	0.12	0.4	1.3	2 1 2
85 918	17 116.49	3411.89	10648.45	11.10	0.28	15	16	79	0.09	0.3	1.0	2 1 2
85 918	171455.85	3411.96	10648.62	9.42	-0.10	15	16	80	0.06	0.2	0.6	2 1 2
85 918	171644.12	3411.75	10648.56	11.45	-0.38	10	16	104	0.07	0.3	1.0	2 1 2
85 918	18 2 7.11	3411.75	10648.44	10.76	0.59	16	16	75	0.06	0.2	0.7	2 1 2
85 918	182214.38	3411.54	10648.33	9.97	0.79	13	16	74	0.05	0.2	0.8	2 1 2
85 918	1823 3.09	3411.68	10648.58	10.28	0.01	14	15	75	0.09	0.4	1.3	2 1 2
85 918	191930.85	3411.90	10648.43	11.37	1.28	15	16	76	0.08	0.3	0.9	2 1 2
85 918	192050.85	3410.82	10648.25	10.68	-0.51	10	16	159	0.12	0.7	1.2	2 1 3
85 918	1923 9.00	3411.89	10648.51	9.00	0.69	15	16	76	0.10	0.4	1.2	2 1 2
85 918	1926 3.36	3411.90	10648.41	9.21	-0.07	14	16	80	0.10	0.3	1.2	2 1 2
85 918	1938 0.31	3411.67	10648.51	9.94	0.57	13	16	75	0.07	0.3	0.9	2 1 2
85 918	194029.13	3411.57	10648.42	10.45	-0.55	13	16	103	0.08	0.3	1.0	2 1 2
85 918	195017.74	3411.71	10648.64	8.99	0.06	13	15	78	0.07	0.3	0.9	2 1 2
85 918	20 019.64	3411.73	10648.74	9.24	-0.07	11	15	104	0.08	0.4	1.4	2 1 2
85 918	202323.97	3411.80	10648.68	7.00	0.36	14	15	78	0.06	0.2	1.0	2 1 3

DATE	ORIGIN	LAT N	LONG W	DEPTH	MAG	NO	DM	GAP	RMS	ERH	ERZ	Q/QS/QD
85 918	212551.88	3411.67	10648.49	11.18	0.00	12	16	78	0.09	0.4	1.2	2 1 2
85 918	2140 6.57	3412.25	10648.60	8.48	0.04	14	16	82	0.13	0.5	1.8	2 1 2
85 919	224 5.31	3411.36	10648.29	10.37	1.68	12	16	73	0.07	0.3	1.1	2 1 2
85 919	22725.90	3411.81	10648.05	11.71	0.39	14	16	80	0.11	0.5	1.7	2 1 2
85 919	22812.97	3411.81	10648.87	9.97	1.23	12	15	93	0.09	0.4	1.2	2 1 2
85 919	3 324.82	3411.82	10648.65	7.00	0.14	13	15	79	0.08	0.3	1.6	2 1 3
85 919	63037.40	3411.50	10648.80	10.41	0.65	12	15	133	0.06	0.3	0.7	2 1 2
85 919	93841.58	3411.65	10648.61	11.55	1.65	12	15	114	0.06	0.3	0.9	2 1 2
85 919	94439.14	3411.85	10648.44	8.40	0.62	13	16	115	0.09	0.3	1.1	2 1 2
85 919	10 5 3.58	3411.66	10648.61	10.95	0.24	13	15	114	0.08	0.4	0.9	2 1 2
85 920	142651.02	3411.46	10648.56	7.00	0.89	12	15	102	0.14	0.6	1.8	2 1 3
85 920	143733.90	3411.78	10648.56	11.54	0.69	12	16	76	0.09	0.4	1.3	2 1 2
85 920	162028.23	3411.44	10648.46	7.00	0.08	12	16	102	0.10	0.4	1.4	2 1 3
85 920	1927 2.82	34 8.40	10649.77	7.00	0.26	13	13	78	0.13	0.5	1.7	2 1 2
85 920	22 0 6.66	34 8.20	10649.47	8.59	0.04	13	13	87	0.12	0.5	1.0	2 1 2
85 921	6 027.03	3419.28	10652.68	7.00	0.14	15	19	117	0.13	0.4	2.0	2 1 3
85 921	7 918.73	34 7.51	10649.45	7.00	0.47	11	13	86	0.12	0.6	1.7	2 1 2
85 921	8 4 0.36	34 7.71	10649.86	7.74	0.38	15	12	70	0.08	0.3	0.9	2 1 2
85 923	21147.44	3419.38	10652.32	7.00	0.33	12	3	149	0.11	0.6	1.1	2 1 3
85 923	45828.43	3413.21	107 4.79	7.00	-0.19	11	11	102	0.15	0.6	1.8	2 1 2
85 925	73437.36	3419.46	10652.14	7.00	0.07	9	3	144	0.12	0.7	1.4	2 1 3
85 929	35449.06	34 7.41	10650.21	11.04	0.68	10	12	112	0.12	0.7	1.3	2 1 2
8510 2	91711.36	34 1.82	10659.71	7.66	-0.08	14	6	141	0.12	0.5	0.9	2 1 3
8510 3	163317.22	3417.67	10649.53	8.88	1.55	14	8	110	0.09	0.4	1.0	2 1 2
851013	112520.70	3422.03	107 2.87	6.41	-0.70	8	9	164	0.07	0.6	1.5	2 1 3
851016	6 842.10	3432.88	107 5.82	10.97	0.54	16	17	155	0.09	0.4	0.9	2 1 3
851018	616 5.63	3417.94	10651.38	5.78	-0.17	10	6	127	0.12	0.6	1.6	2 1 2
851019	132551.89	34 7.15	10649.70	10.29	-0.24	12	14	89	0.13	0.5	1.4	2 1 2
851023	35345.06	3413.33	10653.64	11.27	0.61	13	13	68	0.07	0.3	0.8	2 1 2
851023	191637.01	3417.39	10648.82	9.36	0.17	12	9	137	0.09	0.4	1.1	2 1 3
851028	82938.91	34 7.24	10649.77	7.00	0.64	17	12	72	0.13	0.4	1.4	2 1 2
851031	181234.99	3416.64	10648.90	10.85	0.35	8	10	104	0.09	0.8	1.5	2 1 2
8511 2	151618.52	3417.85	10648.74	9.37	0.48	10	9	112	0.14	0.8	1.9	2 1 2
8511 3	24023.95	34 5.17	10651.55	7.81	0.30	10	8	116	0.05	0.2	0.7	2 1 2
8511 4	13 224.45	34 1.24	107 0.25	6.65	-0.11	10	8	151	0.06	0.4	0.7	2 1 3
851110	14325.95	3415.12	10654.47	10.63	-0.16	11	9	75	0.15	0.7	1.5	1 1 1
851111	83236.74	34 7.64	10649.58	10.74	-0.05	8	13	128	0.08	0.6	1.5	2 1 2
851116	2255 6.70	34 2.04	107 0.40	7.75	-0.01	13	7	124	0.10	0.4	0.8	2 1 2
851120	34344.72	3420.07	10649.44	8.83	0.13	7	7	173	0.07	0.8	1.4	2 1 3
851127	135228.05	3415.73	10653.20	6.48	0.36	11	8	97	0.10	0.4	1.4	2 1 2
8512 1	211357.45	34 2.20	107 0.20	8.44	0.26	11	7	137	0.09	0.5	0.7	2 1 3
8512 1	223747.21	3415.90	10653.22	7.15	0.30	12	8	83	0.14	0.6	1.6	2 1 2
8512 2	24133.69	3356.67	107 0.87	7.00	0.93	17	16	101	0.14	0.4	1.7	2 1 3
851210	15554.98	34 3.76	10657.62	9.72	0.00	13	2	71	0.12	0.5	1.0	1 1 1
851213	213734.26	34 0.17	10658.54	8.24	0.10	10	8	125	0.08	0.3	0.6	2 1 2
851214	138 1.27	3414.09	10652.02	5.68	0.52	7	12	98	0.04	0.3	1.7	2 1 3
851225	73814.17	34 6.03	10649.22	10.36	0.35	12	12	101	0.10	0.4	1.2	2 1 2
851228	20 923.84	3416.70	10652.35	7.75	0.16	11	7	98	0.13	0.6	1.6	2 1 2
851230	223511.10	34 1.51	10649.78	8.15	0.48	14	12	89	0.14	0.5	1.4	2 1 2